Analysis of Freeway Bottlenecks

by

Srinivasa Srivatsav Kandala

A Dissertation Presented in Partial Fulfillment
of the Requirements for the Degree
Doctor of Philosophy

Approved June 2014 by the
Graduate Supervisory Committee:

Soyoung Ahn, Chair
Ram Pendyala
Kamil Kaloush

ARIZONA STATE UNIVERSITY

August 2014

ABSTRACT

Traffic congestion is a major externality in modern transportation systems with negative economic, environmental and social impacts. Freeway bottlenecks are one of the key elements besides the demand for travel by automobiles that determine the extent of congestion. The primary objective of this research is to provide a better understanding of factors for variations in bottleneck discharge rates. Specifically this research seeks to (i) develop a methodology comparable to the rigorous methods to identify bottlenecks and measure capacity drop and its temporal (day to day) variations in a region, (ii) understand the variations in discharge rate of a freeway weaving bottleneck with a HOV lane and (iii) understand the relationship between lane flow distribution and discharge rate on a weaving bottleneck resulted from a lane drop and a busy off-ramp. In this research, a methodology has been developed to de-noise raw data using Discrete Wavelet Transforms (DWT). The de-noised data is then used to precisely identify bottleneck activation and deactivation times, and measure pre-congestion and congestion flows using Continuous Wavelet Transforms (CWT). To this end a methodology which could be used efficiently to identify and analyze freeway bottlenecks in a region in a consistent, reproducible manner was developed. Using this methodology, 23 bottlenecks have been identified in the Phoenix metropolitan region, some of which result in long queues and large delays during rush-hour periods. A study of variations in discharge rate of a freeway weaving bottleneck with a HOV lane showed that the bottleneck discharge rate diminished by 3-25% upon queue formations, however, the discharge rate recovered shortly thereafter upon high-occupancy-vehicle (HOV) lane activation and HOV lane flow distribution (LFD) has a significant effect on the bottleneck discharge rate: the

higher the HOV LFD, the lower the bottleneck discharge rate. The effect of lane flow distribution and its relationship with bottleneck discharge rate on a weaving bottleneck formed by a lane drop and a busy off-ramp was studied. The results showed that the bottleneck discharge rate and lane flow distribution are linearly related and higher utilization of the median lane results in higher bottleneck discharge rate.

Dedicated to my parents

Ratna and Gopala Rao

ACKNOWLEDGMENTS

First and foremost, I offer my deepest gratitude to my advisor Dr. Soyoung Ahn for her supervision, advice and guidance. She provided me unflinching encouragement and support throughout the course of my graduate study and this research work. I would like to thank Dr. Ram Pendyala and Dr. Kamil Kaloush for serving in my committee.

I am as ever, indebted to my parents, brothers and friends for their love and support throughout my life. I am also thankful to Tejasri Buddha, Sravani Vadlamani, Zuduo Zheng, Karthik Konduri, Madhav Garikapati and Priya Gudipudi for their cheerful company and help in making my graduate study, a memorable experience.

TABLE OF CONTENTS

Page

LIST OF TABLES

LIST OF FIGURES

Figure Page

Figure Page

CHAPTER 1

INTRODUCTION

Traffic congestion is a major externality in modern transportation systems and has a negative economic, environmental, and social impact. The 2012 Urban Mobility Report (Schrank and Lomax, 2012) states that the cost of congestion, in terms of delay and wasted fuel, is estimated to be about $103 billion in urban areas in the United States. This cost has steadily increased since 1982, and the trend will likely continue.

One of the key elements that determine the extent of congestion, besides the demand for travel by automobiles, is freeway bottlenecks. Some studies (e.g. Cassidy and Bertini, 1999) have shown that the discharge rate of a merge bottleneck can drop by 10 percent upon bottleneck activation (i.e., onset of queue/congestion). (Note that an "active" bottleneck is characterized by a queued state upstream and a free-flow state downstream.) In traffic science literature, this phenomenon is referred to as "capacity drop." Thus, identifying freeway bottlenecks and studying the mechanism of their activation and capacity drop are important in improving operational efficiency and reducing freeway delay. Further, while freeway bottlenecks are observed to exhibit reproducible features, they still display temporal variations. For example, the reduction in bottleneck capacity upon activation is observed to vary (e.g. as low as 1.5 percent). Whether these variations are merely stochastic fluctuations (and therefore statistically insignificant) or occur due to the changes in traffic features (e.g. on-ramp inflow, lane-changing rates) is an open question yet to be explored in detail.

In recent years, there have been efforts to understand the characteristics of freeway bottlenecks. Many studies have shown that the features related to bottleneck activations exhibit regularities and are often reproducible. For example, researchers have observed over multiple

days that the reduction in bottleneck discharge rate is attributable to systematic lane-change maneuvers from the rightmost lane (shoulder lane) upstream of the merge to faster lanes to the left (Cassidy and Rudjanakanoknad, 2005). Moreover, the resulting queues propagate in ways predictable by a simple kinematic wave theory (Newell, 1993). For example, the wave marking the onset of a queue propagates backward in space at the speed of approximately 10 mph as predicted by the kinematic wave theory, and numerous studies (e.g. Smilowitz and Daganzo, 2000) reported similar findings. However, freeway bottlenecks still present many puzzling aspects including variation of capacity reduction and influencing factors.

There have not been many efforts in the past to systematically identify bottlenecks and measure the capacity drop on a regional network. This could be done by developing a methodology comparable to the rigorous methods to provide a better understanding of detailed features of freeway bottlenecks in a region and their temporal (day-to-day) variations. Developing effective countermeasures to improve freeway operations would benefit from more detailed analysis of various bottleneck features, particularly the capacity drop. Prioritizing the bottlenecks by ranking them based on the capacity drop would help the local governing body to focus on the bottlenecks that require immediate attention.

The primary objective of this research is to provide a better understanding of factors for variations in bottleneck discharge rates. Specific objectives are:

Regional Bottleneck Analysis: The objective here is to develop a methodology which could be used efficiently to identify and analyze freeway bottlenecks in a region in a consistent, reproducible manner. To this end, a simple analysis methodology was developed for a regional analysis and compared to a more rigorous method based on a spectral analysis technique. The

comparative analysis was conducted for the Phoenix metropolitan region to gauge the trade-off between precision and efficiency.

Using the regional analysis methodology, 23 bottlenecks have been identified, some of which result in long queues and large delays during rush-hour periods. For these bottlenecks, a number of performance measures were obtained, such as the duration of congestion, length of the congestion, vehicle miles traveled (VMT), vehicles hours traveled (VHT), and bottleneck discharge rate (where it can be measured or estimated). The identified bottlenecks were ranked according to the capacity drop in terms of flow and percent reduction in flow.

Bottleneck Features and The Smoothing Effect of the HOV lane on a Freeway Weaving Bottleneck: The objective here is to study the variations in discharge rate of a freeway weaving bottleneck. Data obtained near a freeway weave bottleneck show that the bottleneck discharge rate diminished by 3-25% upon queue formations. The discharge rate, however, recovered shortly thereafter upon high-occupancy-vehicle (HOV) lane activation. A statistical analysis showed that HOV lane flow distribution (LFD) has a significant effect on the bottleneck discharge rate: the higher the HOV LFD, the lower the bottleneck discharge rate. This finding supports the existence of "smoothing effect" which has been shown to arise at a merge bottleneck due to fewer disruptive lane changes with activation of HOV lane.

The Effect of Lane Flow Distribution (LFD) on the Reduction of Bottleneck Discharge Rate: Cassidy et.al (Cassidy and Bertini, 1999) observed that before the bottleneck activation high flows were created as a result of vehicle lane changing towards the median lane. They observed a decrease in discharge rate in all the lanes after the bottleneck activation. This research focusses on examining the relationship between lane flow distributions and bottleneck discharge rate

(variation and magnitude). The work is ongoing using the data obtained from a bottleneck on US-101 southbound in Los Angeles County in California.

Note that a spectral analysis method is used for II and III using high-resolution 20-second and 30-second data. Noise in the data is a major problem especially when dealing with high resolution data. In this research, a methodology has been developed to de-noise raw data using Discrete Wavelet Transforms (DWT). The de-noised data is then used to precisely identify bottleneck activation and deactivation times, and measure pre-congestion and congestion flows using Continuous Wavelet Transforms (CWT).

The rest of the document is organized as follows. Chapter 2 describes the literature review, Chapter 3 discusses the methodology that has been used in this research, and Chapter 4 presents the regional analysis of bottlenecks in Phoenix metropolitan region. Chapter 5 presents empirical analysis of bottleneck features at a freeway weaving bottleneck using a spectral analysis technique, called wavelet transform. Chapter 6 will provide analysis of the relationship between lane flow distribution (LFD) and bottleneck discharge rate.

CHAPTER 2

LITERATURE REVIEW

Chapter 2 describes the review of literature in three areas: (i) the features of bottleneck discharge rate, (ii) effectiveness of HOV lane (including the smoothing effect), and (iii) lane flow distribution. A number of prominent papers on bottlenecks and their related features are reviewed and described below.

Features of bottleneck discharge rate

This section summarizes several key empirical studies that analyzed traffic features around freeway bottlenecks.

Empirical evidence of capacity drop

Hall et al. (Hall and Agyemang-Duah, 1991) studied the bottleneck capacity drop phenomenon using 30-second data collected from a segment on Queen Elizabeth Way, Toronto, Canada (see Figure 1) in 1990. An active bottleneck typically occurred between stations 22 and 23 in the figure near the Cawthra Rd. interchange. The times of queue onsets and dissipations and the transition periods (i.e., the periods during which high pre-queue flows were observed momentarily, followed by marked drops in flow) were measured using the loop detector data obtained downstream of the active bottleneck (station 25). These times were confirmed by a *t*-test, e.g., the differences in flow during transition and after were statistically different. Hall and Agyemang-Duah computed the mean pre-queue and queue discharge flows by averaging the flow rates before and after the start of the queue, respectively, at station 25. They found based on the *t*-test that the difference between them was significant for 16 of 20 days at 5 percent significance level. The pre-queue flow rates were larger than the queue discharge rates by about

5-6 percent, indicating a capacity drop at the onset of the queues. Finally, they found that the distribution of queue discharge flows were Gaussian-distributed.

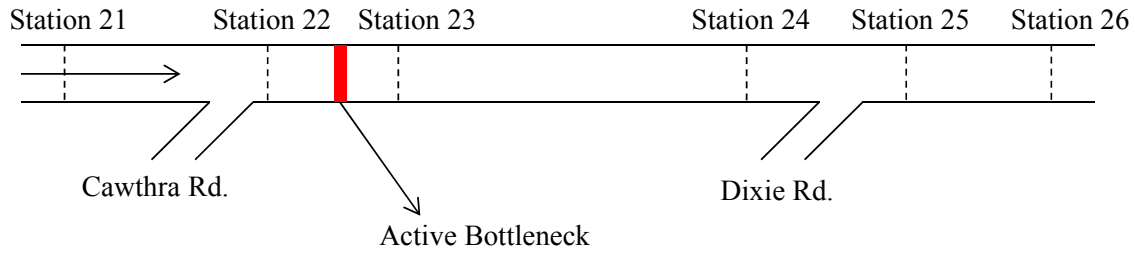

Figure 1. Study section of QEW, Toronto, Canada. (Recreated based on Hall and Agyemang-Duah (1991))

Cassidy et al. (Cassidy and Bertini, 1999) analyzed bottleneck discharge rates at two freeway bottleneck locations, Queen Elizabeth Way (QEW) and Gardiner Expressway near Toronto, Canada using high-resolution 30-second (QEW) and 20-second (Gardiner Expressway) loop detector data for three days. Oblique N-curves (cumulative vehicle counts vs. time on an oblique time axis) were constructed for each detector station to better reveal changes in traffic flow/state. Furthermore, the vertical displacements between two N-curves (after correcting for inflows and outflows) at neighboring detector stations represented vehicle accumulations between the stations. Similarly oblique T-curves (cumulative occupancy vs. time on an oblique time axis) were constructed to reveal changes in traffic occupancy/density. Based on these cumulative N- and T-curves, the active bottleneck locations and the start and end times of queues were identified systematically; for instance, the start of queue was accompanied by a sharp increase in occupancy and a reduction in flow. A capacity drop of nearly 8 percent was observed on QEW, while it varied from 4 percent to 10 percent on Gardiner Express. They observed that the bottlenecks occurred at the same locations and the discharge rates upon bottleneck activation were nearly constant over time.

Bertini et al. (Bertini and Leal, 2005) studied the traffic features at a freeway lane drop at two sites, M4 motorway (U.K.) and I-494 (Minneapolis, USA). They used oblique curves of cumulative vehicle count, time-mean speed, and occupancy vs. time to analyze bottleneck discharge rate. Upon bottleneck activation, they observed reductions in bottleneck discharge rate of nearly 10 percent, accompanied by propagations of shock waves at 3-4 mph. They also observed that oscillations (stop and go traffic) traveled upstream of the bottleneck at nearly constant speeds independent of the location within the queue. No oscillations were observed downstream of the bottleneck.

There are other studies (Elefteriadou et al., 1995; Chung and Cassidy, 2004; Cassidy and Rudjanakanoknad, 2005; Laval et al., 2005; Chung et al., 2007; Yeon et al., 2007; Lee and Cassidy, 2009; Rudjanakanoknad and Akaravorakulchai, 2011) that have reported evidence of capacity drop. These studies were described later in the chapter.

Traffic models that capture capacity drop

It is well documented that the seminal Kinematic Wave model (Lighthill and Whitham, 1955; Richards, 1956; Newell, 1993a; 1993b; 1993c) is unable to reproduce the capacity drop phenomenon (see Nagel and Nelson, (2005) for example). Earlier remedies included defining reverse-lambda shaped fundamental diagrams, thereby inducing capacity drop exogenously (e.g., Koshi et al., 1983; Hall and Hall, 1990). Laval and Daganzo (2006) sought to describe the physical mechanism by developing a hybrid model that incorporates lane-changing, bounded vehicle acceleration and heterogeneous vehicle characteristics in a macroscopic framework. They conjectured that lane-changes by merging vehicles create voids in traffic streams due to bounded accelerations and that the voids persist and propagate downstream with the traffic,

resulting in a reduction in bottleneck discharge flow. Leclercq et al. (2011) further developed a merge model that endogenously incorporate capacity drop.

Elefteriadou et al. (Elefteriadou, Roess and McShane, 1995) studied the stochastic nature of breakdowns at freeway merge junctions using the database from NCHRP Project 3-37, *Capacity of Ramp-Freeway Junctions*. At three sites, one in Chicago, Illinois and two in Orlando, Florida, they observed that the breakdowns occurred at these sites at relatively lower flows compared to maximum observed flows, indicating that breakdowns need not occur only at capacity flows, thereby contradicting the Highway Capacity Manual. Using videos at the sites, they observed breakdowns whenever there were clusters of vehicles approaching the freeway through the on-ramps. In their study, clusters were defined as groups of three or more vehicles with headways not exceeding 3 seconds or spacing of 54 m (0.033 miles) traveling at a speed approximately equal to 64 km/h (~40 mph). They concluded that occurrence of breakdowns at freeways is a probabilistic process and formulated a probabilistic model of breakdown occurrence as a function of the occurrence of vehicle clusters on the on-ramp and vehicles on the right-most lane (shoulder lane). However, the model was not fully validated due to limited data availability. They further observed that the probability of breakdown occurrence increases with respect to on-ramp flow up to 1,500 vehicles per hour (vph) but does not change much beyond 1,500 vph.

Polus et al. (Polus and Pollatschek, 2002) defined momentary capacity as the intersection of best-fit regression lines of unstable (congested) and dense (near-capacity) flows against speed as shown in Figure 2. They found that the momentary capacity was stochastic in nature. They used 5-minute loop data for speed and flow for three days from three busy urban freeway facilities in Tel Aviv. Based on the 5-minute data, they obtained regression lines and the

corresponding estimated parameters for unstable and dense flows and determined a momentary capacity. Using Monte Carlo simulations, they estimated the distribution of the capacity based on the properties of the estimated regression parameters (i.e. the expected values and the standard errors), after which they generated 1,000 random regression lines for unstable and dense flows and estimated the momentary capacity for each simulation run. The simulation result showed that the momentary capacity is gamma-distributed.

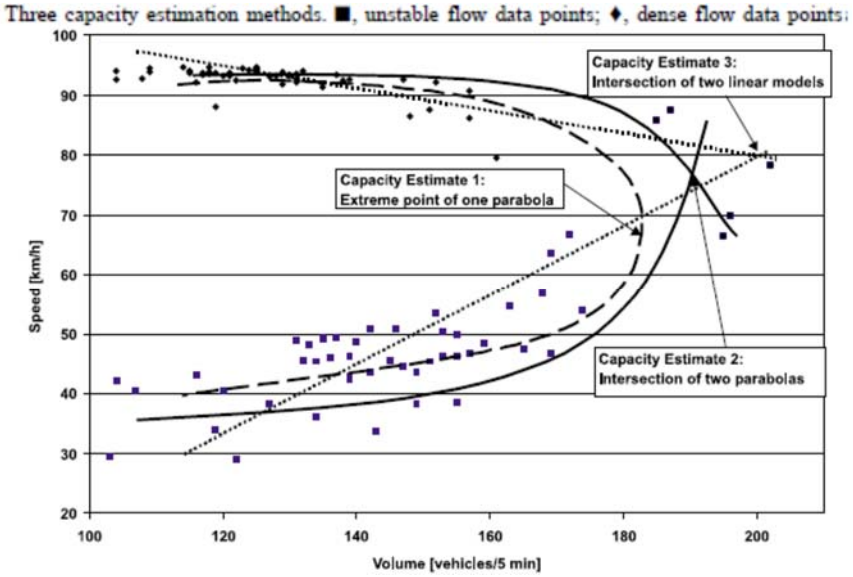

Figure 2. Best-fit regression of unstable-dense flows against speed. (Courtesy: Polus and Pollatschek (2002))

Brilon et al. (Brilon, Geistefeld and Regler, 2005) defined capacity as "*the traffic volume below which traffic still flows and above which the flow breaks down into stop-and-go or even standing traffic*." They analyzed data from 15 freeway sections near Cologne, Germany. Using the Product Limit method, they found that capacity, which is stochastic in nature, follows a Weibull distribution with a nearly constant shape parameter. (The Product Limit method is normally used for lifetime data analysis where death is termed as a failure event. In Brilon et al., traffic breakdown is termed as a failure event.) They defined three different traffic states: fluent,

synchronized, and congested. They concluded that transitions between traffic states occur spontaneously in the order of fluent traffic, breakdown, synchronized state (transition state), and then congested state. They further observed that the flow after traffic recovery to the fluent state was less than the flow prior to the breakdown, representing traffic hysteresis. An average capacity drop of 1,180 vph was observed across the 15 freeway sections analyzed, but the values varied widely from site to site. The risk of breakdown was particularly high when the freeway was saturated over 90 percent of its estimated capacity. They also found that capacity was reduced by 11 percent on a wet surface and that darkness (light conditions) did not affect the capacity distributions. They also concluded that a controlled-access freeway section has a higher capacity (by 3 percent) than a highway with intersections.

Yeon et al. (Yeon, Henrandez and Elefteriadou, 2007) defined four different types of capacity flows: maximum pre-breakdown flow (maximum flow within 2 hours before the breakdown), breakdown flow (5-minute flow per lane just before the breakdown), maximum queue discharge flow (maximum flow during congestion), and average queue discharge flow (average flow during the congestion). They measured these flows on different freeway segments along US-202 southbound near Philadelphia, PA. In their study, they observed that diverging segments have larger capacity flows than merging segments on average. Based on the analysis of variance (ANOVA), they reported that these capacity flows are statistically different across time of day, though they did not change much across day of the week. Of the different types of capacity flows, the maximum pre-breakdown flow was found to be the largest, while the average queue discharge flow was the smallest.

Factors influencing capacity drop

Cassidy et al. (Cassidy and Mauch, 2001) examined the relationship between flow and density on queued freeway segments using 20-second loop data during two morning periods on QEW. This site experienced higher on-ramp flows than off-ramp flows, which resulted in improvement in queued vehicular speeds toward the bottleneck. They used oblique N- and T-curves to verify bottleneck capacity drops and examine the features of queues upstream. Notably, they found that there is a well-defined relationship between flow and vehicle accumulation (thus density) on a homogenous freeway segment. Moreover, the simple hydrodynamic theory of Newell (1993) is adequate to predict the propagation of a freeway queue.

Cassidy et al. (Cassidy and Rudjanakanokand, 2005) have studied the effect of on-ramp metering at an isolated merge bottleneck. They observed that the queue initially formed in the shoulder lane and spread to the left lanes as slow vehicles maneuvered toward the left lanes. They found that by metering the on-ramp, the shoulder lane accumulation reduced and higher bottleneck discharge flows were attained. However, they cautioned that the on-ramp metering schemes should be adopted based on freeway conditions, such as vehicle accumulations near the on-ramp, to gain significant increase in the capacities.

Ogut et al. (Ogut and Banks, 2005) studied the nature of transitions from uncongested to congested flow using 30-second vehicle counts and occupancy data from five freeway sections in San Diego. They defined speed drop as an event that satisfies the following conditions: a speed reduction of 10km/hr (6.2 mph) or larger that lasts for at least 15 minutes, or a speed reduction that propagates upstream as a shock wave, accompanied by reductions in flow at upstream locations. They analyzed the spatial sequences of speed drops at each site and identified three patterns. Type A, which is the most typical pattern, is characterized by a speed drop occurring at the most downstream detector of the study section and then moving upstream. Type B is

characterized by two or more bottlenecks with a upstream bottleneck activating first. Type C displays more complex patterns. There, authors observed that some of speed sequences were out of order; for example, speed drops occurred at the upstream-most detector first and then at another detector in the middle. These patterns indicated the presence of more than one bottleneck. They computed the percentage of breakdowns corresponding to these types of speed drops at each site. Among the five study sites, the observed speed drops corresponded mostly to types A and B, with an exception of one site, where complex patterns (type C) were observed. To verify if variations in demand or a variation in capacity caused these patterns, a sample of speed drops observed during 15 days was further analyzed. Oblique cumulative plots were examined for increases in flow prior to the breakdowns, and the results showed that these variations in breakdowns were due to variations in capacity rather than variations in demand.

Chung et al. (Chung, Rudjanakanoknad and Cassidy, 2007) obtained a correlation between density and capacity drop on three bottlenecks: a merge bottleneck on I-805 near San Diego, CA, a reduced-lane bottleneck on SR 24 near San Francisco, CA, and a horizontal-curve bottleneck on Gardiner expressway in Toronto, Canada. A reduction in bottleneck discharge flow occurred shortly after the density increased beyond a certain threshold level. For the three bottlenecks in the study, the capacity drops ranged from 3 percent to 18 percent. The authors further concluded that capacity drops can be avoided by implementing traffic control schemes that regulate density.

Liu et al. (Liu and Wu, 2009) considered the influence of downstream traffic in defining freeway operational capacity. They noted that freeway capacity depends on the prevailing traffic conditions and is not a single value. They studied the stochasticity of freeway capacity using loop detector data at three stations along Trunk Highway 169 northbound in the Twin Cities area.

They defined freeway operational capacity as "*the maximum hourly rate at which vehicles reasonably can be expected to traverse a point or uniform section of a lane or roadway during a given time period under prevailing traffic conditions.*" They used a flow-density (FD) method, which is based on the flow-density or flow-occupancy curves, to determine the operational capacity. The maximum flow rates under different congestion levels (categorized by occupancy in increments of 5 percent as shown in Figure 3) on multiple days were used to determine the probabilistic distribution of operational capacities. It was found that, within each congestion level, the operational capacities are normally distributed. Further, a sensitivity analysis revealed that the categorization of the congestion level affects the operational capacity. They further plotted the mean operational capacities at different congestion levels, which showed the same general trend that an increase in occupancy results in lower operational capacity. The authors defined a probabilistic function for capacity as a function of occupancy to determine the risk level (defined as the probability of traffic breakdown) of freeway capacity.

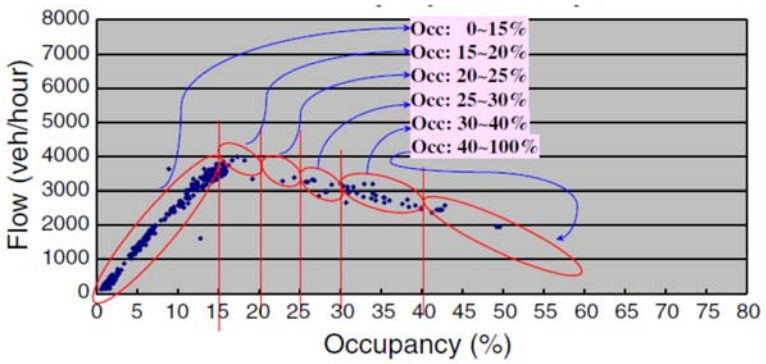

Figure3. Flow-occupancy curves with categorization of congestion levels. (Courtesy: Liu and Wu (2009))

Zhang et al. (Zhang and Levinson, 2009) studied the effectiveness of ramp metering in the Twin Cities in mitigating the impact of 27 bottlenecks. They analyzed data collected from nearly 4,000 single-loop detectors for seven weeks without ramp metering and another seven

weeks with ramp metering in 2000. To identify active bottlenecks, they defined three traffic regimes based on traffic density: a congested regime if the density is larger than 39 vehs/km/lane (24.23 vehs/mile/lane), a free-flow regime if the density is smaller than 31 vehs/km/lane (19.26 vehs/mile/lane), and a transition regime if the density is in between. The threshold values for the density were determined from visual inspection of the time-series occupancies and cumulative count curves obtained from more than 30 breakdowns on Trunk Highway 169 and I-94. They formulated a number of hypotheses to determine the impact of ramp metering on capacity (e.g., if pre-queue transitions, defined as the period in which the flow is higher than the queue discharge flow prior to the breakdown, exist, if pre-queue or queue discharge flows are higher with metering, if ramp metering can prolong the pre-queue transition period) and concluded that overall, ramp metering can increase the bottleneck capacity.

Patire et al. (Patire and Cassidy, 2011) studied the congestion mechanism of a three lane uphill expressway segment, with no ramps, in Japan. They analyzed 14 days of loop detector data and observed persistent congestion in all the three lanes in the upstream detector and free flow conditions at the immediately downstream detector. They observed a long run output flow drop (capacity drop) ranging from 4-11 percent during the study period. They found an increase in the shoulder lane flow (increased utilization) during the congestion period. They observed low shoulder lane flows in the initial duration of congestion. Due to the high demand and speed disturbances induced on the median and central lanes, the vehicles migrated to the shoulder lane during this period. They observed that once the flow on the shoulder lane increased due to the increase in the demand the lane changes became more disruptive resulting in the capacity drop.

Studies on weaving bottlenecks

Most existing studies in the literature analyzed bottlenecks around merge or diverge sections, and studies on weaving bottlenecks are relatively rare. Some notable exceptions are Lee et al. (Lee and Cassidy, 2009) and Rudjanakanoknad et al. (Rudjanakanoknad and Akaravorakulchai, 2011). Lee et al. (Lee and Cassidy, 2009) studied the mechanism of bottleneck activations on two freeway weaving sections in California that each formed due to a busy on-ramp and a busy off-ramp immediately downstream. Each of these sections has an auxiliary lane connecting the on-ramp and the off-ramp. They found that the bottleneck became active when freeway-to-ramp (F-R) maneuvers occurred near the on-ramp and that the bottleneck discharge rate varied by the rate of F-R maneuvers. Moreover, lower on-ramp flows induced greater F-R maneuvers near the on-ramp and resulted in lower discharge rates. In contrast, higher on-ramp flows induced F-R maneuvers away from the on-ramp and resulted in higher discharge flows. Based on the empirical findings, they formulated a mandatory lane changing model in which the lane changing decision is a function of the distance to the weaving section's diverge area, number of lanes to be crossed to reach the target lane and the difference in densities in the current and the target lanes.

Rudjanakanoknad et al. (Rudjanakanoknad and Akaravorakulchai, 2011) studied a weave bottleneck in central Bangkok that formed due to busy on-ramp and off-ramp. They analyzed video data collected during morning peak hours on two days. They observed that the capacity of the weaving bottleneck varied over time, and the variations were correlated with the upstream freeway flow, on-ramp and off-ramp flows. Specifically, lane changes from slow to fast lanes due to a surge in on-ramp flow resulted in an increase in bottleneck discharge rate, whereas lane changes from fast to slow lanes due to an increase in off-ramp flow resulted in reduction of bottleneck discharge rate. Based on their findings, they formulated a basic structure to model the

capacity of a weaving bottleneck in terms of several factors: lane-wise flows, on-ramp and off-ramp flows, and number of lane changing maneuvers (fast to slow lanes or slow to fast lanes.

It is evident from the literature review that traffic breakdown is probabilistic, highly site-specific, and not always reproducible. It has also been found that the capacity drop varies by time and site and that many factors may be responsible for its variations.

Effectiveness of HOV lane and smoothing effect

This section summarizes several key studies that focusses on the effectiveness of HOV lanes and smoothing effect and their influence on the traffic flow conditions.

Dahlgren (Dahlgren, 1998; 2002) studied the effectiveness of implementation of HOV vs. HOT lanes on freeways. The author concluded that if the delay is relatively low (< 35 minutes) and a proportion of HOVs is less than 20 percent, adding a general purpose lane to the existing freeway is more effective than adding either an HOV or HOT lane. If the initial delay is high and accompanied by a high proportion of HOVs (mu ch larger than 20 percent) then adding an HOV lane is more effective. If the delay is high but the proportion of HOVs is close to 20 percent, an HOT lane serves as a better alternative to an HOV lane.

Chen et al. (Chen, Varaiya and Kwon, 2005) evaluated HOV lane effectiveness on a freeway in the San Francisco Bay area and concluded that the HOV lane would increase the overall congestion on the freeway. They observed that the activation of HOV lane decreases the capacity of the non-HOV lanes, thereby affecting the overall capacity in a negative way. They termed this phenomenon as “HOV congestion penalty”. They also observed reductions in speed and flow in the HOV lane in spite of being in the free flow regime. They termed this as “HOV capacity penalty”. They explained that the low speed in the HOV lane could be a result of HOV

vehicles entering the HOV lane from slow, non-HOV lanes and reduction in speed due to risk perception induced by the large speed difference between the HOV and non-HOV lanes.

Kwon et al. (Kwon and Varaiya, 2008) have further computed the "HOV capacity penalty" to be 20 percent. They suggested that the HOV lane actuation increases the demand on the non-HOV lanes and thus increases the net delay. They also concluded that the HOV lane actuation does not increase the person throughput significantly and is also insensitive to travel time saving in both long term and short term.

On the contrary, Menendez et al. (Menendez and Daganzo, 2007) showed using simulations that the presence of an HOV lane diminishes the disruptive lane changes (smoothing effect) and therefore can increase the capacity of the general purpose lanes. They studied the effect of HOV lanes in three different scenarios, one without bottlenecks, one with a diverge bottleneck and one with a merge bottleneck. They observed increases in capacity in the general purpose lanes at isolated bottlenecks and decreases in capacity of the general purpose lanes only at some idealized locations (freeway sections without bottleneck). They also concluded that if properly deployed, HOV lanes can reduce the person-hours of delay in the system.

Cassidy et al. (Cassidy, Jang and Daganzo, 2010) found that the smoothing effect in fact exists and is reproducible at different sites and on different days. It was observed that the smoothing effect is the largest in the lane immediately adjacent to the HOV lane and decreases as away from the HOV lane. The smoothing effect is the least or negligible in the shoulder lane. They observed an increase in bottleneck discharge flow as high as 21 percent due to the smoothing effect. They observed a reduction in both person delay and vehicle delay due to the smoothing effect.

In summary, the studies cited above suggest that lane-changes, induced by merging and diverging flows, diminish the bottleneck discharge rate and that the activation of a HOV lane can remedy this impact by discouraging disruptive lane-changes. These previous studies primarily analyzed the smoothing effect on merge and curve bottlenecks. The present study corroborates the existence of smoothing effect on a weave bottleneck. Moreover, this study examines the smoothing effect in more depth by analyzing its temporal trends and influencing factors in a statistically rigorous manner. We analyzed data from 33 days using a spectral analysis tool called wavelet transform to systematically de-noise the raw data, unveil underlying trends, and identify times of queue onset and steady-state periods.

Lane flow distribution (LFD)

This section summarizes several key studies on lane flow distribution.

Carter et.al (Carter, Rakha and Van Aerda, 1999) studied the lane to lane variations in flow and speed on data from 30 days at 27 detector locations on Queen Elizabeth Way, Canada. They observed that the interaction between speed and flow on different lanes is significantly different. The study used analysis of variance (ANOVA) approach to find out if the lane to lane variations in speed and flow are significantly different. Using ANOV approach they also studied the interaction between speed and flow across different lanes. They also concluded that the capacity parameters varied significantly across different sites and day of the week has a relatively less effect on the variability of flow and speed in different lanes.

Cassidy et.al (Cassidy and Bertini, 1999) studied the bottleneck features upstream and downstream of a bottleneck located on Gardiner expressway in Toronto, Canada. They observed that before the bottleneck activation, high flows were created as a result of vehicle lane changing

towards the median lane. They observed a decrease discharge rate in all the lanes after the bottleneck activation.

Amin et al. (Amin and Banks, 2005) have studied the effects of freeway and ramp flows on the lane flow distribution on five freeway segments in the San Diego, California. They looked at how the relationships between freeway/ramp volumes and lane flow distributions varied by time and location. They found that the lane flow distribution of the lanes is significant effected by the freeway flow and not by the on-ramp flow. They concluded that there was a significant variation in the lane flow distributions of the lanes by time of day. They noticed that these variations by time of the day are consistent at different locations in the same freeway segment however, they differed for different segments. They found that the lane flow distribution in the median lane increases with an increase in freeway volume.

Hong et al. (Hong and Oguchi, 2007) have studied the lane flow distributions and speed-flow relationships under unsaturated flow conditions on roadways in Japan. They studied the lane-use patterns by different vehicles and speed-flow relationships in different lanes for different roadways sections on multi-lane motorways in Japan. They concluded that the passenger cars and heavy vehicles showed significant difference in their lane use patterns. They also found that rainfall has a significant effect on the speed-flow relationship and heavy vehicle proportion on the motorway. They developed models to estimate the average patterns of lane use and speed-flow relationships on a lane given the proportion of vehicle type on each lane not considering the roadway geometric conditions.

Lee et.al. (Lee and Park, 2010) have studied the lane flow distributions on a 2, 3 and 4 lane freeway segments during different traffic conditions. They used density measure instead of flow to represent lane flow distributions. They found that during uncongested traffic regime, lane

flow ratio of median lane increased continuously and the magnitude of the lane flow distribution across all lanes was nearly the same as the congestion level increased. They also observed an increase in lane flow ratio in the median lane during the transition regime and lane flow ratio in middle and right most lanes decreased with increase in density. They also concluded that the lane flow ratio is effected by the truck volume on the freeway segments.

Knoop et al. (Knoop et al., 2010) studied the effect of variable speed limits on lane flow distribution near merging zones on A12 motorway eastbound in Netherlands. They observed that the right-most lane is underutilized on the motorway near a merging zone. They found that a variable speed limit of 60 km/h has a significant effect on the lane flow distribution and during this variable speed limit, the flow on the right increased thereby increasing the road capacity. However, they noticed that at the speed limit of 60km/h the merging process from the on-ramp to the motorway became more difficult which increased the congestion on the on-ramp. They concluded that variable speed limits near an on-ramp have significant effect on the lane flow distribution and should be considered when implementing variable speed limits on a motorway.

Duret et al., (Duret, Ahn and Buisson, 2012) studied the lane flow distribution in free-flow regime on a three-lane freeway in France. Their study was based on the data collected from the site located on A7/E15 south Lyon, France. They found that in free-flow regime, the proportion of flow in the median flow is directly proportional to the total flow. They observed a reverse trend in the center and shoulder lanes. They found that the relationship between lane flow distribution and the total is linear. They observed significant under-utilization of the shoulder lane, which could contribute to lower flow at the onset of congestion. They found that the under-utilization of the shoulder lane can be in part mitigated by banning trucks and/or implementing VSLs, both of which had a speed harmonization effect across lanes.

In summary, the studies explored the relationship of speed and flow across different lanes with the total flow on the freeway segments. They observed that high flows before the bottleneck activation were associated with vehicle lane changes towards the median lane and observed reduction in flows in all the lanes after the bottleneck activation. However, not much work has been done on studying the relationship of lane flow distributions at bottleneck locations and their effect on the reduction/variation in bottleneck discharge rate. This research focuses on examining the relationship between lane flow distribution and its effect on bottleneck discharge rate at a bottleneck location on US-101 southbound in Los Angeles County in California.

CHAPTER 3

METHODOLOGY

This Chapter describes the methodology of the current research used in the regional bottleneck study and a rigorous methodology based on a spectral technique called wavelet transform.

Regional analysis methodology

This section describes the regional methodology procedures for identifying major recurrent freeway bottlenecks and measuring or estimating the reductions in their discharge rates (i.e., capacity drop). Specifically, the section provides the definition of an "active bottleneck" and the methods to measure or estimate bottleneck discharge rates.

Measurement or estimation of bottleneck discharge rate. A bottleneck is "active" if traffic downstream of the bottleneck is freely flowing and traffic upstream is congested, as illustrated in Figure 4. In this study, speed below 45 mph is classified as "congestion" in using the 5-minute data. Thus, an active bottleneck is located by identifying a pair of neighboring detector stations with the upstream detectors exhibiting congested speed and the downstream detectors exhibiting free-flow speed (> 45 mph). We analyzed all recurrent active bottlenecks that persisted over 30 minutes or longer.

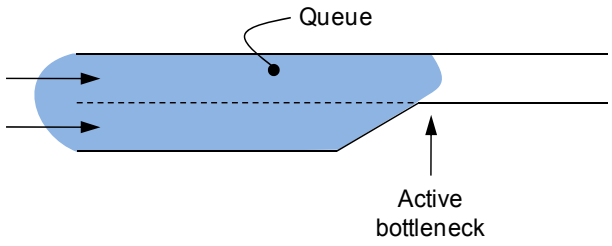

Figure4. Illustration of an active bottleneck; the shaded area represents a queue.

To analyze the reduction in bottleneck discharge rate (i.e., capacity drop), the maximum flow prior to a bottleneck activation and the discharge rate during congestion are measured. More specifically, the pre-congestion flow is the maximum flow prior to the bottleneck activation, and the bottleneck discharge rate during congestion is measured as the average flow during congestion. Then the capacity drop is measured as the difference between these two flows. The details of how these flows are measured are discussed later.

Ideally, bottleneck discharge rates should be measured at a location immediately downstream of a bottleneck with flows conserved throughout. This is illustrated in Figure 5. In this hypothetical example, a merge bottleneck is located between stations 1 and 2; thus, bottleneck discharge rates can be measured directly at station 2 since flow is conserved between the bottleneck and station 2.

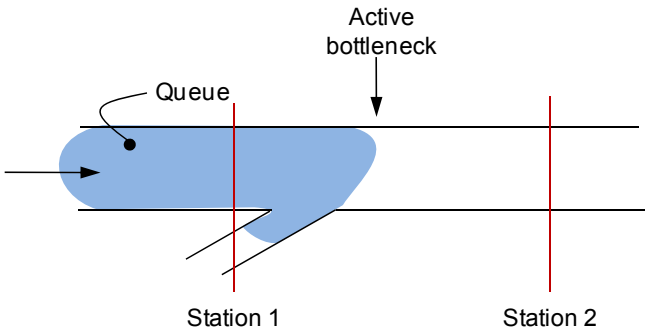

Figure5. Illustration of bottleneck discharge rate measurement.

For other types of recurrent bottlenecks, discharge rates are estimated rather than directly measured. For instance, Figure 6 shows a typical detector configuration around a merge bottleneck. Detectors (at station 1) are placed on the mainline and the on-ramp immediately upstream of the hypothetical merge; and an off-ramp is located between the bottleneck and the downstream detector station (station 2 in the figure). In cases like this, the bottleneck discharge

rate cannot be measured at station 2 since flow is not conserved due to diverging flow; i.e., the flow at station 2 represents the bottleneck discharge rate minus the diverging flow. Instead, the bottleneck discharge rate is estimated by summing the mainline and the on-ramp flows at station 1. Alternatively, the off-ramp flow can be added to the flow at station 2; however, off-ramp counts were not available at most locations.

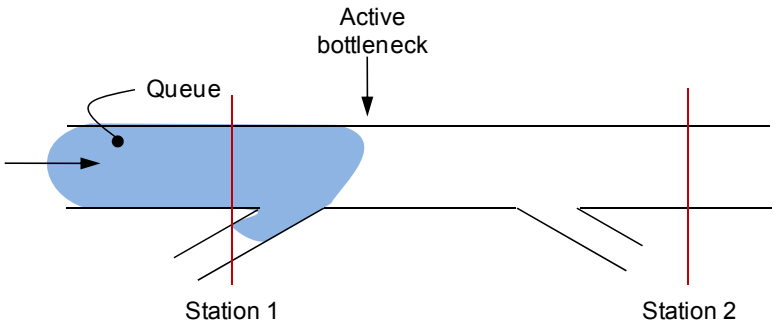

Figure6. Illustration of most common case of bottleneck discharge rate estimation.

Finally, bottleneck discharge rates cannot be measured or estimated on several freeways because on-ramp counts were not available or bottlenecks were not contained within the detector coverage area. For these cases, we report flows (rather than bottleneck discharge rates) before, during, and after congestion at the stations nearest to the bottlenecks.

Wavelet transform

In this research, the wavelet transform (WT) is used to de-noise the raw data, precisely identify bottleneck activation and deactivation times, and measure pre-congestion and congestion flows. These events are typically marked by sharp changes in speed and/or flow, which can be detected effectively by WT. In this chapter, we provide detailed background information of WT.

In the presence of noise, it is often not feasible to obtain critical information precisely from the raw signal (e.g., 20-second detector speed or flow data). Mathematical transformations, such as Fourier transforms (FT), short-term Fourier transforms, and WT, are often used to

process the raw signal to de-noise and obtain underlying frequency information hidden in the raw signal. Fourier transform is given by the following equation.

$$X(f) = \int_{-\infty}^{\infty} x(t)\, e^{-2j\pi ft}\, dt \qquad (1)$$

Equation (1) represents FT of a raw signal, $x(t)$, that is obtained by multiplying, or convolving, the signal with an exponential term at a particular frequency, f, and integrating it over time. The resulting spectrum shows the sine-wave frequencies that constitute $x(t)$. Figure 7(a) shows a simple, infinite sinusoidal signal, expressed as

$$x(t) = \sin 2\pi f \qquad (1a)$$

In the frequency domain, as shown in Figure 7(a), the FT spectrum consists of a single spectral line, or "spike," of signal energy with amplitude 1. Thus, the signal has only one rate of change, namely its sole frequency$f$. However, traffic flow is far from infinitely sinusoidal. A somewhat more realistic example is steady traffic that may become oscillatory at a point in time, then even out again. Such a case is drawn in Figure 7(b). Here, the FT produces a broadened complex spectrum that shows the sine wave's frequency with other frequencies produced by the starting and ending of the signal. The FT of the signal gives information about what frequency components are present over the entire period of signal, but it does not represent what frequency components exist at a particular time and how they change over time.

Due to this limitation, FT is effective in characterizing a *stationary* signal, like that of equation (1a) and Figure 7(a), in which the frequency content does not change over time. Traffic patterns may be stationary in certain circumstances, but they often exhibit *non-stationary* features due to the emergence of stop-and-go traffic, onset of congestion, incidents, work zones, and so on, and FT may not be effective in decomposing and analyzing them. One cannot get the

time-frequency information of the signal using FT as seen in Figure 7(c); hence FT may not be effective in decomposing and analyzing traffic data.

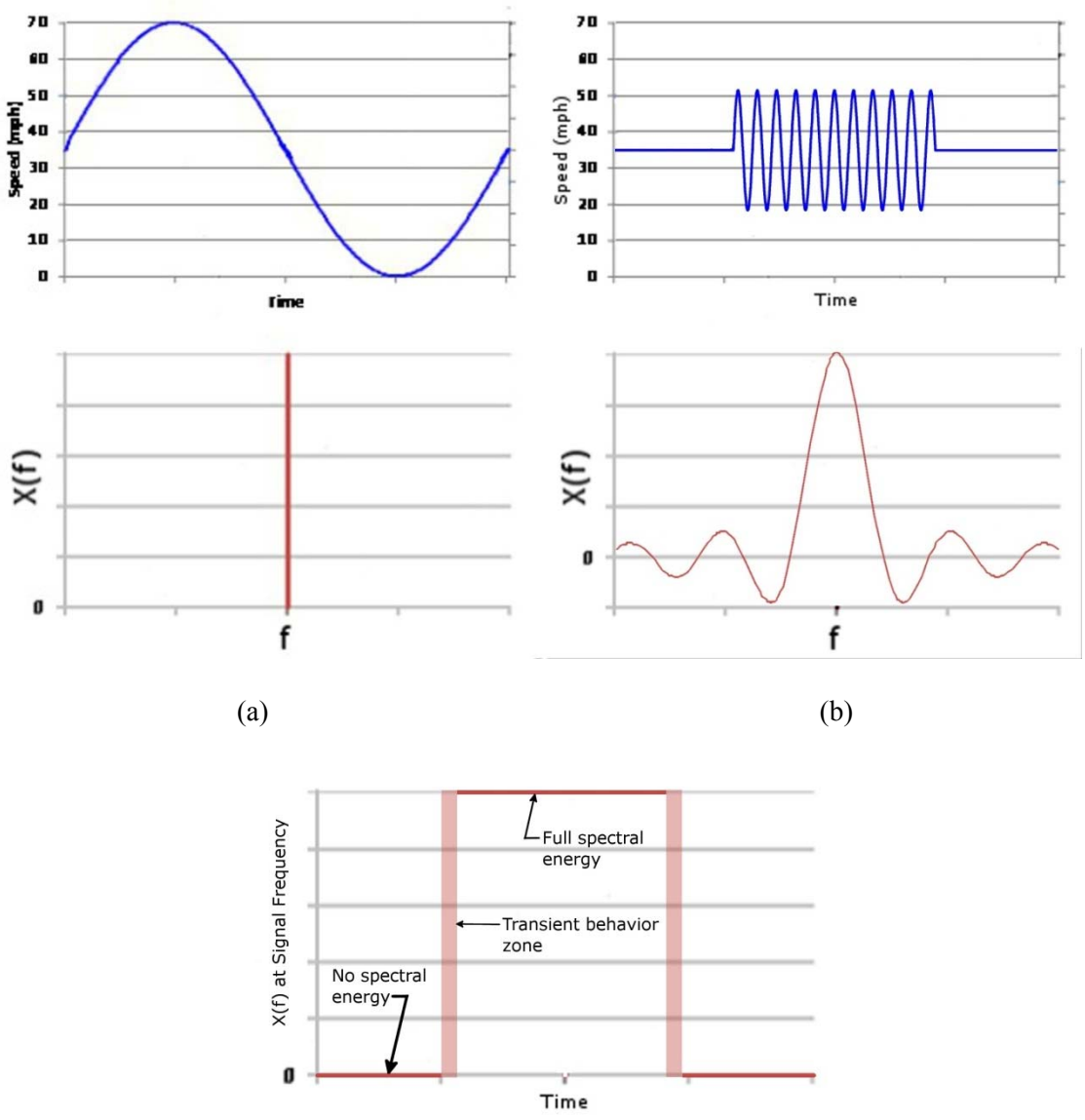

Figure 7. (a) Fourier Transform of a Continuous Sine Wave Signal (b) Fourier Transform of a Finite-Length Sine Wave Signal (c) Single-Frequency Spectral Energy vs. Time of a Finite-Length Sine Wave Signal Unattainable with Fourier Transforms

Wavelet transform (WT) is a powerful spectral analysis tool that provides time-frequency information of the given signal rather than only frequency information as in FT. That is, rather than providing spectral energies over the entire time period as in Figures 7(a) and 7(b), WT reveals the signal's spectral energy over any time period as in Figure 7(c). Thus, WT can effectively analyze non-stationary signals, such as speed and flow time series.

A wavelet coefficient, $\varphi_x^{\varphi}(s,\tau)$, is a complex mathematical function given by,

$$\varphi_x^{\varphi}(s,\tau) = \frac{1}{\sqrt{|s|}} \int x(t)\varphi\left(\frac{t-\tau}{s}\right) dt \qquad (2)$$

where $x(t)$ is the raw signal, in this case either speed or flow time-series. $\varphi(t)$is the transformation function or *mother wavelet* function. τ, a real number (Note that a real number may be an integer or a fraction, but it has no imaginary component as in complex or vector mathematics), is the time-translation parameter, which determines where the center of the mother wavelet function is placed along the time-domain graph of the signal. s, a real number that does not include zero because s appears in a denominator, is the scale parameter that determines the width of the mother wavelet function. The magnitude of s governs the *dilation* and *contraction* of the mother wavelet function and is defined as the inverse of frequency. That is, high s refers to low frequencies in the given signal representing non-detailed or global views of the signal. In contrast, low s refers to high frequencies representing more detailed views of the signal (e.g., noise). Because $x(t)$ is convolved with a transformation function $\varphi\left(\frac{t-\tau}{s}\right)$that is a function of both scale (frequency) and time, WT provides the time-frequency information of the non-stationary signal unlike FT. Without delving into mathematical details, these wavelet coefficients (spectral energies) of the given signal essentially represent the rates of change of the signal with time. In theory, the analyst using WT computes the wavelet coefficients by applying equation (2)

for all time translations τ and all scales s. In practice, however, the τ, dependent on the data resolution, are not continuous, and neither are the s. The resulting wavelet coefficients are therefore considered averages. 20- second detector data (speed/flow) have been used in this study, and WT is computed for each detector output on a given study day. Thus, as we will see in the following example, changes in the signal (e.g., a speed drop) generate large absolute values of wavelet coefficients.

To illustrate the *convolution* of the signal $x(t)$ with the wavelet function $\varphi\left(\frac{t-\tau}{s}\right)$ as in Eq. 2, the top panels of Figure 8 shows a representative raw speed signal $x(t)$ with time represented on the *x*-axis and speed on the *y*-axis. However, unlike the top panels of Figures 8, these signals are each superimposed with two wavelets, the left side with wavelets having s=1 and the right side with wavelets having s=3. Notice that the wavelets with larger s are more dilated than those with smaller s. Note that the Mexican Hat wavelet $\varphi(t)$ is used in this example (and for our analysis), which is one of several wavelet functions proven effective for a wide range of signals. The Mexican Hat wavelet function is the negative normalized second derivative of the Gaussian function and is represented by

$$\varphi(t) = \frac{2}{\sqrt{3\sigma}\pi^{\frac{1}{4}}}\left(1-\frac{t^2}{\sigma^2}\right)e^{\frac{-t^2}{2\sigma^2}} \qquad (3)$$

Haar, Daubechies, biorthogonal and Meyer are some of the other widely used mother wavelet functions. The bottom left panel of Figure 8 shows the wavelet coefficients (spectral energies) that result when the raw signal is convolved with the s=1 wavelet for all τ using equation (2). The coefficient value that results when the wavelet passes τ=15:06 hours is

specially denoted for illustrative purposes, as is that at 15:12 hours. The bottom right panel does likewise, except that the more dilated wavelet, s =3,is used.

Figure 8 shows the effects of choosing various wavelet dilations. The red wavelet on the left focuses narrowly on a part of the signal that is changing rapidly at 15:06 hours and thus produces a relatively large wavelet coefficient. By contrast, the other red wavelet almost fully envelops the oscillatory part of the signal and renders it as a region with little rate of change, yielding a low wavelet coefficient. On the other hand, the green wavelet on the left captures only a small part of a long decline of the signal and thus produces a relatively small wavelet coefficient. By contrast, the other green wavelet envelops much more of the decline and renders it as a region with a high rate of change, yielding a high wavelet coefficient. This behavior shows that the wavelet coefficients for $s = 1$ reveal more detailed information of the signal, such as small local changes and noise on the signal. By contrast, the coefficients with $s = 3$ reveal a more approximate/global trend and expose longer-term changes in traffic flow while suppressing signal noise.

For a non-stationary signal, which is often the case for speed and flow time series, wavelet coefficients are computed for a range of scales to represent different frequency information of the signal. Then, the average coefficients are computed to identify significant changes, such as a significant speed drop, in the signal. The maximum scale is typically a function of sample size. Although the wavelet coefficients in Figure 8 are graphed like time-domain functions along time axes, they are very much like spectral energies shown in Figures 7(a) and 7(b). Each point on a wavelet coefficient trace in the lower half of Figure 7 represents the tip of a spectral line of $x(t)$ at that instant and at a frequency that is the inverse of s from the mother wavelet's scale parameter.

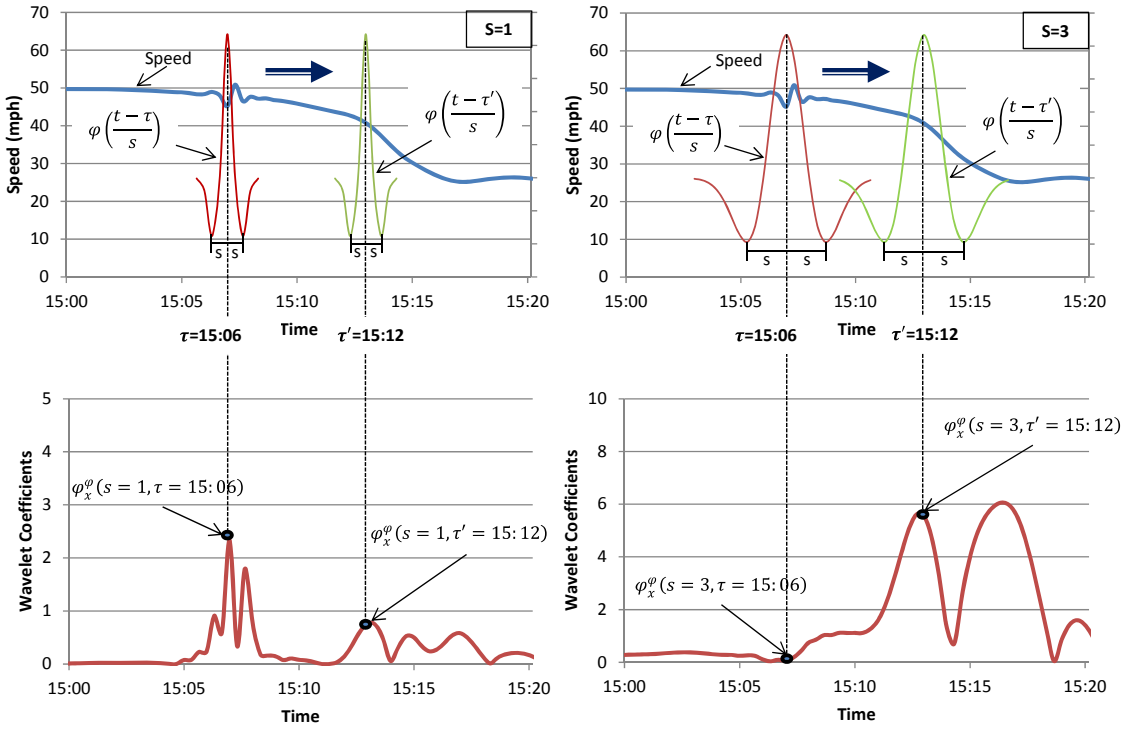

Figure8. Mexican hat wavelet illustration

There are two types of wavelet transforms, continuous wavelet transforms (CWT) and discrete wavelet transforms (DWT). In CWT, the scale and translation parameters are continuous, and thus wavelet coefficients are obtained continuously over s and τ (as in Equation (Eq.2)), thereby leading to redundancy in the information obtained. This redundancy allows one to identify event times (e.g., bottleneck activation) more precisely, albeit at the expense of efficiency. In DWT, the signal is decomposed in a discrete fashion; wavelet coefficients are computed with discrete values of s and τ. This can be achieved by adjusting the wavelet function as shown in equation (4).

$$\varphi_x^{\varphi}(s,\tau) = \frac{1}{\sqrt{|s|}} \int x(t)\varphi\left(\frac{t-\tau}{s}\right) dt \qquad (4)$$

Where $s \in 2^j, \tau = k \cdot s, (j,k) \in Z^2$(Z is set of integers, s≠0 because $s$is in the denominator). In this case, the initial value of s is set to 2 and increased by the power of 2 in the next iterations. The maximum scale is restricted to the sample size. τ is a linear function of s with k as a multiplying factor. (Note that in certain applications, τ can be independent of s). DWT decomposes the signal more efficiently than CWT since the coefficients are computed based on a subset of s and τ, albeit at the expense of resolution. More importantly, the DWT scheme allows one to reconstruct the signal via inverse transform, thereby enabling noise filtering. This process is described below in more detail. In light of the properties of CWT and DWT, DWT is used to de-noise the raw speed and flow data, and CWT is used to identify the bottleneck activation and de-activation times and steady-state periods.

Filtering data noise. For the purpose of de-noising, a raw signal, $\boldsymbol{x(t)}$, can be expressed as

$$x(t) = f(t) + \sigma\, e(t) \tag{5}$$

Where t is the (discrete) time in equal intervals; $f(t)$ is the signal in the absence of noise; $e(t)$ is white noise assumed to be Gaussian distributed, $N(0,1)$ and σ is the standard deviation. The goal is essentially to extract $f(t)$ from the raw signal. This is achieved by (i) decomposing the raw signal into different frequency components via DWT, (ii) determining noise components by applying threshold(s) on the wavelet coefficients, and (iii) reconstructing the signal (without the noise components) via inverse WT (Misiti et al., 2010). More details of each step follow.

The raw signal is filtered according to the wavelet based subband algorithm; see Figure 9 for the basic principle. (The details of this algorithm are provided in Polikar (2001).) The raw signal is passed through three levels of high-pass and low-pass filters using the Daubechies wavelet to decompose the signal into high frequency and low frequency components. In level 1

the signal is decomposed into "detail" wavelet coefficients representing high frequency components, $f_{max}/2 - f_{max}$, and "approximation" wavelet coefficients representing low frequency components, $0 - f_{max}/2$, where f_{max} is the maximum frequency in the raw signal. In level 2, the low frequency components are again bisected and decomposed into *approximation* ($0 - f_{max}/4$) and *detail* ($f_{max}/4 - f_{max}/2$) wavelet coefficients. In level 3, the lowest frequency components are once again decomposed into *approximation* ($0 - f_{max}/8$) and *detail* ($f_{max}/8 - f_{max}4$) wavelet coefficients. Note that the lowest frequency components are successively passed through the filters because they have low temporal resolution and are not well represented in the time domain (Robi and Polikar, 2001). After the three levels of decomposition, wavelet coefficients representing frequencies of $0 - f_{max}/8$ are considered as *approximation* wavelet coefficients and others are considered as level-1, level-2, and level-3 *detail* coefficients. Noise in the signal, which typically displays high frequencies, is assumed to be present in the *detail* wavelet coefficients.

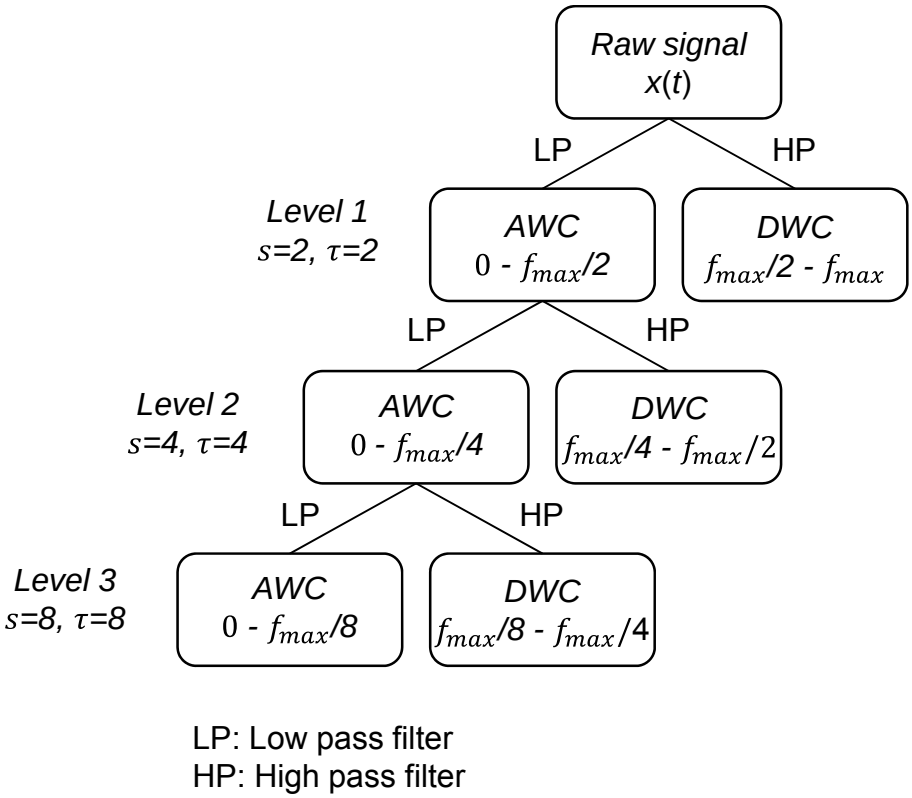

Figure9. Wavelet based the subband algorithm.

Note that the scale parameter and the increment of the translation parameter of the wavelet function increase by power of 2 to better decompose lower frequency components and avoid redundancy for efficiency. This means that the sample size decreases by power of 2. Therefore, the number of decomposition levels depends on the sample size. Three levels of decomposition were deemed sufficient in the present study.

Once the signal is decomposed, we determine the noise components by applying hard thresholds (λ's) on all three-levels of detail wavelet coefficients. Specifically, the wavelet coefficients below the thresholds are considered high-frequency noise components and are therefore removed: i.e.,

$$d(x) = \begin{cases} d(x), |d(x)| > \lambda \\ 0, |d(x)| \leq \lambda \end{cases} \qquad (6)$$

Where $d(x)$ represents *detail* wavelet coefficients of the raw signal x. The threshold values, λ's, are determined based on the Rigorous SURE method that is found to be most effective in de-noising real signals (Rosas-Orea et.al., 2005). In this method, λ is determined as:

$$\lambda = \sqrt{2\ \log_e(N \log_2 N)} \tag{7}$$

where N is the sample size. Note that since N varies with the level, different threshold values are used for different levels.

Finally, the signal is reconstructed via inverse wavelet transform using the approximation coefficients and the detail coefficients remaining after removing the noise components. Examples of de-noised speed and flow data are shown in Figure 10(a) and 10(b), respectively.

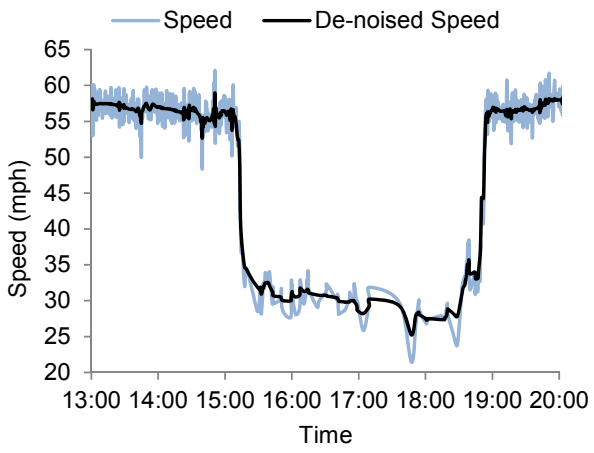

(a)

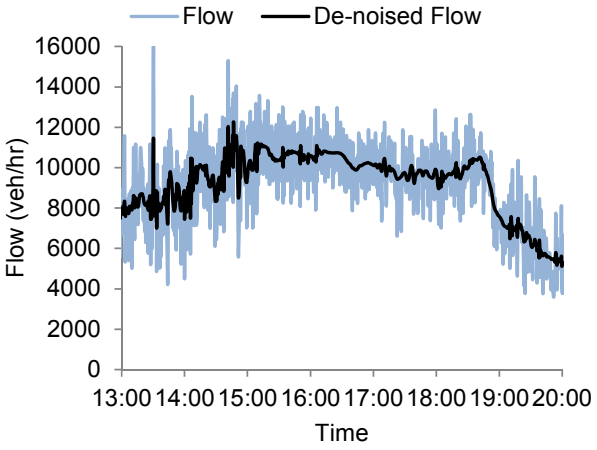

(b)

Figure10. (a) De-noised speed; (b) De-noised flow on 01/08/09, I-10 eastbound, Phoenix.

Bottleneck activation and discharge rate. Using the de-noised data, the characteristics of bottlenecks are analyzed. We first identify the times of onset and clearance of queue using the speed data obtained from measurement location 1 (immediately upstream of the bottleneck). These times are identified in a systematic manner using CWT and used later to estimate the times at the downstream measurement location. Among several mother wavelet functions, the Mexican Hat wavelet is adopted based on the previous finding that it is effective in analyzing traffic data (Zheng et al., 2011). The Mexican Hat wavelet function is the negative normalized second derivative of the Gaussian function and is represented by

$$\varphi(t) = \frac{2}{\sqrt{3\sigma}\pi^{1/4}} \left(1 - \frac{t^2}{\sigma^2}\right) e^{\frac{-t^2}{2\sigma^2}} \tag{8}$$

Based on its shape, the Mexican Hat wavelet generates peaks and dips whenever there are changes in the signal. In this research, absolute values of wavelet coefficients are used so that changes in speed or flow correspond to peaks. As shown in Figure 11(a), the onset of congestion marked by a sharp decrease in speed corresponds to a peak in the (absolute value of) wavelet coefficients. Note that there is another pronounced peak immediately after the onset of congestion. This marks the end of transition to the congested regime. Similarly, the clearance of congestion marked by a recovery in speed also corresponds to a peak. The peak prior to the clearance represents the start of transition to the free-flow regime. For this example, the start and the end of congestion are identified to be at 14:42:40 p.m. and 18:52:17 p.m., respectively. The same technique is used on flow data to identify the periods of near-steady traffic states, in which the flows remain nearly constant (i.e., the periods between two neighboring peaks in wavelet coefficients); see Figure 11(b). Specifically, we identify the near steady-state period immediately

before the onset of congestion to measure the pre-congestion congestion flow (to be used in computing the capacity drop).

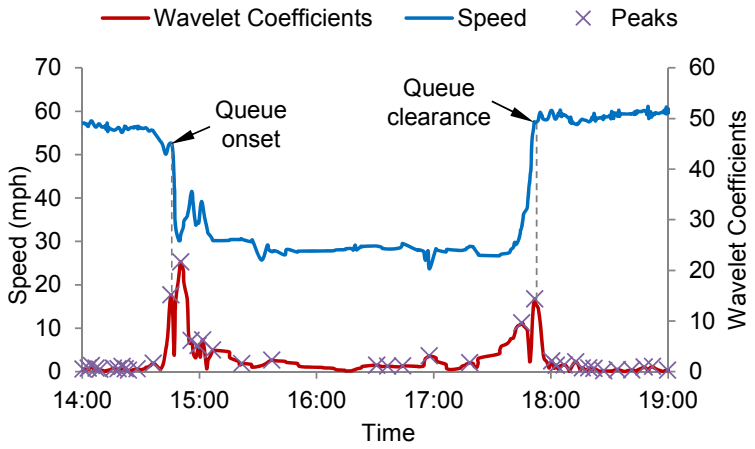

(a)

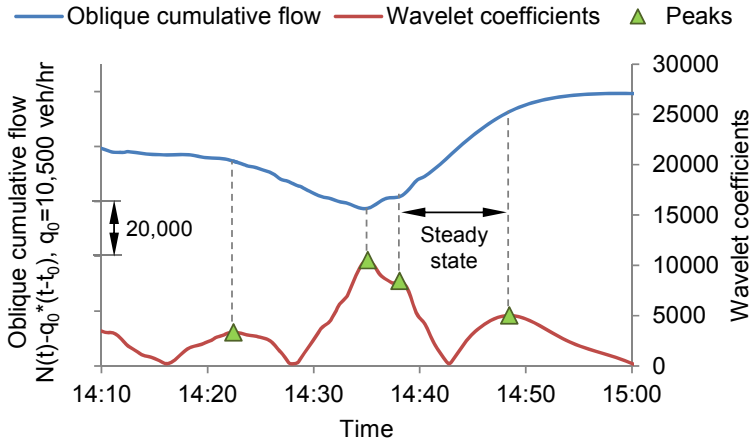

Figure11. (a) Times of queue onset and clearance based on continuous wavelet transform; (b) Near-steady state periods based on continuous wavelet transform (06/06/2008).

CHAPTER 4

REGIONAL BOTTLENECK ANALYSIS

The objective of this study is to develop a methodology which could be used efficiently to identify and analyze freeway bottlenecks in a region in a consistent, reproducible manner. In recent years, there have been efforts to understand the characteristics of freeway bottlenecks and found that freeway bottlenecks are observed to exhibit reproducible features even though they display temporal variations which could be mere stochastic fluctuations or due to changes in several traffic features like on-ramp flows, lane changing etc. It was found that the bottleneck discharge rate decreased upon bottleneck activation and thus identifying freeway bottlenecks and studying the mechanism of their activation and capacity drop are important in improving operational efficiency and reducing freeway delay. However they are not many efforts to systematically identify active bottlenecks and measure the capacity drop on a regional network. Choe et al. (Choe, Skabardonis and Varoaiya, 2002) and Wieczorek et al. (Wiezorek, Moctezuma and Bertini, 2010) have worked on identifying the bottlenecks at regional level but in this study a methodology comparable to the rigorous methods was developed to measure capacity drop and its temporal (day to day variations) and also provide a better understanding of detailed features of freeway bottlenecks in a region.

To this end, Phoenix metropolitan region has been chosen as the case study site. The Phoenix metropolitan region has several recurrent bottlenecks, some of which result in long queues and large delays during rush-hour periods. All Interstates, US Routes and State Routes with available detector data in the region were analyzed. Recurrent bottleneck locations were identified based on several criteria including congestion pattern, sensor coverage, data quality and (absence of) incident/construction activities. Chapter 4 presents the analysis results of all 23

bottlenecks identified, including some general observed congestion patterns, affected locations, number of days observed, and the feasibility of measuring or estimating bottleneck discharge rates. The identified bottlenecks were ranked according to the capacity drop in terms of flow and percent reduction in flow. This chapter also presents the comparison of the results obtained using WT with the result based on the regional analysis of 5-minute data to gauge the trade-off between precision and efficiency. This research shows that the 5-minute data could be effectively used in identifying and prioritizing active bottlenecks in a region. However, for studying the detailed mechanism of the high ranked active bottlenecks identified through the regional analysis it is advisable to use higher resolution data with an effective de-noising methodology as many traffic phenomena like lane changing, traffic stationary periods, oscillations etc. occur at a frequency less than 5 minutes.

Case study site and data

For this study, all interstates (I), US Routes (US), and State Routes (SR) in the Greater Phoenix area, where detector data are available, were analyzed to identify locations of recurrent bottlenecks and measure or estimate bottleneck discharge rates. The coverage of traffic sensors is illustrated in Figure 12 using ArcGIS 9.3. Most freeways and highways are equipped with inductive loop detectors except for I-17 and SR 51, which are equipped with passive acoustic detectors (PADs). Six months of data from these detectors were analyzed, spanning from July, 2009 through July, 2010 (though much data after January, 2010 were missing.) The data provides vehicle counts, time-mean speeds, and occupancies that were aggregated over 5-minute intervals. We further analyzed a bottleneck using the regional methodology using 5-minute data which has been described in detail in Chapter 3and compared the results with those based on the

wavelet analysis to evaluate the results from the regional-level analysis. The 20-second data were taken from July, 2008 to March, 2009. In this research, a.m. peak is considered from 6-10 a.m. and p.m. peak is considered from 3-7 p.m.

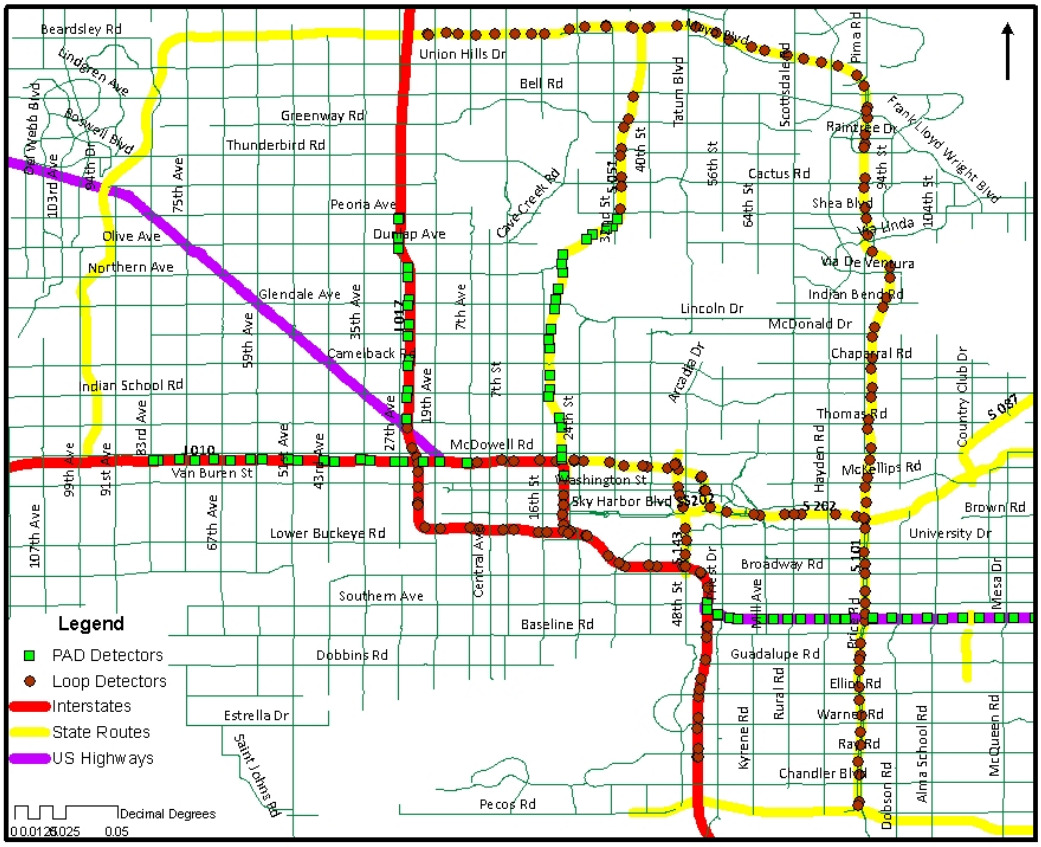

Figure12. Map of Greater Phoenix congested freeway segments with coverage of loop detectors and passive acoustic detectors. (Source: Samuelson (2011), Application: ArcGIS 9.3)

Identification of recurrent bottlenecks

In identifying major recurrent bottlenecks, the following criteria were considered:

- Congestion Level
- Sensor Coverage of the Queue
- Data Quality
- Non-recurrent congestion

Congestion level. In this study, speed below 45 mph is classified as congestion. Ideally, it should be site-specific but for a regional analysis, a reasonable value was selected based on examination of speed data from various freeway sections. There are studies that use similar values (Choe, Skabardonis and Varoaiya, 2002; Wiezorek, Moctezuma and Bertini, 2010**)**. The sites for which the temporal (>30 minutes) and spatial extent of the congestion are large are identified. Localized and non-recurrent congestion (these can be due to incidents, weather, etc.) are not considered for analysis. These sites are identified in the forthcoming figures with the help of speed contours that represent spatiotemporal distributions of speed in different color schemes.

Sensor coverage of the queue. The head of a queue is the farthest downstream part of the queue, at the bottleneck, containing vehicles that are discharging from the congested area. The tail of the queue is the farthest upstream part of the bottleneck, containing vehicles that are entering the shockwave part of the queue and coming into the congestion. Ideally, the entire queue fits within the study section with sufficient sensor coverage to measure or estimate bottleneck discharge rates and queue length. Such an idealization is shown in Figure 13.

In Figure 13, the time-space region is colored according to the speed based on the color scheme provided in the legend. Dark areas correspond to low speeds, indicating presence of congestion. However, given the objectives of study, it was not deemed critical to measure the queue length. Thus, we considered all the sites where the bottleneck discharge rate can be measured or estimated using the detector data. For example, in Figure 14(a), a queue formed at bottleneck 3 (labeled as “BN 3”) and propagated beyond MP160.23. Thus, the queue length cannot be measured. Nevertheless, it is still possible to measure or estimate the bottleneck discharge rate around MP 152. On the other hand, if a bottleneck location resides downstream of the detector coverage region, the bottleneck discharge rate cannot be measured or estimated; see

Figure 14(b). Of note, it was common to observe multiple bottlenecks on a study corridor; and often times, a bottleneck was "de-activated" due to the spill-over of a downstream queue. Figure 14(a) illustrates three major bottlenecks, two of which (BN 1 and 2) were de-activated due to the queues from the downstream bottlenecks (BN 2 and 3, respectively). In such circumstances, the most downstream bottleneck (BN 3 in Figure 14(a)) was analyzed where the discharge rate can be measured consistently throughout the time.

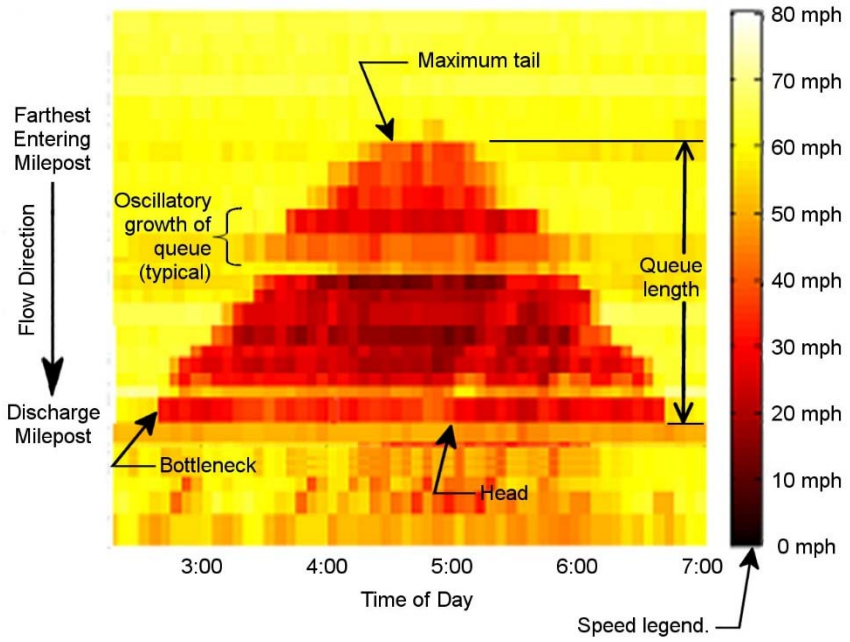

Figure 13. Speed contour plot from Matlab of ideally located bottleneck having entire queue contained within detector coverage area.

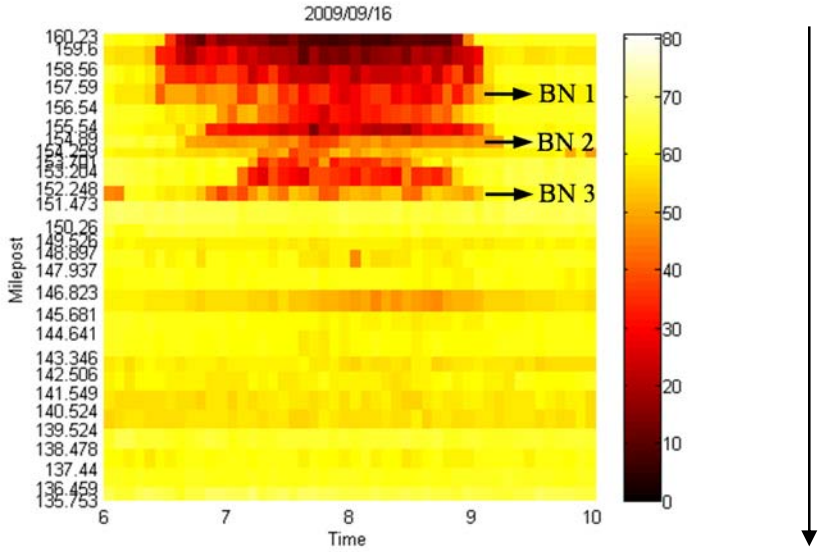

(a)

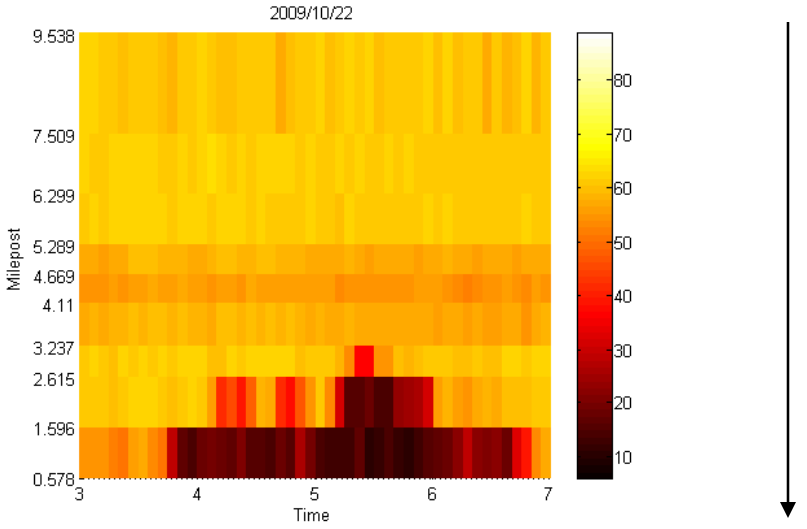

(b)

Figure14. (a)Tail of a queue not contained within the detector coverage area. (I-10 WB AM peak) (b) Head of a queue not contained within the detector coverage area (Loop 202 WB a.m. peak)

Data. To obtain meaningful results, the following procedure was implemented to assess the quality of data and take appropriate actions:

- Days with a majority of missing data were excluded from the analysis.
- Days with a significant amount of missing data in congested time-space regions were used only for classifying congestion patterns (e.g., bottleneck locations) but not for quantitative analysis of capacity drop and performance statistics (e.g., VMT and VHT).

For the remaining days in which quantitative analyses were performed, further assessment of data quality was performed as follows.

- If a significant amount of data was missing in uncongested time-space regions, the missing data were imputed using the valid data from neighboring detectors.
- Erroneous data were identified using the following filtering criteria established by TTI (Turner, Margiotta and Lomax 2004) and replaced by an average of the two nearest valid data points in time (one preceding and one following the time of interest, not exceeding 15 minutes):
  - 5-minute flow < 3,060 vph
  - Speed < 100 mph
  - Speed > 5 mph and 5-minute flow > 0

Non-recurrent congestion. Ideally, days with incidents and work zones can be identified from the archives (e.g., highway condition reports). Alternatively, days with recurrent congestion can be identified conveniently from speed contour plots, as exemplified in Figure 14. For our analysis, we selected the days for which the congestion/spatial extent of the queue were relatively consistent. The recurrent congestion pattern for I-10 eastbound during p.m. peak is shown in Figure 15(a). The bottleneck around MP 154.63 activates around 3:20 p.m. and remains active until 7 p.m., resulting in a 6.7-mile-long queue. This pattern was prevalent on the selected study days. In this research, we define recurrent congestion as a freeway condition in which the travel demand exceeds the freeway capacity resulting in congestion (below 45 mph) for 30 minutes of longer on an incident-free weekday. In contrast, Figure 15(b) represents a day with non-recurrent congestion, in which a much longer queue is observed due to an obvious restriction around MP 141.826. This non-recurrent congestion could be attributed to accidents, breakdowns, construction, or inclement weather.

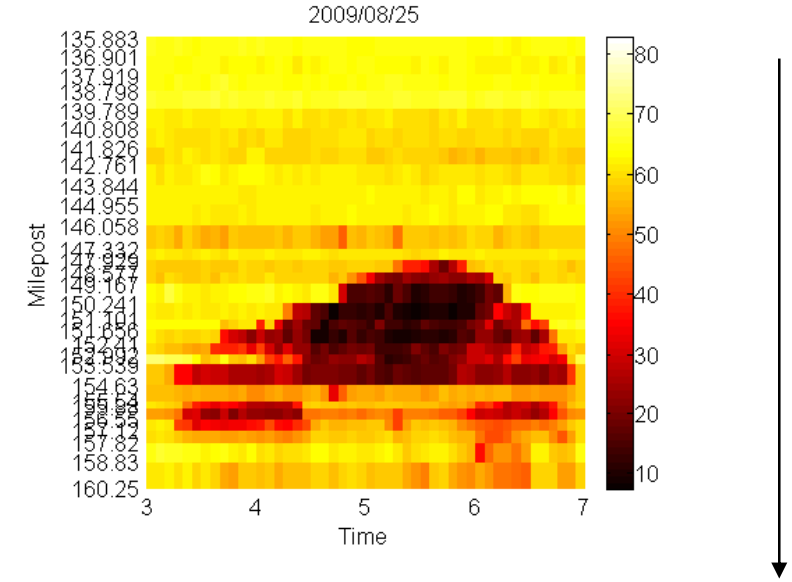

(a)

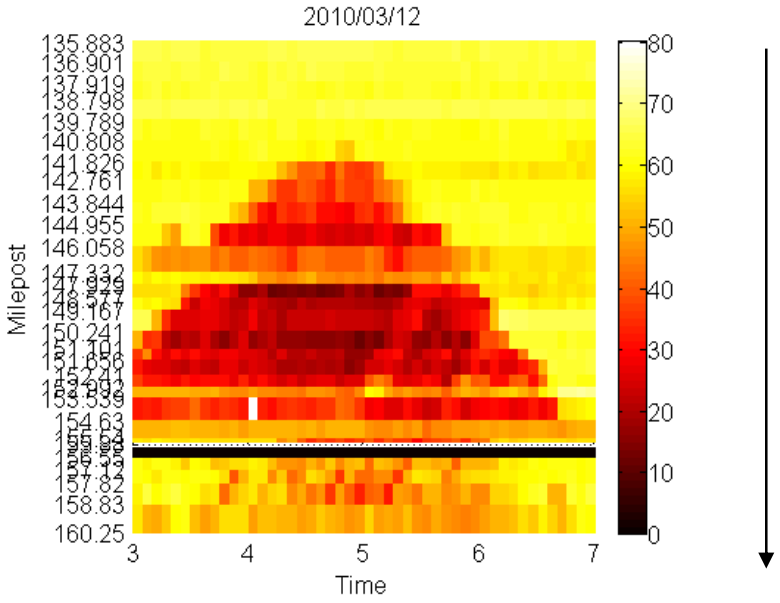

(b)

Figure 15. (a) Speed contour for the day with recurrent congestion on I-10 EB. (p.m. peak) (b) Speed contour for the day with non-recurrent congestion on I-10 EB. (p.m. peak)

Evaluation of regional analysis

Bottleneck mechanism is studied in detail based on the WT technique described in Chapter 3 using 20-second data for the I-10 eastbound bottleneck between S. 53rd St. and W. Southern Ave. The period of analysis is from July 2008 to March 2009. The selected site is a weaving bottleneck due to a busy on-ramp from W. Broadway Rd. with an average flow of 1,454 vph during congestion and a major exit to US-60 eastbound with an average flow of 5,205 vph during congestion; see Figure 16 for the schematic of the site. The analysis results are shown in Table 1. Bottleneck activation times are fairly consistent, varying from 14:31 p.m. to 14:51 p.m. However, bottleneck de-activation times varied to a larger degree from 16:38 p.m. to 18:48 p.m. The pre-congestion flow ranged from 10,616 to as high as 12,442 vph, whereas the average flow during congestion varied from 9,746 to 10,765 vph. As a result, the capacity drop varied from 3 to 17 percent.

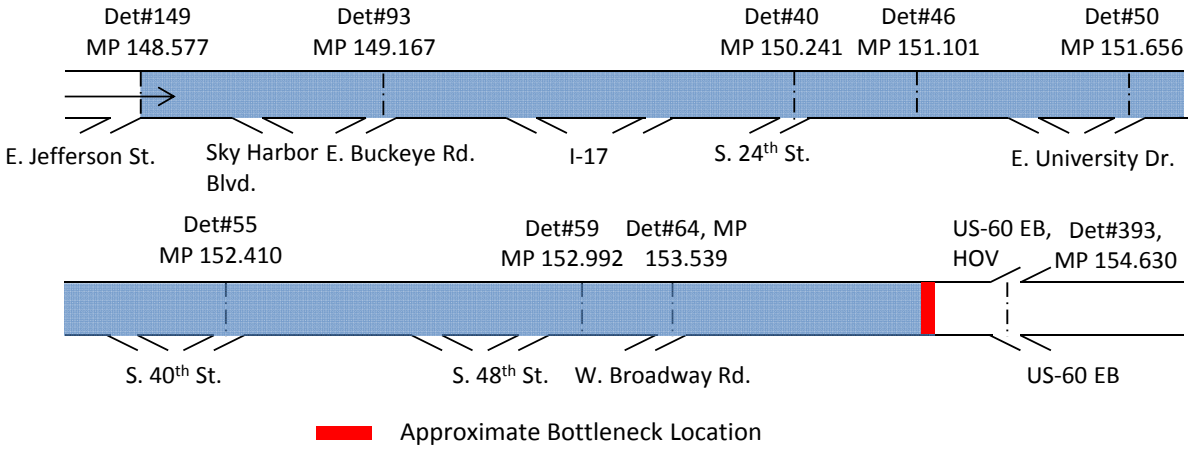

Figure 16. Schematic of I-10 eastbound bottleneck

We further analyzed the same bottleneck for the same period based on the simple method using 5-minute data which has been described in detail in Chapter 3.1 and compared the results

with those based on the wavelet analysis to evaluate the results from the regional-level analysis. More specifically, the pre-congestion flow was measured by taking the maximum 5-minute flow within 30 minutes prior to the bottleneck activation. The bottleneck discharge rate during congestion was measured by taking the average of all 5-minute flows during congestion. Reasonably close results would justify the implementation of the simpler analysis in favor of efficiency. The results based on the regional analysis are shown in Table 2. It is notable that the ranges of the reported values are fairly close to those in Table 1, although some daily differences are apparent.

Table 3 and Figure 17 present the summary of the comparison result. The average bottleneck activation and de-activation times are fairly comparable between the two methods, especially given the difference in the data resolution (5 minutes vs. 20-second). The average values of both pre-congestion and congestion flows are slightly higher in the wavelet analysis than in the simple analysis;. Finally, there is little difference in the average capacity drop (~11 percent) between the two methods. In summary, the results obtained from the two methods are similar on average, which justifies the use of the simple method for the regional analysis. However there is a systematic underestimation of pre-queue flow and discharge rate with the simple method underlying the importance WT based analysis for detailed analysis. The regional analysis underestimates both the pre-activation flow and average congestion flow by around 3%.

Table 1.

Results: bottleneck analysis using wavelet analysis.

Date	BN activation time	BN deactivation time	Pre-activation flow (vph)	Average congestion flow (vph)	Capacity drop (percent)
6/3/2008	14:45:27	18:09:45	11,435	10,516	8.04
6/4/2008	14:40:47	18:26:25	12,127	10,321	14.89
6/6/2008	14:39:47	17:47:05	11,859	10,358	12.65
6/11/2008	14:39:34	18:13:14	10,894	10,360	4.9
7/9/2008	14:44:18	18:21:56	10,616	10,345	2.55
7/11/2008	14:42:58	17:33:56	11,904	10,174	14.54
7/30/2008	14:42:58	18:26:35	11,564	10,055	13.05
8/6/2008	14:43:38	18:34:15	11,945	9,872	17.35
8/8/2008	14:30:38	17:47:16	11,432	10,128	11.41
8/13/2008	14:44:58	18:23:36	11,798	10,416	11.71
8/29/2008	14:42:45	17:13:45	11,307	10,541	6.77
9/3/2008	14:40:18	18:39:35	12,442	10,456	15.96
9/15/2008	14:46:36	17:45:36	11,315	10,743	5.05
9/16/2008	14:45:56	18:35:56	11,618	10,419	10.33
9/19/2008	14:45:09	17:18:07	11,589	10,578	8.72
10/6/2008	14:48:09	18:22:47	11,697	10,410	11
10/8/2008	14:48:09	18:21:07	12,172	10,399	14.57
10/9/2008	14:48:49	18:14:07	11,549	10,609	8.14
10/20/2008	14:50:16	17:54:36	12,090	10,526	12.94
11/3/2008	14:43:49	17:19:07	11,784	10,722	9.01
11/4/2008	14:40:49	18:14:27	11,754	10,505	10.63
11/10/2008	14:45:49	17:19:47	11,422	10,656	6.71
11/12/2008	14:40:29	16:37:48	11,988	10,765	10.2
11/20/2008	14:42:20	18:00:18	11,557	10,193	11.8
11/24/2008	14:45:27	17:30:27	11,876	10,619	10.59
12/3/2008	14:50:47	17:33:47	11,737	10,406	11.35
12/15/2008	14:44:00	18:39:17	10,976	9,746	11.21
12/17/2008	14:39:40	18:39:17	11,465	10,287	10.28
1/5/2009	14:44:00	18:21:37	11,940	10,656	10.76
1/7/2009	14:44:40	18:47:37	12,098	10,230	15.44
1/8/2009	14:48:20	18:37:37	11,436	10,205	10.76
1/13/2009	14:42:40	18:42:17	11,537	10,043	12.94
1/23/2009	14:46:00	18:28:37	12,220	10,376	15.1

Table 2.

Results: bottleneck analysis using regional analysis.

Date	BN activation time	BN deactivation time	Pre-activation flow (vph)	Average congestion flow (vph)	Capacity drop (percent)
6/3/2008	14:35:00	18:10:00	10,488	10,363	1.19
6/4/2008	14:35:00	18:25:00	10,920	10,210	6.5
6/6/2008	14:40:00	17:50:00	11,784	10,194	13.5
6/11/2008	14:35:00	18:05:00	10,824	10,240	5.4
7/9/2008	14:35:00	18:15:00	10,344	10,264	0.77
7/11/2008	15:10:00	17:50:00	10,812	10,066	6.9
7/30/2008	15:10:00	18:35:00	11,772	9,917	15.76
8/6/2008	15:05:00	18:40:00	12,060	9,643	20.04
8/8/2008	14:40:00	17:55:00	10,812	9,987	7.63
8/13/2008	15:15:00	18:25:00	11,100	10,230	7.83
8/29/2008	14:40:00	17:15:00	11,028	10,457	5.18
9/3/2008	15:40:00	18:40:00	11,304	10,233	9.48
9/15/2008	15:10:00	18:05:00	11,124	10,578	4.91
9/16/2008	14:40:00	18:35:00	11,832	10,270	13.2
9/19/2008	15:10:00	18:00:00	11,388	10,246	10.03
10/6/2008	15:35:00	18:15:00	11,148	10,246	8.09
10/8/2008	15:10:00	18:40:00	11,928	10,019	16
10/9/2008	15:10:00	18:25:00	11,556	9,993	13.53
10/20/2008	15:15:00	18:40:00	11,964	10,131	15.32
11/3/2008	15:10:00	18:30:00	11,208	10,288	8.21
11/4/2008	14:35:00	18:30:00	11,436	10,225	10.59
11/10/2008	15:15:00	18:05:00	10,872	10,324	5.04
11/12/2008	14:55:00	19:00:00	11,880	9,659	18.69
11/20/2008	15:00:00	19:00:00	11,652	9,456	18.85
11/24/2008	15:05:00	18:35:00	11,616	10,222	12
12/3/2008	14:45:00	19:00:00	11,820	9,577	18.98
12/15/2008	14:40:00	18:45:00	11,028	9,331	15.39
12/17/2008	14:40:00	18:45:00	11,532	9,941	13.8
1/5/2009	15:10:00	18:30:00	12,780	10,482	17.98
1/7/2009	15:10:00	18:45:00	11,664	10,079	13.59
1/8/2009	15:10:00	18:50:00	11,520	10,038	12.86
1/13/2009	14:40:00	18:50:00	11,400	9,896	13.19
1/23/2009	14:35:00	18:35:00	10,896	10,234	6.08

Table 3.

Comparison of wavelet analysis and simpler analysis.

	Wavelet analysis	**Simpler analysis**
No. of days	33	33
Data resolution	20-second data	5-min data
Average BN activation time	2:43:56 p.m.	2:57:35 p.m.
Average BN de-activation time	6:05:30 p.m.	6:26:13 p.m.
Average pre-congestion flow (VPH)	11671	11379
Average congestion flow (VPH)	10383	10092
Average capacity drop (percent)	10.95	11.11

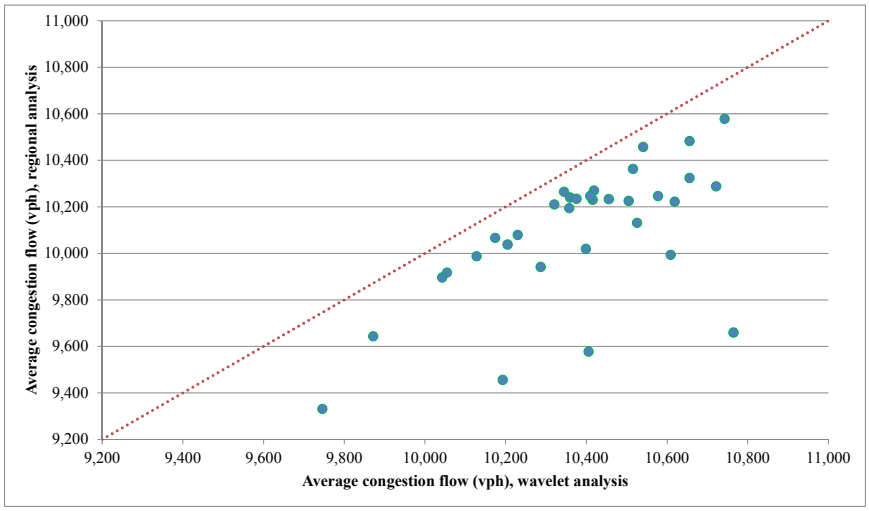

(a)

Figure 17. Comparison of wavelet and regional analysis (a) average congestion flow (b) pre-activation flow

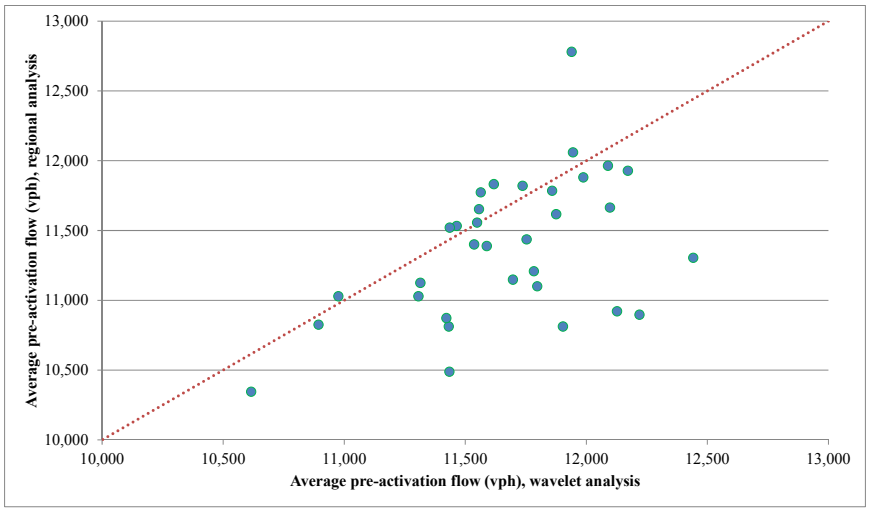

(b)

Figure 17(contd.). Comparison of wavelet and regional analysis (a) average congestion flow (b) pre-activation flow

Regional bottleneck analysis

In this study, 23 bottlenecks that recurred during morning and evening peak hours were identified. Of these 23 recurrent bottlenecks 13 bottlenecks were selected based on the selection criteria discussed in the Chapter 4.2. These bottlenecks were attributed to a variety of factors, such as merging at busy on-ramps or freeway-to-freeway connectors, weaving due to busy merges followed by busy diverges (especially near major freeway-to-freeway interchanges), and curves. Tables 4 and 5 show the recurrent bottlenecks identified during a.m. and p.m. peak hours in the Phoenix metropolitan region.

Table 4.

Recurrent congestion identified during a.m. peak hours (6 - 10 a.m.).

ID	Route	Bottleneck location	No of days observed (out of 131 weekdays)	Bottleneck discharge rate
A1	I-10 EB	MP:146.058-147.332, b/w N.9th St. & 19th St.	90	Estimated
A2-1	I-10 WB	MP: 154.89-154.259, b/w Meadowclark Cir. & W. Alameda Dr.	44	Measured
A2-2	I-10 WB	MP: 152.248-151.473, b/w S. 32nd St. & S. 31st St.	68	Estimated
A2-3	I-10 WB	MP: 155.54-154.89, b/w W. Donner Dr. & Meadowclark Cir.	29	Measured
A3	I-17 SB	MP: 204.71-203.7, b/w W. Solano Dr. & W. Elm Dr.	42	Estimated
A4-1	L-101 NB	MP: 58.34-57.46, b/w W. Palomino Dr. & W. Newton Ct.	11	Not measured or estimated
A4-2	L-101 NB	MP: 57.46-55.88, b/w E. Newton Ct. & E. Watson Dr.	63	Not measured or estimated
A5-1	L-202 WB	MP: 7.509-6.299, b/w E. Newton Ct. & E. Watson Dr.	78	Estimated
A5-2	L-202 WB	d/s of 0.578, d/s of N.22 St.	58	Not measured or estimated
A6-1	SR-51 SB	MP: 6.16-5.48, b/w E. Northern Ave. & E. Lamar Rd.	33	Estimated
A6-2	SR-51 SB	MP: 2.53-1.32, b/w E. Amelia Ave. & E. Virginia Ave.	56	Estimated
A7	US-60 WB	d/s of 172.37, d/s of S. Albert Ave.	63	Not measured or estimated

Table 5.

Recurrent congestion identified during p.m. peak hours (3 - 7 p.m.).

ID	Route	Bottleneck location	No of days observed (out of 131 weekdays)	Bottleneck discharge rate
P1-1	I-10 EB	MP: 153.539-154.63, b/w S. 53rd St. & W. Southern Ave.	87	Estimated
P1-2	I-10 EB	d/s of MP:160.25, d/s of E. Gold Poppy Way	84	Not measured or estimated
P2	I-10 WB	MP:140.524-139.524, b/w N. 44th Ave. & N. 52nd Ave.	50	Estimated
P3	I-17 NB	d/s of MP: 208.69, d/s of W. Beryl Ave.	70	Not measured or estimated
P4-1	L-101 SB	MP: 53.784-54.49, b/w E. Golf Ave. & US-60	38	Estimated
P4-2	L-101 SB	MP: 56.08-56.8, b/w E. Pegasus Dr. & E. Tempe Water Trmt.Drwy	68	Estimated
P5	L-202 WB	d/s of MP: 0.579, d/s of N. 22nd St.	57	Not measured or estimated
P6-1	SR-51 NB	MP: 2.71-3.97, b/w E. Devonshire Ave. & E. Georgia Ave.	21	Estimated
P6-2	SR-51 NB	MP: 4.82-5.8, b/w E. Keim Dr. & E. Aurelius Ave.	41	Could not be analyzed
P6-3	SR-51 NB	MP:1.79-2.71, b/w E. Avalon Dr. & E. Devonshire Dr.	43	Not measured or estimated
P7	US-60 EB	MP:172.65-175.45, b/w S. Shafer Dr. & S. Kachina Dr.	90	Not measured or estimated

The following performance measures are reported in these sections for each recurrent congestion location identified in Tables 4 and 5:

- Duration of congestion (minutes)
- Length of congestion (miles)
- VMT (for the entire detector coverage area during the peak hour)
- VHT (for the entire detector coverage area during the peak hour)
- If bottleneck discharge rates can be measured directly or estimated (Chapter 3, Figure 4)

- Bottleneck discharge rates and speeds before and during congestion
- Amount and percentage of a reduction in bottleneck discharge rate during congestion

- If bottleneck discharge rates cannot be measured (Chapter 3, Figure 5)
  - Flows and speeds before and during congestion at the nearest detector station upstream of a bottleneck

Note that VMT and VHT for each freeway are computed using the following equations.

$$VMT = \sum_{i=1}^{n} c_i L_I \qquad (9)$$

$$VHT = \sum_{i=1}^{n} c_i \frac{L_i}{v_i} \qquad (10)$$

where n represents the total number of detector stations on a freeway; c_i represents vehicle counts (for all lanes) at detector station i; L_i represents the length of station i's influence area; and v_i represents time-mean speed across all lanes, where v_i is given by

$$v_i = \frac{1}{m} \sum_{k=1}^{m} v_k \qquad (11)$$

where m is the number of vehicles k passing the station's influence area. The influence area of a detector station is defined as the area bounded by the midpoints to neighboring detector stations. We assumed that traffic conditions measured from a detector station were representative of conditions within its influence area.

The results of the regional analysis have been tabulated in Table 6.

Conclusion

The objective of this chapter is to apply the regional methodology which was described in detail in the previous chapter to both identify and analyze freeway bottlenecks in a region. The Phoenix metropolitan region has been chosen as the case study site. To this end, all Interstates, US Routes and State Routes with available detector data were analyzed. Recurrent bottleneck locations were identified based on several criteria including congestion pattern, sensor coverage, data quality and (absence of) incident/construction activities.

Bottleneck features were studied by measuring bottleneck activation and de-activation times, pre-congestion and congestion flows, and capacity drop. For a select bottleneck (the bottleneck on I-10 eastbound between S. 53rd St. and W. Southern Ave.), two methods were employed: a sophisticated method based on wavelet transform (WT) on 20-second data to improve precision and accuracy (at the expense of efficiency) and a simple, automated method using 5-minute data to improve efficiency (at the expense of precision and accuracy). The WT-based method was employed to de-noise the detector data and identify key event times such as the times of congestion onset and change in near steady state flow. With the simpler method, congestion was defined as speed below 45 mph, and 5-minute data were used instead of identifying times of flow change. It was found that the two methods generated comparable results, justifying the use of the simpler method for efficiency without much loss of accuracy.

Based on the above finding, the regional analysis was conducted using the simple method. Throughout the Phoenix region, 23 recurrent bottlenecks were identified: 12 during a.m. peak hours and 11 during p.m. peak hours. Of these 23 recurrent bottlenecks, 13 bottlenecks were selected for bottleneck performance analysis based on the selection criteria discussed in Chapter 4.2. Most of these bottlenecks were attributed to heavy merging and weaving. For these

bottlenecks, a number of performance measures were obtained, such as the duration of congestion, length of the congestion, VMT, VHT, and bottleneck discharge rate (where it can be measured or estimated). Bottleneck discharge rates were measured directly at 2 locations and estimated (using ramp counts) at 11 locations. Due to the limited sensor coverage, the bottleneck discharge rate could not be measured or estimated for the other 10 bottlenecks. Although these bottlenecks did not meet our selection criteria, congestion flows at the nearest detector station upstream of the bottleneck were provided instead along with other performance measures. The identified bottlenecks were ranked according to the capacity drop in terms of flow and percent reduction in flow.

Table 6.

Regional Bottleneck Analysis.

ID	Route	Bottleneck Throughput	Duration		Pre-Congestion Flow (vph)		Congestion Flow (vph)		Pre-Congestion Speed (mph)		Congestion Speed (mph)		VMT		VHT		Throughput Reduction (vph)		Throughput Reduction (%)	
			Avg.	Std. Er	Avg.	Std. Er	Avg.	Std. Er	Avg.	Std. Er	Avg.	Std. Er	Avg.	Std. Er	Avg.	Std. Er	Avg.	Rank	Avg.	Rank
A6-1	SR-51 SB	Estimated	75	7.9	7,408	110	5,243	87	55.4	0.5	37.4	0.7	34,375,437	177,829	603,572	6,274	2,165	1	29	1
P6-1	SR-51 NB	Estimated	51.9	13	5,576	2,58	4,235	115	55.1	1	40.7	1.5	39,339,935	147,873	690,879	5,180	1,341	3	22.6	2
P4-1	L-101 SB	Estimated	58.1	8.2	6,092	58	4,949	99	53.1	0.6	41.7	0.8	33,775,670	151,346	657,237	7,164	1,143	5	18.7	3
A5-1	L-202 WB	Estimated	79	5.5	8,626	84	7,020	96	57.9	0.4	33.4	0.8	24,878,825	139,754	484,773	139,754	1,606	2	18.3	4
P2	I-10 WB	Estimated	42	7.1	7,552	57	6,255	95	51.1	0.2	43.9	0.5	73,489,534	513,806	1,452,809	21,675	1,297	7	17.2	5
A3	I-17 SB	Estimated	56.1	11.8	6,425	61	5,489	181	53.6	0.6	39.1	2.2	50,392,274	554,915	950,944	14,602	936	8	14.35	6
A6-2	SR-51 SB	Estimated	41.2	4.1	6,481	37	5,575	54	53.4	0.5	42.6	0.5	34,000,156	164,930	595,230	4,706	906	9	13.9	7
P1-1	I-10 EB	Estimated	199.7	6.8	9,879	94	8,585	65	55.5	0.2	26.8	0.4	70,473,368	222,796	1,436,327	16,292	1,294	4	12.7	8
A2-3	I-10 WB	Measured	102.5	13.4	5,970	132	5,207	47	55.7	1	32.7	2.1	69,863,756	450,179	1,271,750	16,233	763	11	12.5	9
A2-1	I-10 WB	Measured	76.7	17.3	10,102	614	8,978	598	55.6	0.62	53	1.7	69,372,600	302,863	1,267,157	9,867	1,124	6	11.4	10
A2-2	I-10 WB	Estimated	36.8	5.2	8,476	157	7,682	149	55.9	0.7	41.3	0.6	69,167,739	261,007	1,313,970	6,261	794	10	9.2	11
P4-2	L-101 SB	Estimated	88.6	9.7	7,954	210	7,357	198	54.2	0.3	39.8	0.5	35,455,844	292,748	688,506	6,139	597	12	7.4	12
A1	I-10 EB	Measured	75.9	9.4	8,060	73	7,521	75	51.9	0.6	42.5	0.9	71,614,838	318,683	1,323,225	10,718	539	13	6.6	13
A4-1	L-101 NB	Not Measured/Estimated	42	19.8	5,139	752	4,565	557	55.6	2.1	34.5	2.6	28,578,411	2,409,458	526,931	48,591	-	-	-	-
A4-2	L-101 NB	Not Measured/Estimated	75.6	10.7	7,408	282	6,149	224	60.1	1.4	40.9	1.2	29,109,817	543,106	572,006	17,783	-	-	-	-
A5-2	L-202 WB	Not Measured/Estimated	78.4	9.9	3,681	96	3,009	98	54.2	0.5	34	0.9	24,513,529	147,284	483,484	5,012	-	-	-	-
A7	US-60 WB	Not Measured/Estimated	85	6.9	8,307	172	7,806	243	59.9	0.1	57.5	1.2	63,228,196	347,320	1,090,158	7,223	-	-	-	-
P1-2	I-10 EB	Not Measured/Estimated	72.2	12.5	5,547	111	4,958	132	63.6	1.6	61.1	2.4	70,841,250	368,658	1,488,668	28,302	-	-	-	-
P3	I-17NB	Not Measured/Estimated	94.4	5.8	6,738	43	6,027	42	51.7	0.4	38.2	0.6	53,505,566	202,553	1,123,729	11,711	-	-	-	-
P5	L-202 WB	Not Measured/Estimated	199.2	59.5	2,994	164	1,764	309	48.1	6.1	22	4.1	17,648,365	201,591	373,842	11,459	-	-	-	-
P6-3	SR-51 NB	Not Measured/Estimated	82.7	7.1	5,850	43	4,453	115	58.2	0.4	33.7	0.8	38,937,417	176,943	641,916	5,311	-	-	-	-
P7	US-60 EB	Not Measured/Estimated	150.2	8.4	6,254	44	4,435	61	55.8	0.3	19.2	0.9	62,068,837	506,735	1,122,827	9,919	-	-	-	-

CHAPTER 5

FREEWAY WEAVING BOTTLENECK: BOTTLENECK FEATIRES AND THE SMOOTHING EFFECT OF THE HOV LANE

This study analyzed the characteristics of a freeway weave bottleneck with a HOV lane. Previous studies suggested that lane-changes, induced by merging and diverging flows, diminish the bottleneck discharge rate and that the activation of a HOV lane can remedy this impact by discouraging disruptive lane-changes. These previous studies primarily analyzed the smoothing effect on merge and curve bottlenecks. The present study corroborates the existence of smoothing effect on a weave bottleneck. Most previous studies on bottlenecks analyze few days of data, neglect steady-state periods, or fall short of characterizing steady-state periods in a systematic, reproducible manner.

In this study 33 days of data had been analyzed using a spectral analysis tool called wavelet transform to systematically de-noise the raw data, unveil underlying trends, and identify times of queue onset and steady-state periods. From this study we found that: (i) a higher (lower) flow can be sustained prior to traffic breakdown with higher diverging (merging) flow, suggesting that ramp-to-freeway maneuvers are more disruptive; (ii) higher bottleneck discharge rates are attained with higher diverging flow and lower utilization of HOV lane. The latter indicates that a smoothing effect exists around a weave bottleneck; and importantly, the smoothing effect was more significant than the effect of diverging flow. By knowing the bottleneck mechanism it would enable one to fine tune current traffic controls to improve the bottleneck discharge rate on the freeways.

Data obtained near a freeway weave bottleneck show that the bottleneck discharge rate diminished by 3-22% upon queue formations. The discharge rate, however, recovered upon the

high-occupancy-vehicle (HOV) lane activation, confirming the existence of the "smoothing effect." The recovery was substantial; the discharge rate improved by 4% and occasionally exceeded the maximum pre-queue flow. The smoothing effect persisted for about 1.5 hours and waned thereafter as the relative utilization of the HOV lane gradually recovered. A statistical analysis corroborates that the HOV lane flow distribution significantly (and negatively) affects the bottleneck discharge rate, more so than the amount of diverging flow.

Site and data

The selected study site is an eastbound section of Interstate 10, located between Broadway Rd. and eastbound US 60 in the Phoenix metropolitan area; see Figure 18(a). This section of freeway is approximately one mile long and has five regular-use lanes that split into three exit lanes (to US 60) and three continuing lanes. The site also contains a HOV lane that splits into an exit lane (to US 60) and a continuing lane. Two or more passengers are required for the vehicles traveling in the HOV lane during peak hours (6-9 a.m. and 3-7 p.m.). Note that with the dedicated HOV exit lane to US 60, we expect very few lane-changes from the HOV lane to the exit lanes. A recurrent bottleneck (Figure 18(b)) resides in this freeway section presumably due to heavy weaving maneuvers induced by high merging flows from the Broadway Rd. on-ramp (>1,400 veh/hr during peak hours) and high diverging flows to US 60 (>3,500 veh/hr during peak hours), often resulting in queues exceeding 5 miles. A typical speed contour is shown in Figure 18(c).

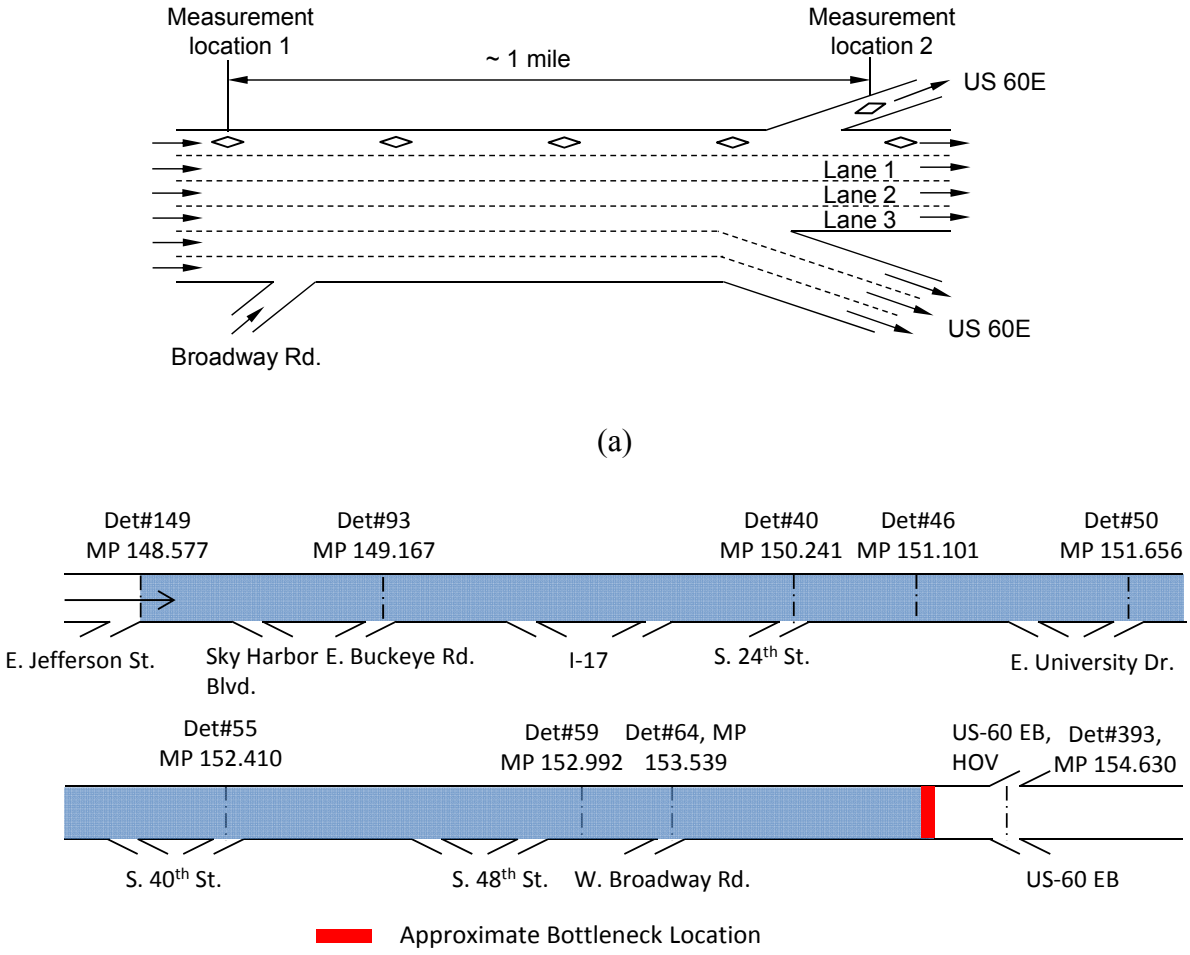

Figure 18. (a) Schematic of the study site at I-10 EB, Phoenix, AZ (b) Location of recurrent bottleneck on I-10 EB, Phoenix AZ (c) Typical speed contour of recurrent congestion (I-10 EB)

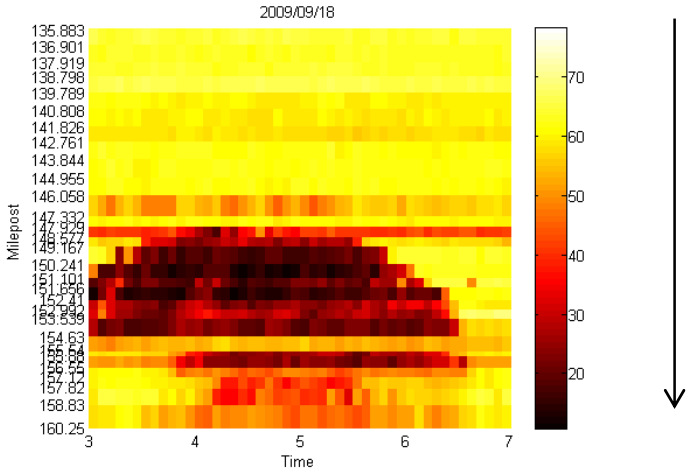

(c)

Figure 18 (contd.). (a) Schematic of the study site at I-10 EB, Phoenix, AZ (b) Location of recurrent bottleneck on I-10 EB, Phoenix AZ (c) Typical speed contour of recurrent congestion (I-10 EB)

Data come from two measurement locations, as labeled in Figure 1, and consist of vehicle count, occupancy (dimensionless measure of density) and time-mean speed aggregated over 20-second intervals. Data from 33 days between July 2008 and February 2009 were analyzed when the study section was free of reported incidents and adverse weather conditions, and was an active bottleneck; i.e., traffic was freely flowing at the downstream measurement location (location 2 in the figure) whereas it was congested at the upstream location (location 1). On these days, queues consistently formed around 2:40 p.m. and persisted for at least three hours. Bottleneck discharge flows and off-ramp flows were taken at measurement location 2, and on-ramp flows were taken at measurement location 1.

Bottleneck activation and discharge rate

In this research, the wavelet transform (WT) is used to de-noise the raw data, precisely identify bottleneck activation and deactivation times, and measure pre-congestion and congestion flows. These events are typically marked by sharp changes in speed and/or flow, which can be detected effectively by WT. Please note that some text in this section is a repetition from Chapter 3 but has been included here for the convenience of the readers.

Using the de-noised data (obtained from DWT analysis described in Chapter 3), the characteristics of bottlenecks are analyzed. We first identify the times of onset and clearance of queue using the speed data obtained from measurement location 1 (immediately upstream of the bottleneck). These times are identified in a systematic manner using CWT and used later to estimate the times at the downstream measurement location. Among several mother wavelet functions, the Mexican Hat wavelet is adopted based on the previous finding that it is effective in analyzing traffic data (Zheng et al. 2011). The Mexican Hat wavelet function is the negative normalized second derivative of the Gaussian function and is represented by

$$\varphi(t) = \frac{2}{\sqrt{3\sigma}\pi^{1/4}} \left(1 - \frac{t^2}{\sigma^2}\right) e^{\frac{-t^2}{2\sigma^2}} \qquad (12)$$

Based on its shape, the Mexican Hat wavelet generates peaks and dips whenever there are changes in the signal. In this research, absolute values of wavelet coefficients are used so that changes in speed or flow correspond to peaks. As shown in Figure 19(a), the onset of congestion marked by a sharp decrease in speed corresponds to a peak in the (absolute value of) wavelet coefficients. Note that there is another pronounced peak immediately after the onset of congestion. This marks the end of transition to the congested regime. Similarly, the clearance of congestion marked by a recovery in speed also corresponds to a peak. The peak prior to the

clearance represents the start of transition to the free-flow regime. For this example, the start and the end of congestion are identified to be at 14:42:40 p.m. and 18:52:17 p.m., respectively. The same technique is used on flow data to identify the periods of near-steady traffic states, in which the flows remain nearly constant (i.e., the periods between two neighboring peaks in wavelet coefficients); see Figure 19(b). Specifically, we identify the near steady-state period immediately before the onset of congestion to measure the pre-congestion congestion flow (to be used in computing the capacity drop).

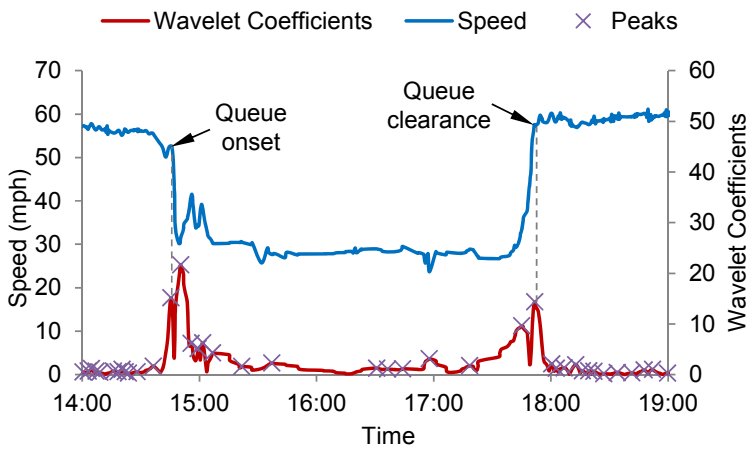

(a)

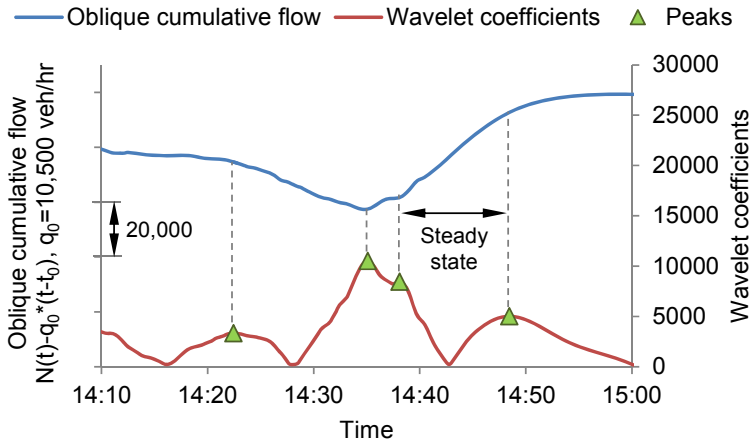

(b)

Figure 19. (a) Times of queue onset and clearance based on continuous wavelet transform; (b) Near-steady state periods based on continuous wavelet transform (06/06/2008).

However, bottleneck de-activation times varied to a larger degree from 16:38 p.m. to 18:48 p.m. The pre-congestion flow ranged from 10,616 to as high as 12,442 vph, whereas the average flow during congestion varied from 9,746 to 10,765 vph. As a result, the capacity drop varied from 3 to 17 percent as shown in Table 7.

Table 7.

Results: bottleneck analysis using wavelet analysis.

Date	BN activation time	BN deactivation time	Pre-activation flow (vph)	Average congestion flow (vph)	Capacity drop (percent)
6/3/2008	14:45:27	18:09:45	11,435	10,516	8.04
6/4/2008	14:40:47	18:26:25	12,127	10,321	14.89
6/6/2008	14:39:47	17:47:05	11,859	10,358	12.65
6/11/2008	14:39:34	18:13:14	10,894	10,360	4.9
7/9/2008	14:44:18	18:21:56	10,616	10,345	2.55
7/11/2008	14:42:58	17:33:56	11,904	10,174	14.54
7/30/2008	14:42:58	18:26:35	11,564	10,055	13.05
8/6/2008	14:43:38	18:34:15	11,945	9,872	17.35
8/8/2008	14:30:38	17:47:16	11,432	10,128	11.41
8/13/2008	14:44:58	18:23:36	11,798	10,416	11.71
8/29/2008	14:42:45	17:13:45	11,307	10,541	6.77
9/3/2008	14:40:18	18:39:35	12,442	10,456	15.96
9/15/2008	14:46:36	17:45:36	11,315	10,743	5.05
9/16/2008	14:45:56	18:35:56	11,618	10,419	10.33
9/19/2008	14:45:09	17:18:07	11,589	10,578	8.72
10/6/2008	14:48:09	18:22:47	11,697	10,410	11
10/8/2008	14:48:09	18:21:07	12,172	10,399	14.57
10/9/2008	14:48:49	18:14:07	11,549	10,609	8.14
10/20/2008	14:50:16	17:54:36	12,090	10,526	12.94
11/3/2008	14:43:49	17:19:07	11,784	10,722	9.01
11/4/2008	14:40:49	18:14:27	11,754	10,505	10.63
11/10/2008	14:45:49	17:19:47	11,422	10,656	6.71
11/12/2008	14:40:29	16:37:48	11,988	10,765	10.2
11/20/2008	14:42:20	18:00:18	11,557	10,193	11.8
11/24/2008	14:45:27	17:30:27	11,876	10,619	10.59
12/3/2008	14:50:47	17:33:47	11,737	10,406	11.35
12/15/2008	14:44:00	18:39:17	10,976	9,746	11.21
12/17/2008	14:39:40	18:39:17	11,465	10,287	10.28
1/5/2009	14:44:00	18:21:37	11,940	10,656	10.76
1/7/2009	14:44:40	18:47:37	12,098	10,230	15.44
1/8/2009	14:48:20	18:37:37	11,436	10,205	10.76
1/13/2009	14:42:40	18:42:17	11,537	10,043	12.94
1/23/2009	14:46:00	18:28:37	12,220	10,376	15.1

The same technique is used on flow data to identify the periods of near-steady traffic states, in which the flows remain nearly constant; see Figure 19(b) for an example. In the figure, the top curve is the oblique cumulative count curve constructed by taking cumulative vehicle

counts and subtracting background reductions of $q_0 \times (t - t_0)$ to better reveal changes in flow (i.e., slope) (Munoz and Daganzo, 2002), where $q_0(t)$ is the background flow and $(t - t_0)$ is the elapsed time since reference time t_0. The bottom curve represents the wavelet coefficients. It is clear that the peaks in wavelet coefficients correspond to the times of significant changes in flow; therefore, the period between two neighboring peaks is identified as a near-steady state.

On each study day, a surge in freeway flow, accompanied by surges in on-ramp and off-ramp flows preceded the onset of queue; see Figure 20 for an example. Specifically, queues consistently formed on the study days when the on-ramp and off-ramp flows exceeded 1,300 veh/hr and 2,600 veh/hr respectively. Thus, the evidence suggests that weaving activities induced by merging and diverging flows instigated queue formations at this site. Thereafter the bottleneck discharge rate diminished by nearly 3-22% immediately after the onset (referred to as the "immediate" reduction in bottleneck discharge rate). The discharge flow partly recovered but largely remained lower than the flow prior to the onset. (Based on this property, the time of flow drop is taken as the time of queue onset at the downstream measurement location.) The overall amount of reduction is measured by taking the difference between the steady-state flow immediately prior to the onset (referred to as the pre-queue flow hereafter) and the average flow during congestion.

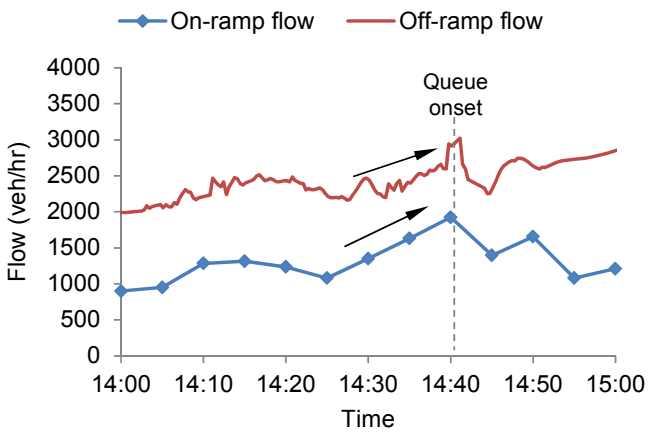

Figure 20. Surges in on-ramp and off-ramp flows around the onset of queue.

Table 8 presents the basic statistics for the times of onset and clearance of queue, pre-queue flow, the overall reduction in bottleneck discharge rate, and the immediate reduction in bottleneck discharge rate over the 33 days analyzed. The times of onset of queue are fairly consistent, varying only from 14:30 to 14:51. However, times of queue clearance vary to a larger degree from 16:37 to 18:47. The average pre-queue flow and bottleneck discharge rate are respectively 11,671 veh/hr and 10,383 veh/hr, resulting in the average reduction of 10.95%. The immediate reduction is larger than the overall reduction at 13.54%.

Table 8.

Statistics of bottleneck capacity drop using wavelet analysis.

	Average (standard error)
No. of days	33
Time of onset of queue	14:30 – 14:51
Time of clearance of queue	16:37 – 18:47
Pre-queue flow (veh/hr)	11,671 (393)
Bottleneck discharge rate (veh/hr)	10,383 (242)
Reduction in bottleneck discharge rate (veh/hr)	1,288 (74)
Reduction in bottleneck discharge rate (%)	10.95 (4)
Immediate reduction in bottleneck discharge rate (veh/hr)	1,592 (99)
Immediate reduction in bottleneck discharge rate (%)	13.54 (5)

Variation in bottleneck discharge rate reduction

We further find that the percent reduction of overall bottleneck discharge rate varies from 3 to 17%, and the immediate reduction from 3 to 22%. Based on the result in Table 7, the variations in the percent reduction are attributable to variations in both pre-queue flow and bottleneck discharge rate after the queue formations. In this section, we examine the variations in pre-queue flow, the maximum flow sustained prior to traffic breakdown, and bottleneck discharge rate during congestion.

Variations in pre-queue flow. The variations in pre-queue flow, the maximum flow sustained prior to traffic breakdown, are analyzed with respect to merging and diverging flows. The motivation for choosing these explanatory variables stems from the earlier findings that lane-changes due to merging and weaving can instigate queue formations (Yeon et al., 2007; Rudjanakanoknad and Akaravorakulchai, 2011) but that freeway-to-ramp maneuvers to exit the freeway may have a different impact than ramp-to-freeway maneuvers (Rudjanakanoknad and Akaravorakulchai, 2011). Indeed Figure 6 shows that the pre-queue flow is positively related to

the diverging flow (Figure 21(a)), whereas it is negatively related to the merging flow (Figure 21(b)). The latter relationship is not as clear, and a multiple regression analysis verifies that the merging flow is not statistically significant at the 95% confidence level. This is attributable to (i) the low resolution of the on-ramp data (5 minutes) and/or (ii) disproportionately large diverging flow, which may have a dominant influence. Nevertheless, the result suggests that ramp-to-freeway lane-changes may have a more disruptive effect in traffic flow than freeway-to-ramp maneuvers. This finding is also consistent with the finding of Rudjanakanoknad and Akaravorakulchai (2011).

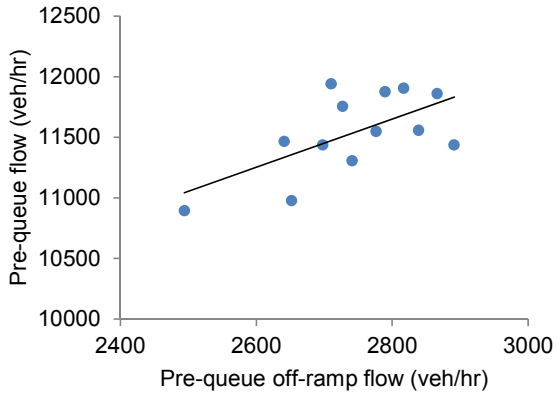

(a)

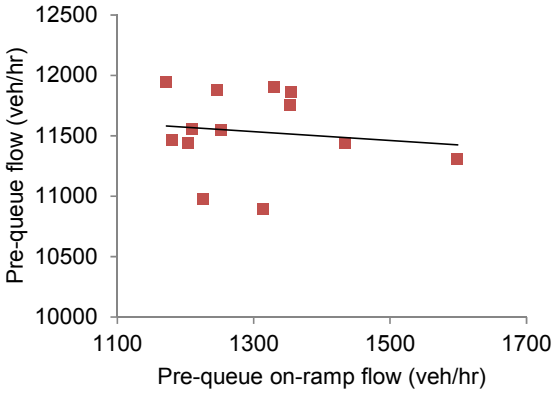

(b)

Figure 21. (a) Pre-queue flow vs. pre-queue off-ramp flow; (b) Pre-queue flow vs. pre-queue on-ramp flow.

Variations in bottleneck discharge rate. We now present the variations in bottleneck discharge rate during congestion. Figure 22(a) shows the total flow across all lanes and the flow in the HOV lane over 5-minute intervals on 10/28/2008. The figure shows that the flow reaches its maximum around 14:40 and instigates the onset of queue. After the queue formation, the bottleneck discharge rate diminishes significantly until the HOV lane becomes active at 15:00. Thereafter, the bottleneck discharge rate partially recovers and remains generally higher than the prior rate for about 1.5 hours. The figure further illustrates that this recovery in discharge rate is attributable to the smoothing effect. Notably, the temporal trend of the HOV lane flow is nearly

opposite to that of the discharge rate, indicating that fewer lane-changes toward the HOV lane promote higher bottleneck discharge rates. The trend is contrary in the regular-use lanes; see Figure 22(b). The regular-use lanes experience markedly higher utilization after the HOV lane activation, presumably induced by restricted access to the HOV lane. (Note that because there is additional capacity downstream of the diverge due to the split of lane 3 (see Figure 18), the changes in lane flow represent the changes in lane utilization, rather than lane-wise bottleneck discharge rates.)

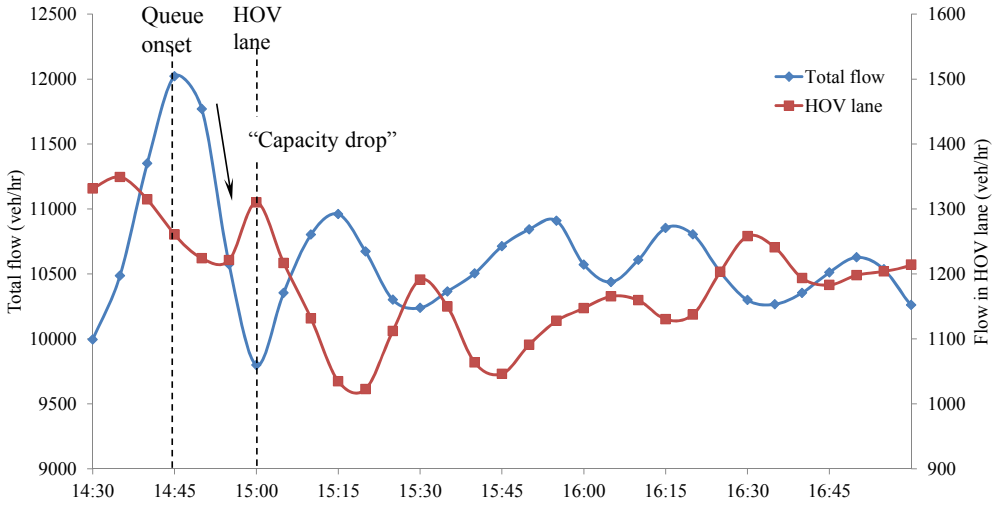

(a)

Figure 22. Smoothing effects over time on 10/20/2008; (a) Temporal trends of total flow vs. flow in the HOV lane; (b) Temporal trends of total flow vs. flows in the regular-use lanes and exit lanes.

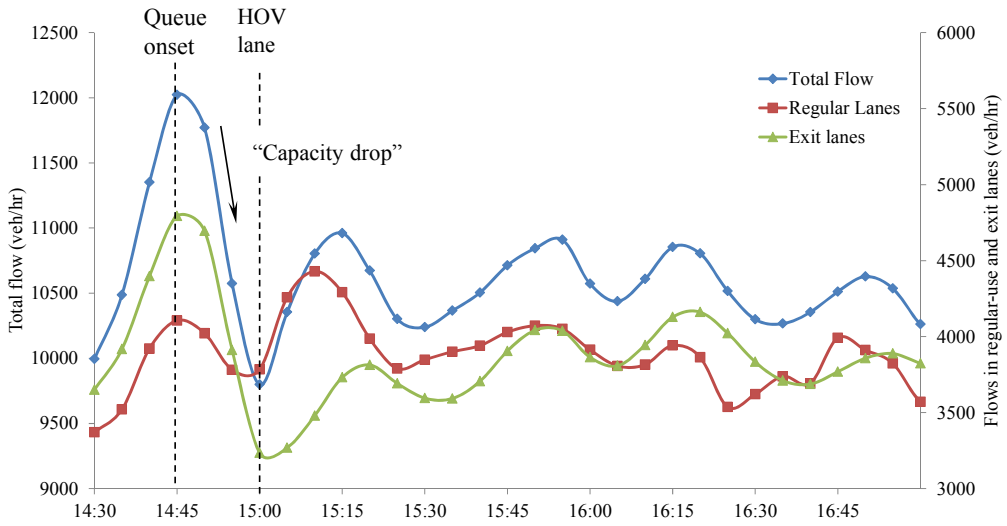

(b)

Figure 22(contd.). Smoothing effects over time on 10/20/2008; (a) Temporal trends of total flow vs. flow in the HOV lane; (b) Temporal trends of total flow vs. flows in the regular-use lanes and exit lanes.

We further investigate the causality between HOV LFD and bottleneck discharge rate at the time of bottleneck activation and HOV lane activation. A cross-correlation analysis revealed that at the time of bottleneck activation, an increase in HOV LFD preceded a reduction in discharge rate (i.e., immediate capacity drop) on nearly 70% of the study days (23 of 33 days). The average lag time was around 3 minutes. Conversely, a reduction in HOV LFD preceded an increase in the discharge rate at the time of HOV lane activation. This trend was observed on 75 % of the study days (25 of 33 days) with the average lag time of 3.6 minutes.

Table 9 provides the basic statistics of the result. The bottleneck discharge rate increases from 10,299 to 10,714 veh/hr on average in the presence of smoothing effect, and this 4% increase is statistically significant. Moreover, judging by the ranges, the discharge rate is as large as 12,943 veh/hr, exceeding the pre-queue flow by more than 18%. Indeed on several days, the discharge rate in the presence of smoothing effect exceeded the pre-queue flow. The smoothing effect persisted for approximately 1.5 hours on average.

Table 9.

Summary statistics of the smoothing effect magnitude and duration.

Summary statistics	**Average (Standard Error)**	**Range**
Bottleneck discharge rate before HOV lane activation (veh/hr)[1]	10,299 (39.5)	9,447 to 10,942
Bottleneck discharge rate with smoothing effect (veh/hr)	10,714 (13.74)	10,714 to 12,943
Duration of smoothing effect (minutes)	92.5 (9.8)	24 to 181

[1] average discharge rate after the immediate capacity drop and before HOV lane activation

Notice in Figure 22(a) that the HOV lane flow gradually recovers after about 1 hour and 15 minutes. However, the trend of the bottleneck discharge rate is contrary; it gradually diminishes over time, implying waning smoothing effect. Clearly, lower utilization of the HOV lane promotes higher bottleneck discharge rates. The highest HOV LFD in the presence of the smoothing effect was 0.288 (standard error = 0.002) on average across study days.

From the Figure 22(a) and 22(b), it is evident that there exists oscillations, where the total flow increases and decreases alternatively. Table 10 provides the day to day variations in the period of these oscillations. It was the found that the average period of oscillation is 32 minutes. The reason for these oscillations should be further investigated and is not in the scope of this research.

Table 10.

Total flow-oscillations statistics.

Day	Avg. Cycle Duration (mins)	Variation Cycle Duration (mins)
6/3/2008	33.05	6.95
6/4/2008	27.09	8.62
6/6/2008	35.71	13.03
6/11/2008	43.16	25.84
7/11/2008	29.17	2.73
7/30/2008	41.44	10.22
8/6/2008	31.23	7.24
8/8/2008	29.33	5.47
8/13/2008	30.1	4.9
9/3/2008	35.44	11.6
9/15/2008	44.42	18.88
9/16/2008	38.19	8.8
9/19/2008	30.19	5.3
10/6/2008	29.66	4.65
10/8/2008	41.47	10.88
10/9/2008	27.07	5.56
10/20/2008	28.18	5.03
11/3/2008	36.29	14.23
11/4/2008	29.38	7
11/10/2008	26.15	7.28
11/20/2008	39.2	11.63
11/24/2008	31.33	5
12/3/2008	30.99	2.71
12/15/2008	26.71	10.91
12/17/2008	39.38	27.82
1/5/2009	27.16	3.66
1/7/2009	29.58	19.12
1/13/2009	26.56	6.32
1/23/2009	43.14	11.59

To gain further insight, Figure 8 presents LFD vs. the bottleneck discharge rate while the HOV lane was active; the data points come from all study days. The LFDs are computed based on the near-steady state flows that are identified via CWT. The trends are approximately linear, as observed by several previous studies (e.g., Duret et al., 2012). More importantly, the bottleneck discharge rate improves as the HOV and exit LFDs decrease. This observation is

further confirmed with a regression analysis; see Table 3 for the result. Notice that the effect of the HOV LFD (and thus the smoothing effect) is more significant than that of the exit LFD. One would expect fewer leftward lane changes with diminishing HOV LFD and similarly, fewer rightward (freeway-to-ramp) lane changes with the diminishing exit LFD.

Table 6.

A summary of regression result: bottleneck discharge rate vs. exit LFD and HOV LFD.

Predictor	Coefficient	Standard error	*t*-value	*p*-value
Constant	17,349.4	636.7	27.25	0.000
Exit LFD	-8,944	1,107	-8.08	0.000
HOV LFD	-13,530	1,127	-12.00	0.000

Analysis of variance

Source	DF	SS	MS	F	P
Regression	2	31,619,226	33,417,851	72.85	0.000
Residual Error	729	158,200,060	215,117		
Total	731	189,819,286			

S= 465.843, R^2 = 0.167, Adjusted R^2 = 0.164

Thus, the findings suggest that (i) higher bottleneck discharge rates are attained with fewer lane changes and that (ii) the smoothing effect by restricting access to the HOV lane has a more profound impact on the bottleneck discharge rate than diverging flow.

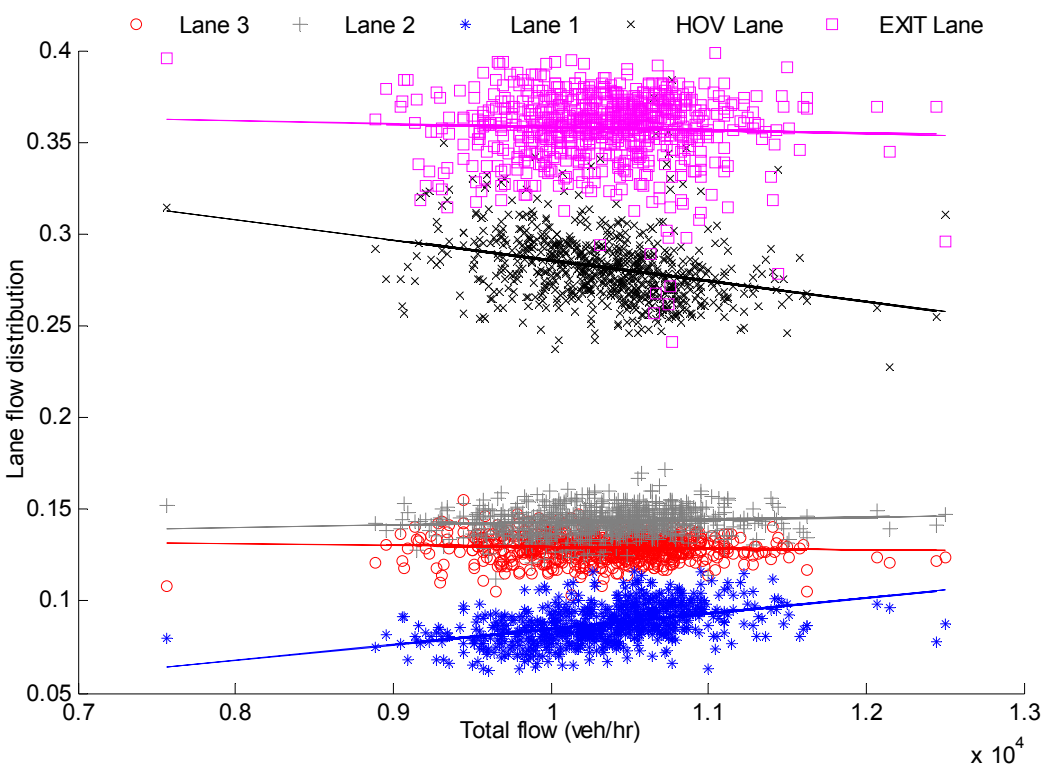

Figure 23. LFDs vs. bottleneck discharge rate after HOV lane activation.

Conclusions

This study analyzed the characteristics of a freeway weave bottleneck with a HOV lane. On each of 33 study days, a queue formed consistently, well before the activation of the HOV lane, upon simultaneous surges in on-ramp and off-ramp flows. Thereafter the bottleneck discharge rate diminished by 3-22% in the presence of queue. The discharge rate, however, recovered substantially with HOV lane activation presumably due to the smoothing effect induced by fewer disruptive lane-changes toward the HOV lane. The discharge rate improved by approximately 4% on average and occasionally exceeded the maximum flow prior to the queue formation. The smoothing effect persisted for 1.5 hours on average, though it waned over time as the HOV lane gradually became more utilized.

This study further examined the variations in bottleneck discharge rate. The HOV LFD and the proportion of flow diverging were found to be significant variables that negatively affect the bottleneck discharge rate. Of the two variables, the HOV LFD, a surrogate measure of the smoothing effect, had a more significant impact on the discharge rate. This finding underscores the significance of the smoothing effect, particularly in light of the fact that the diverging flow constituted a large fraction of flow (≈ 23%) in this study.

The smoothing effect has been conjectured by Menendez and Daganzo (2007) and empirically verified by Cassidy et al. (2010) at a merge and a curve bottlenecks. Our findings corroborated that a HOV lane can also induce the smoothing effect at a weave bottleneck by discouraging lane-changes toward the HOV lane. This effect, measured by the HOV LFD, was evidently the dominant factor for the variations in bottleneck discharge rate. Our findings provided further insight into the characteristics of the smoothing effect, including its magnitude and temporal trend, in a statistically rigorous manner.

Nevertheless, some future studies are needed. Since bottleneck characteristics can be site-specific, it is desirable to verify the reproducibility of the results on a more balanced weaving bottleneck (in terms of merging and diverging flows). Moreover, the waning smoothing effect over time was accompanied by increasing HOV LFD. The reason behind increasing HOV LFD is not clear, although it may be demand driven. Finally, our results suggest that one can sustain high bottleneck discharge rate by limiting the HOV LFD. A more in-depth study would be useful, especially from the control standpoint, to determine the optimal level of HOV LFD that maximizes the bottleneck discharge rate.

CHAPTER 6

LANE FLOW DISTRIBUTION AND ITS RELATIONSHIP WITH BOTTLENECK DISCHARGE RATE

This chapter explores the relationship between lane flow distribution and bottleneck discharge rate at weaving bottleneck occurred due to a lane drop and a busy off-ramp. Previous studies explored the relationship of speed and flow across different lanes with the total flow on the freeway segments. They observed that high flows before the bottleneck activation were associated with vehicle lane changes towards the median lane and observed reduction in flows in all the lanes after the bottleneck activation. However, not much work has been done on studying the relationship of lane flow distributions at weaving bottleneck locations occurred due to a lane drop and a busy off-ramp.

We believe that this study is an important contribution given that the previous studies analyzed weaving bottlenecks that occurred due to busy on-ramp and busy off-ramps. The bottleneck studied in this case is a weaving bottleneck that occurred due to a lane drop and a busy off-ramp. Also the fact that these kind of weaving bottlenecks are quite common and not been studied before adds to the significance of this study. The studies on weaving bottlenecks resulted from a busy merge and diverge flows showed that ramp-to-freeway maneuvers are disruptive in nature. However in this case, a different pattern has been observed given that the weave geometry of this study is different from earlier studies . This Chapter focuses on establishing the relationship of lane flow distribution with variation of bottleneck discharge rate on a bottleneck site located on US-101south in the Los Angeles County in California. The results confirmed that both the pre-queue flow and discharge rate are linearly related with LFD. It was found that more the lane changing towards the median lane, the more is the lane utilization of the

median lane and more is the discharge rate. The lane changes towards the off-ramp from the median lane would be disruptive and would result in lower discharge rate.

Site and data

The selected study site is a southbound section of US route 101, located between Barham Blvd. and Lankershim Blvd. in the Los Angeles County in California. The bottleneck schematic is shown in Figure 24(a). The site contains five regular use lanes which get tapered into four regular use lanes and an off-ramp near the bottleneck location. The shoulder lane (lane 5) becomes an exit only lane just downstream of post mile (PM) 10.2 whereas lane 4 has the option of exiting to the off-ramp. There is no HOV lane at this location. A recurrent bottleneck resides between PM 10.2 and PM 9.9 presumably due to the major diverge in this freeway section and lane reduction at the diverge. A typical speed contour shown in Figure 24(b) further confirms the location of the bottleneck. The length of the queue was found to be greater than 3 miles.

Eighteen days of data during the months spanning from October 2013 to January 2014 were used for this analysis when the study section was free of reported incidents and was an active bottleneck. 5-minute data has been used for the preliminary analysis and 30-second data de-noised using discrete wavelet transforms was used for detailed analysis of the bottleneck. The data are obtained from the California freeway performance measurement system (PeMS) database. Data are available from all the detector locations as labeled in Figure 24(a) and consist of vehicle count, occupancy and time-mean speed aggregated over 5minute and 30-second intervals.

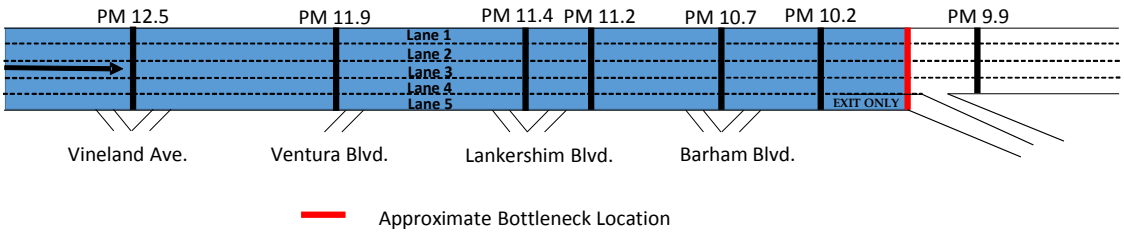

(a)

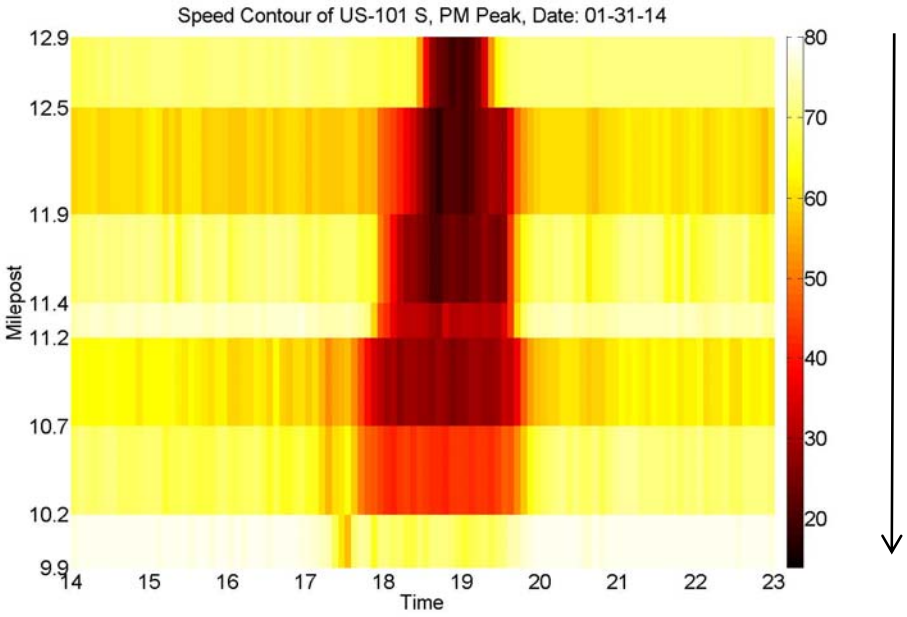

(b)

Figure 24. Bottleneck location on US-101 southbound (a) Schematic (b) Speed contour on 01-31-14.

Bottleneck activation and congestion pattern

For this analysis, the wavelet transform (WT) is used to de-noise the 30-second raw data, precisely identify bottleneck activation and deactivation times, and measure pre-queue flow and discharge rate. The procedure for the application of wavelet transforms is described in detail in Chapter 3. It was observed that the bottleneck activated around 17:22 in the evening with an average duration of 2 hrs and 3 minutes. The average pre-queue flow (maximum flow sustained prior to the bottleneck activation as described in Chapter 3) was found to be 7,726 vph and the

average discharge rate during congestion was found to be 7,037 vph, resulting in an average overall capacity drop of 8.9%. The average off-ramp flow prior to the bottleneck activation when the pre-queue was measured was 1,718 vph whereas the average off-ramp flow during congestion was found to be 1,565 vph. Given that there is high diverge flow through the off-ramp and a lane reduction, the resultant bottleneck is most likely a weave bottleneck. The results are tabulated in the Table 12.

Table 12.

Bottleneck statistics.

	Average (standard error)
No. of days	18
Time of onset of queue	17:22 (5.6 minutes)
Time of clearance of queue	19:25 (4.4 minutes)
Pre-queue flow (veh/hr)	7,726 (62)
Bottleneck discharge rate (veh/hr)	7,037 (82)
Reduction in bottleneck discharge rate (veh/hr)	688 (73)
Reduction in bottleneck discharge rate (%)	8.88 (1)

The speed profile at the detector immediately upstream of the bottleneck on a study day is shown in Figure 25. The times of congestion activation and deactivation were identified using continuous wavelet transforms. The figure shows that lane 4 is the most congested among the lanes whereas lane 1 (median lane) is the least congested. Congestion starts in the lanes associated with the exit lanes, where intense weaving activities likely occur and spreads to the inside lanes. Figure 26 shows the relationship between flow and speed for each lane at the detector immediately upstream of the bottleneck on all days. The figure illustrates that during free flow conditions, the speed is relatively constant. For lanes 3-5, data points during congested periods lie well below those during free-flow periods, and a decrease in speed is associated with the reduction in flow. Interestingly, for lanes 1 and 2, data points during “congested periods” lie

between the free-flow branch and the congested branch (based on lanes 3-5). Moreover, speed is rather insensitive to the flow. These patterns suggest that flows in lanes 1 and 2 are not restricted, and the speeds lower than free-flow speed may be attributable to the low congested speeds in the adjacent lanes; i.e., drivers may choose to travel at lower speeds in response to conditions in the adjacent lanes.

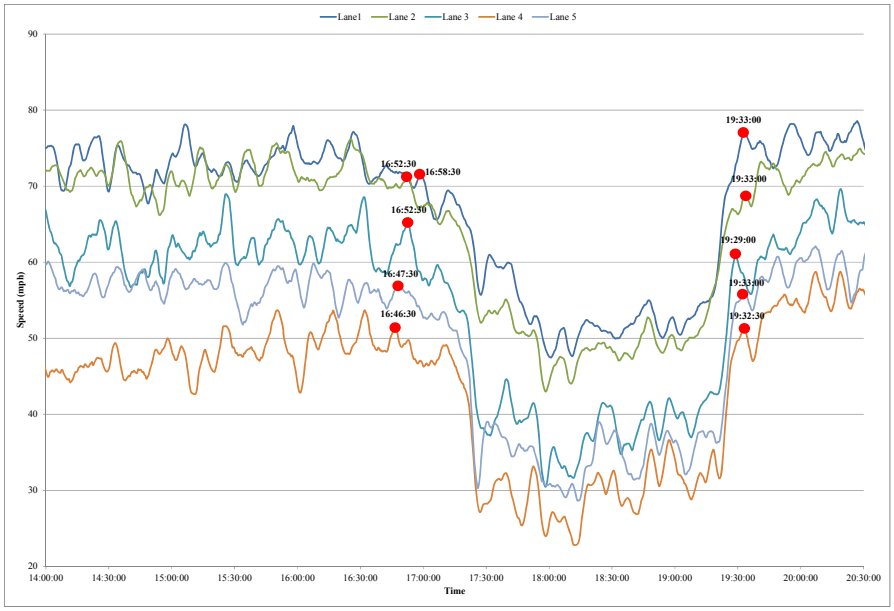

Figure 25. Speed profile of the upstream detector on 01/10/2014.

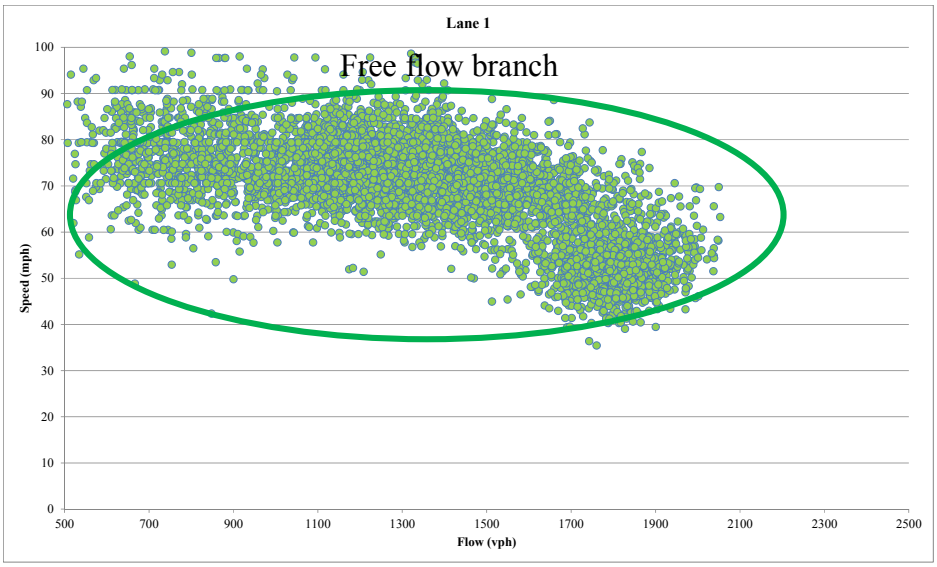

(a)

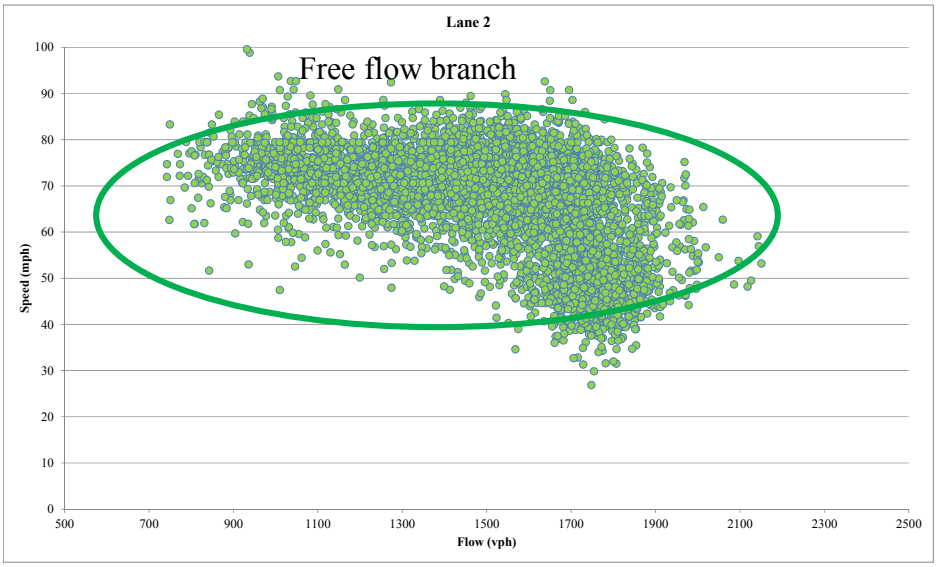

(b)

Figure 26. Flow vs. speed at the upstream detector.

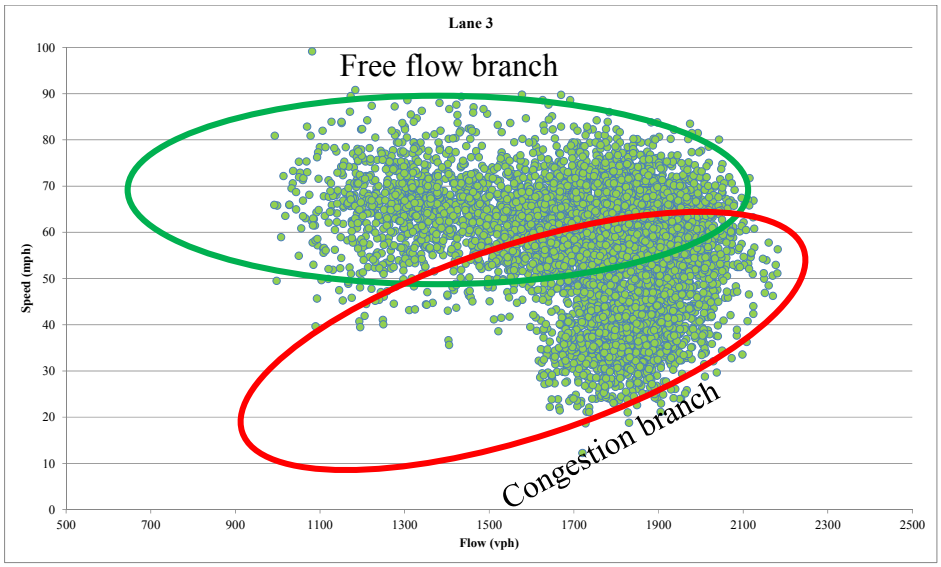

(c)

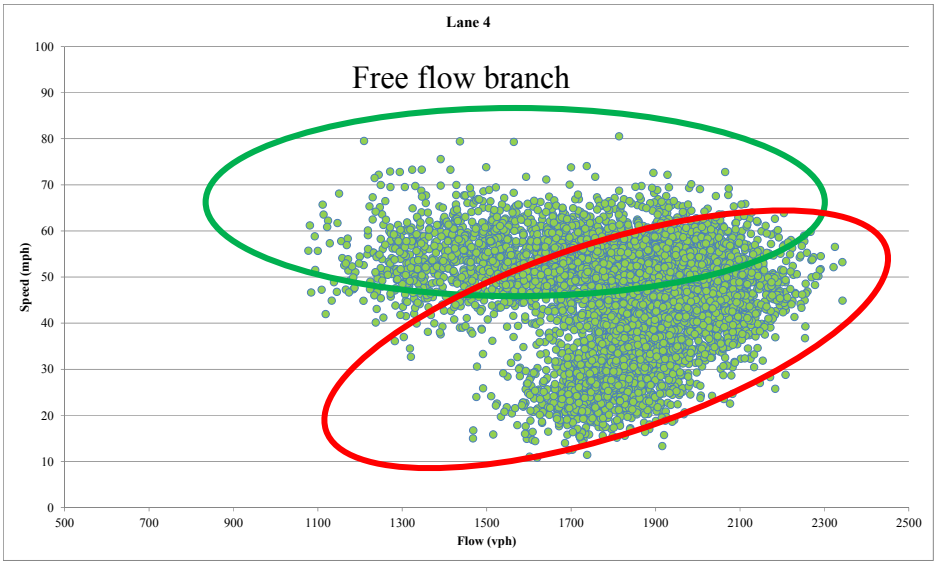

(d)

Figure 26 (contd.). Flow vs. speed at the upstream detector.

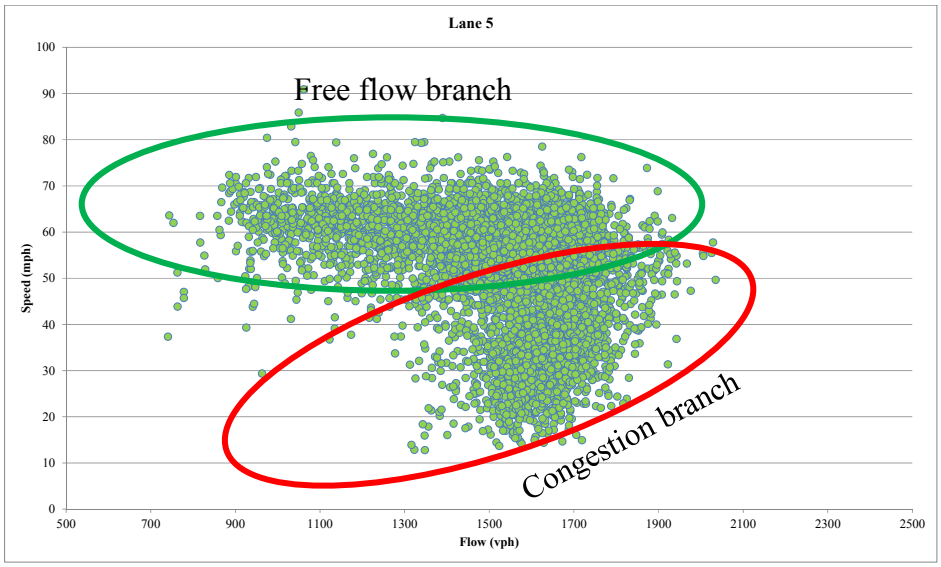

(e)

Figure 26 (contd.). Flow vs. speed at the upstream detector.

Lane flow distribution (LFD) and its effect on discharge rate

Figure 27 shows the LFD of the four lanes on a typical day at the detector located at milepost 9.9, immediately downstream of the bottleneck. The bottleneck activation and de-activation times on this day were 5:15 p.m. and 7:50 p.m., respectively. Figure 27(a) shows that the flow (demand) steadily increased from 3 pm until the bottleneck activated, and then a reduction in discharge rate is observed during congestion. The increase in the flow before congestion is accompanied by an increase in LFD in the median lane and a decrease in the LFD of the shoulder lane as shown in Figure 27(b). There are no significant changes observed in the LFDs of lanes 2 and 3. This shows that as the flow increases before congestion, there is an increase in the utilization of the median lane indicating systematic lane changes towards the median lane. However during congestion, opposite patterns were observed. The reduction in discharge rate was accompanied by a reduction in LFD in the median lane and an increase in LFD in the shoulder lane. The LFD in the median lane at the time of bottleneck activation varied

from 0.20 to 0.26 across the study the days. The LFD in the shoulder lane varied from 0.22 to 0.27 at the time of bottleneck activation.

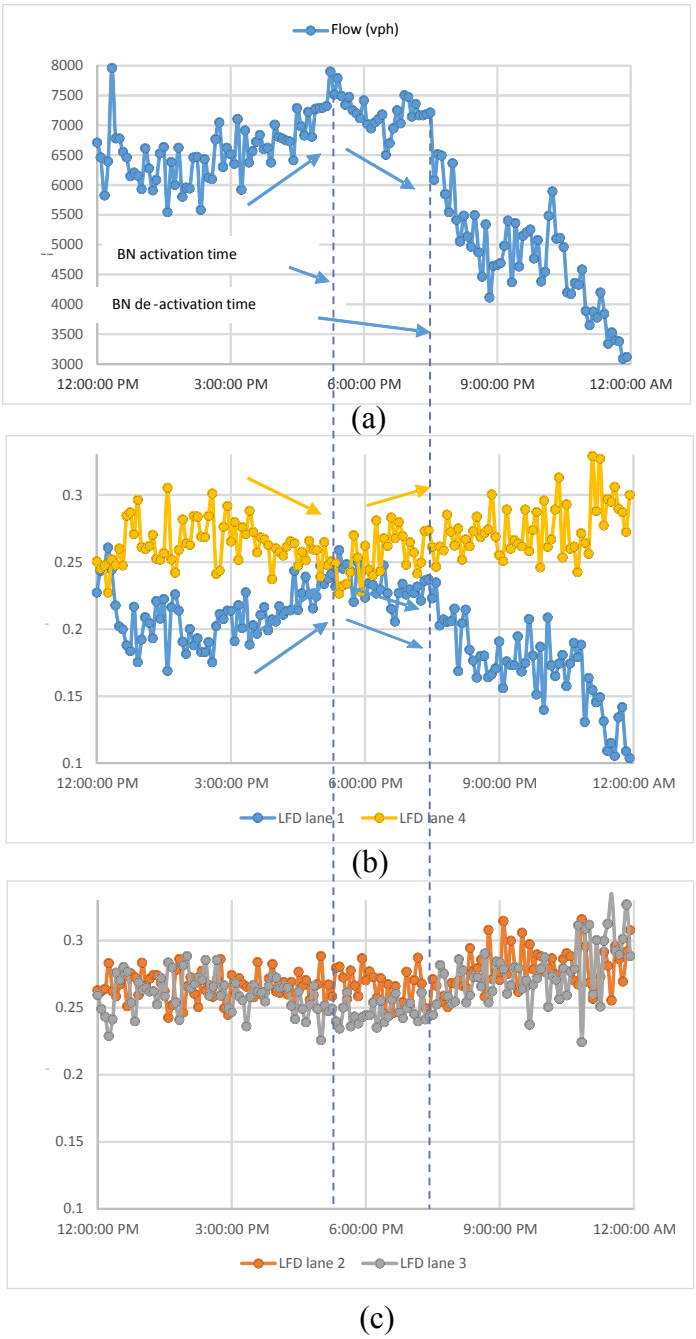

Figure 27. LFD vs. discharge rate on 01/31/14 at detector located milepost 9.9.

To better understand the causality between the change in LFD in the median lane and the change in discharge rate at the bottleneck activation, a cross-correlation analysis has been conducted using 30 second data. Figure 28 shows the cross-correlation at different time lags between the discharge rate and LFD in the median lane on 01/31/14. Each time lag represents a time step of 30-seconds. A positive time lag means that the flow is a leading variable to the HOV LFD where as a negative lag indicated that HOV LFD is the leading variable. The figure shows that the discharge rate is positively correlated to the LFD in the median lane, confirming the observation above (Figure 27). Also it can be seen that the maximum correlation is observed with a negative lag of –3. This result indicates that the change in the LFD in the median preceded the change in discharge rate which implies that higher the utilization of the median lane the higher is the discharge rate. The lag of –3 indicates that the time lag between LFD in the median lane and flow is 1.5 minutes. The cross correlation factor was statistically significant at 95% confidence interval.

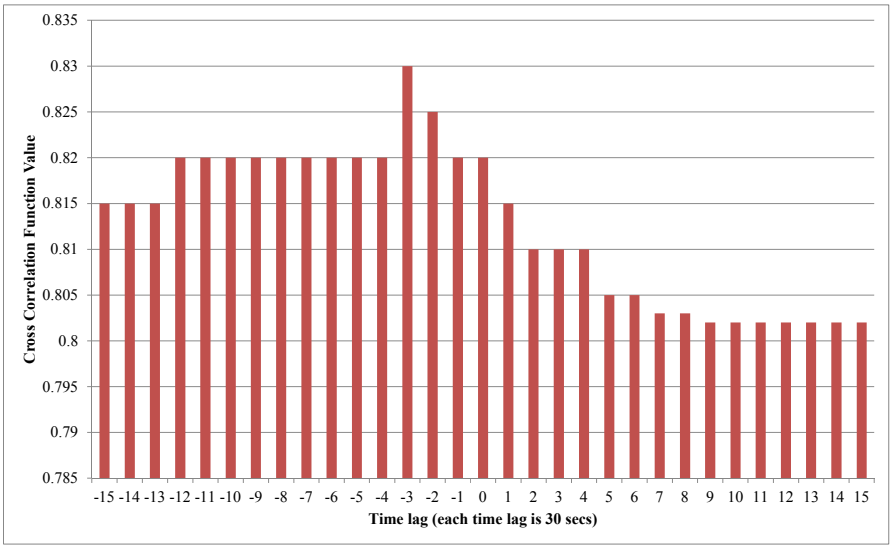

Figure 28. Cross-correlation between the flow and LFD in the median lane (01/31/14).

Relationship between discharge rate and LFD during pre-congestion. Figure 29 shows the relationship between the LFD and the pre-queue just before the activation of the bottleneck for the 18 study days. LFD of the median lane is positively related with the pre-queue flow and this relationship is significant at 90% confidence level. LFD of the shoulder lane is negatively related to the pre-queue flow and this relationship is significant at 95% confidence level. Lanes 2 and 3 have a similar relationship with the pre-queue flow as lanes 1 and lane 4 respectively even though these relationships are not statistically not significant. These results show that the more the median lane is utilized just before the bottleneck activation the higher is the pre-queue flow. As seen earlier in this chapter the congestion is observed in the right most lanes and then progressively proceeds towards the median lanes. Hence the vehicles tried to move away from the right lanes towards the less congested/high speed lanes and thus resulting in higher pre-queue flow.

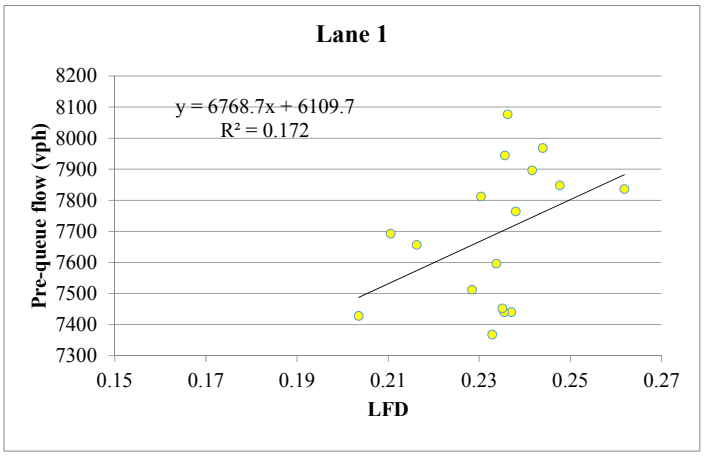

(a)

Figure 29. LFD vs. Pre-queue flow, (a) Lane 1 (b) Lane 2 (c) Lane 3 (d) Lane 4.

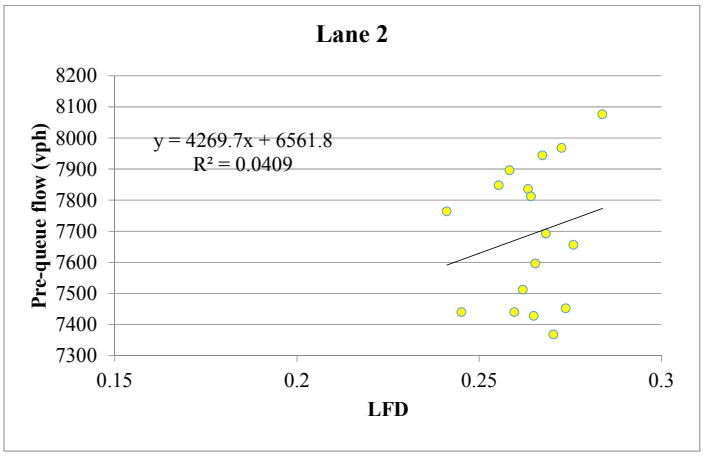

(b)

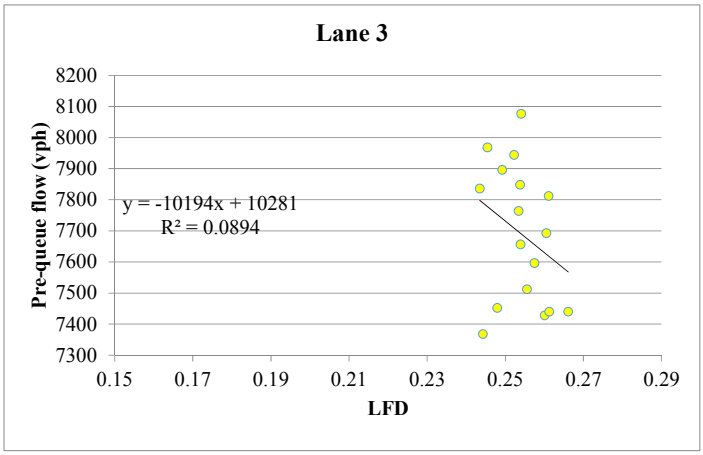

(c)

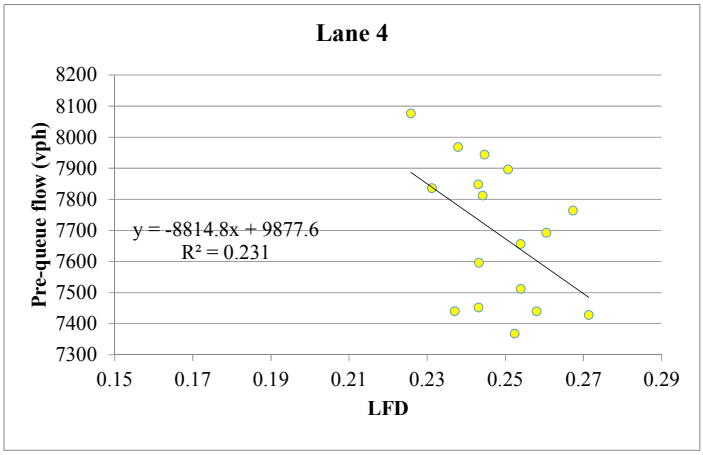

(d)

Figure 29(contd.). LFD vs. Pre-queue flow, (a) Lane 1 (b) Lane 2 (c) Lane 3 (d) Lane 4.

Relationship between discharge rate and LFD during congestion. Figure 30 shows the relationship between LFD and the discharge rate after the activation of the bottleneck for the 18 study days. LFD of the median lane decreases along with the discharge rate after the onset of congestion whereas LFDs of lane 3 and lane 4 increase with the reduction in the discharge rate. Lane 2 LFD does not change significantly during this period. The linear relationships between the discharge rate and LFDs of lane 1, lane 3 and lane 4 were found to be statistically significant at the 95% confidence level. The results show that the more the median lane is utilized during the congestion, the higher is the discharge rate (recall that flows in lanes 1 and 2 were found to be unrestricted). It could be seen that higher the lane utilization of left lanes (lane 1 and lane 2) the higher are the lane changes away from the right lanes (lane 3 and lane 4) and higher is the discharge rate. The linear relationships between the discharge rate and difference in LFDs of lane 1, lane 2 with lane 4 were found to be statistically significant at the 95% confidence level.A more detailed analysis will follow.

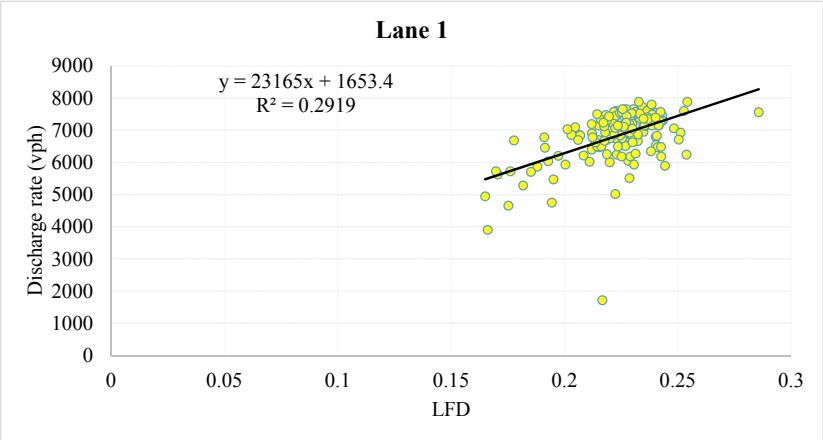

(a)

Figure 30. LFD vs. discharge rate, during congestion (a) Lane 1 (b) Lane 2 (c) Lane 3 (d) Lane 4.

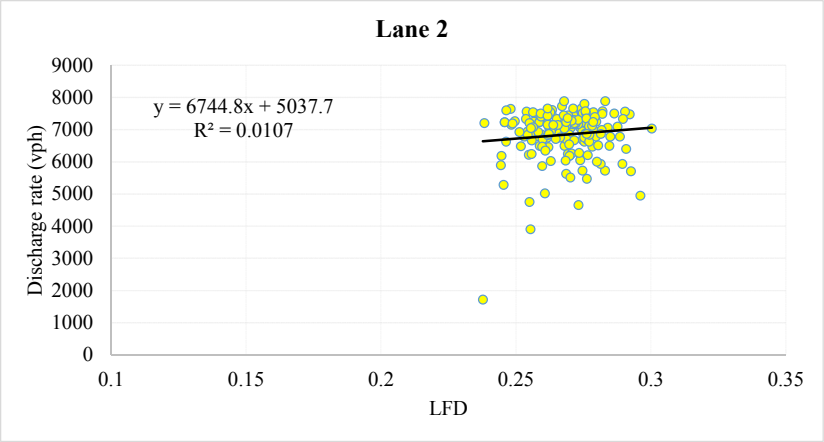

(b)

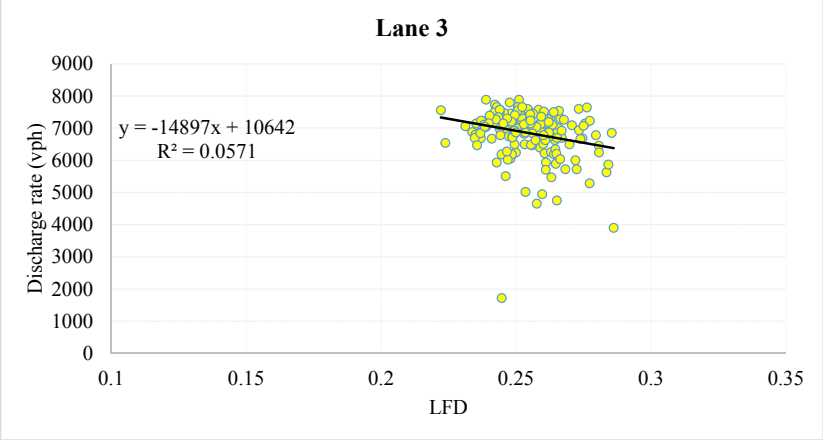

(c)

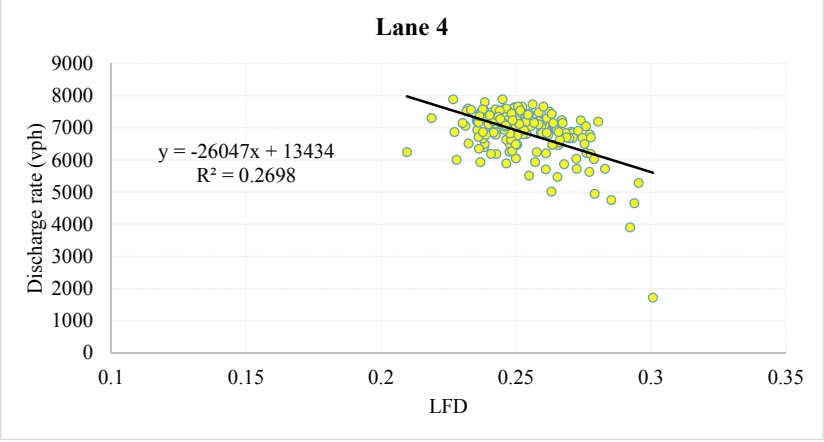

(d)

Figure 30(contd.). LFD vs. discharge rate, during congestion (a) Lane 1 (b) Lane 2 (c) Lane 3 (d) Lane 4.

Figure 31 shows the relationship between the difference in magnitudes of the LFDs between the lanes and discharge rate. These results indicate that the higher the lane utilization of the median and lane 3 (left lanes) the higher is the discharge rate.

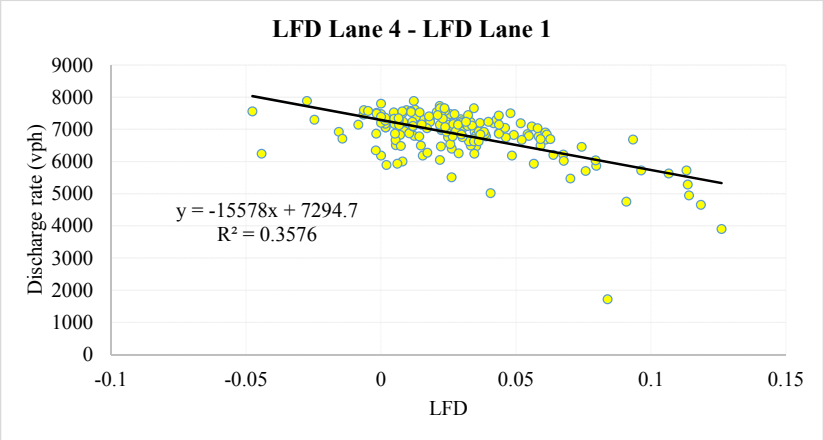

(a)

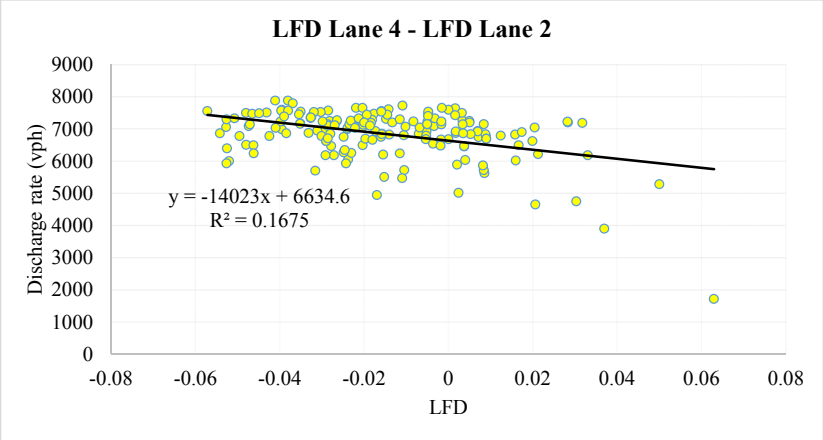

(b)

Figure 31. Difference in magnitudes between lane LFDs vs. discharge rate, during congestion.

To gain more evidence on lane changing, both speed and flow data from the detector located just upstream of the bottleneck were analyzed. The amount of systematic (net) lane changing around the bottleneck was measured by taking the difference in flow between the

upstream and downstream of the bottleneck. Figure 32 shows the relationship between the net lane-changing in individual lanes and the discharge rate. From the figure, it is evident that (i) there are systematic lane changes away from lane 1 judging by negative changes in flow and that (ii) the more the lane changes away from the median lane, the lower is the discharge rate. An increase in lane changes toward lane 2 resulted in an increase in discharge rate. These results indicate that there is a systematic lane changing towards lane 2 indicating merging activity due to the lane reduction in addition to the large diverge flow. This supports that the bottleneck is a weaving bottleneck. The relationships between the changes in flow in lane 3 and lane 4 and the discharge rate were not statistically significant.

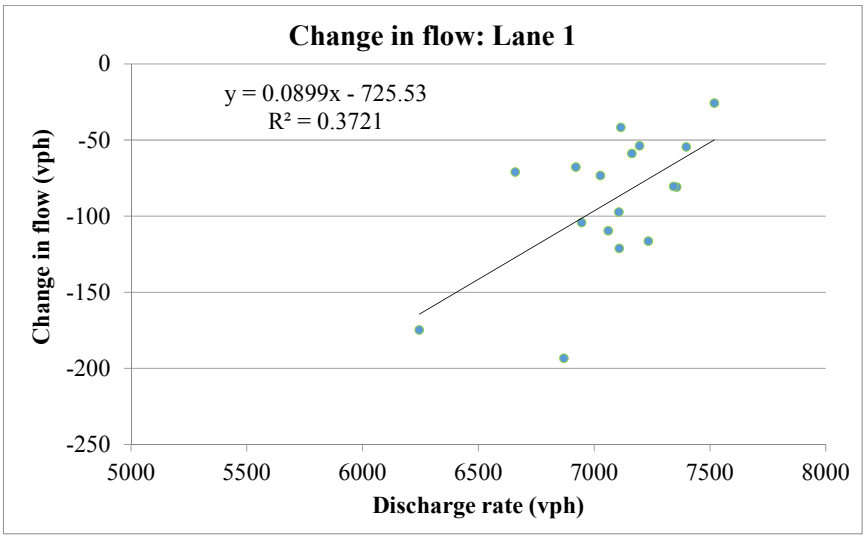

(a)

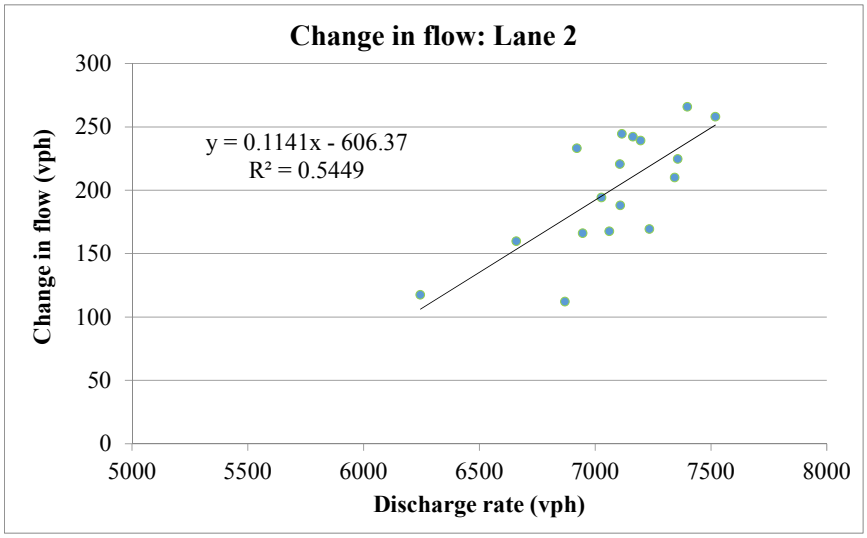

(b)

Figure 32. Relationship between difference in flow between downstream and upstream detector and discharge rate.

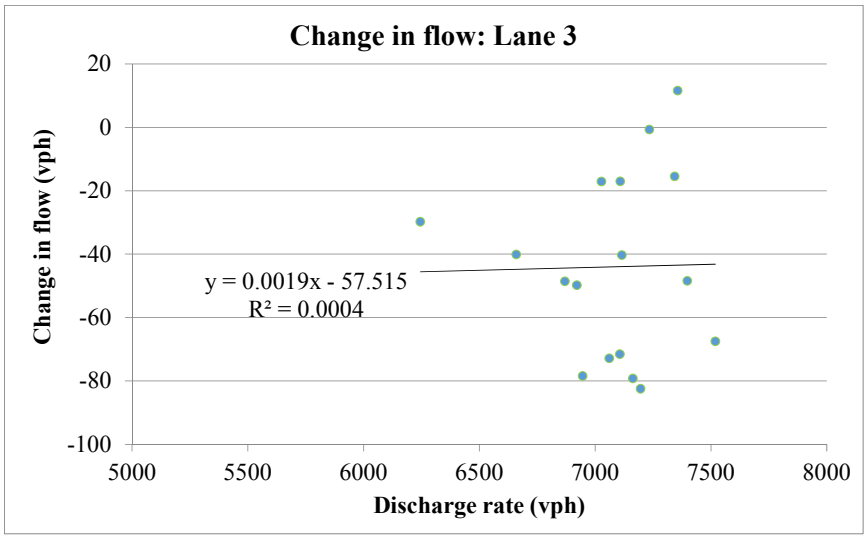

(c)

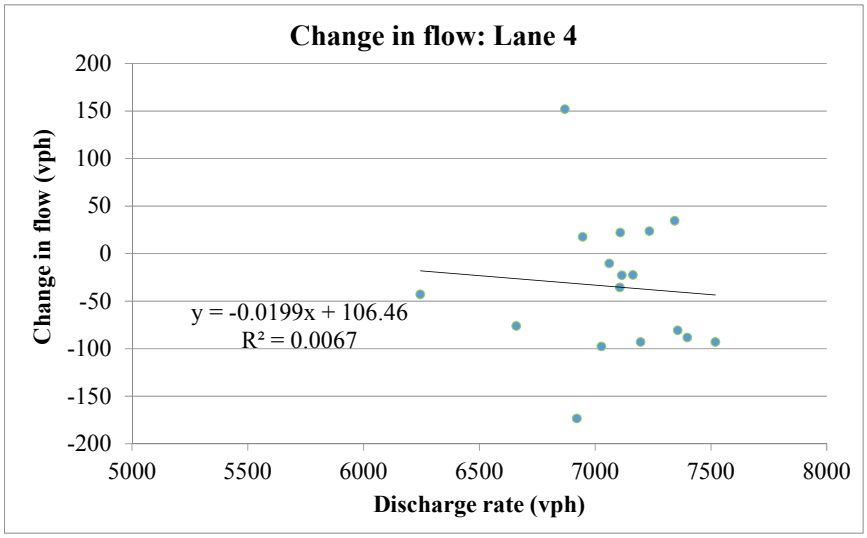

(d)

Figure 32 (contd.). Relationship between difference in flow between downstream and upstream detector and discharge rate.

These results indicate that a higher discharge rate is attained by fewer lane changes toward the off-ramp that likely promote better utilization of the median lane. An increase in off ramp flow results in an increase in lane changes away from the median lane reducing its lane utility thereby reduction in discharge rate. This result is contradicting to an earlier study by Lee

et al. (Lee and Cassidy, 2009) which stated that the lane changes towards the median lanes are disruptive. The weaving bottlenecks previously analyzed in literature involved a busy on-ramp and a busy off-ramp but in this case, the weaving activity is a result of combination of a lane drop and a busy off-ramp. Another significant difference in the geometry in this case, that is, the merge and diverge activities occur at the same location when compared to the other bottlenecks analyzed where the merge (on-ramp) and diverge (off-ramp) activities occur at different locations.

Conclusion

This chapter explored the relationship between lane flow distributions and bottleneck discharge rate on weaving bottleneck involving a lane drop and a busy off-ramp. To this end, 18 study days where the queue has formed consistently due to a diverge/off-ramp and lane reduction. The average reduction in bottleneck discharge rate upon bottleneck activation was found to be around 9%.

The speed profile at the detector immediately upstream of the bottleneck showed that lane 4 is the most congested among the lanes whereas lane 1(median lane) is the least congested. Further it was found that the congestion occurs first in the rightmost lanes and spread progressively towards the inner lanes. Also it was found that during congestion lane 3, lane 4 and lane 5 have lower speeds and high flows whereas lane 1 is the least congested. It was observed that Lane 2 during congestion is associated with relatively high speed and discharge rate respectively indicating that during congestion the inner lanes are more utilized.

It was observed that the increase in flow well before congestion started was accompanied by the increase in the LFD of the median lane and upon bottleneck activation it was found that the LFD in the median decreased with the reduction in the bottleneck discharge rate. Cross

correlation analysis confirmed that the bottleneck discharge rate and LFD in the median lane are positively correlated and the change in LFD in the median lane occurred first followed by the change in the discharge rate. LFD of the median lane is found to be positively related with the pre-queue flow and LFD of the shoulder lane is negatively related to the pre-queue flow. Further, it was found that the LFDs of all the lanes are linearly related to the discharge rate. The LFD in the median lane is positively related to the discharge rate whereas the LFDs in the shoulder lane and lane 3 are negatively related. The relationship is found to be statistically significant in the median lane, lane 3 and lane 4.

To gain more evidence on lane changing, both speed and flow data from the detector located just upstream of the bottleneck were analyzed. It was found that more the lane changing towards the median lane, the more is the lane utilization of the median lane and more is the discharge rate. The lane changes towards the off-ramp from the median lane would be disruptive and would result in lower discharge rate. We believe that this study is an important contribution given the fact that the previous studies analyzed weaving bottlenecks that occurred due to busy on-ramp and busy off-ramps. The bottleneck studied in this case is a weaving bottleneck that occurred due to a lane drop and a busy off-ramp. From the results, it was found that the effect of lane changing patterns in this case are quite opposite to those mentioned in the previous studies.

CHAPTER 7

CONLUSIONS

Traffic congestion is a major externality in modern transportation systems and has a negative economic, environmental, and social impact. One of the key elements that determine the extent of congestion, besides the demand for travel by automobiles, is freeway bottlenecks. In the previous studies, there has been a lack of efforts to systematically identify active bottlenecks and measure the capacity drop on a regional network. Also most of the previous studies have focused on studying the mechanisms of merge and diverge bottlenecks. Mechanisms and features of weaving bottlenecks are not very well understood. Most of these studies have analyzed only a few days of data and have not considered in identifying steady state periods in systematic and reproducible manner.

This research developed an efficient methodology to identify and analyze freeway bottlenecks in a region in a consistent and reproducible manner. To this end, using the regional analysis methodology, 23 bottlenecks have been identified, some of which result in long queues and large delays during rush-hour periods in the Phoenix metropolitan region. For these bottlenecks, a number of performance measures were obtained, such as the duration of congestion, length of the congestion, vehicle miles traveled (VMT), vehicles hours traveled (VHT), and bottleneck discharge rate (where it can be measured or estimated). The identified bottlenecks were ranked according to the capacity drop in terms of flow and percent reduction in flow. This research showed that the 5-minute data could be effectively used in identifying and prioritizing active bottlenecks in a region. However, for studying the detailed mechanism of the high ranked active bottlenecks identified through the regional analysis it is advisable to use higher resolution data with an effective de-noising methodology as many traffic phenomena like

lane changing, traffic stationary periods, oscillations etc. occur at a frequency less than 5 minutes.

This research also investigated the features of two types of weaving bottlenecks in a statistically rigorous manner. It examined the effect of HOV lane on the bottleneck discharge rate and studied the factors that lead to the variation in bottleneck discharge rate. Data ranging from 18 to 33 days has been used in this research and wavelet transforms were used to effectively de-noise the data and identify key bottleneck events like congestion activation/de-activation times and steady state periods in a systematic and reproducible manner. A methodology has been developed to de-noise raw data using Discrete Wavelet Transforms (DWT) and the de-noised data is then used to precisely identify key bottleneck events using Continuous Wavelet Transforms (CWT).

This study specifically analyzed the characteristics of a freeway weave bottleneck with a HOV lane. Results showed that the bottleneck discharge rate diminished by 3-22% upon queue formations and recovered upon the high-occupancy-vehicle (HOV) lane activation, confirming the existence of the "smoothing effect." The recovery was substantial; the discharge rate improved by 4% and occasionally exceeded the maximum pre-queue flow. The smoothing effect persisted for about 1.5 hours and waned thereafter as the relative utilization of the HOV lane gradually recovered. A statistical analysis corroborates that the HOV lane flow distribution significantly (and negatively) affects the bottleneck discharge rate, more so than the amount of diverging flow. From this study we found that: (i) a higher (lower) flow can be sustained prior to traffic breakdown with higher diverging (merging) flow, suggesting that ramp-to-freeway maneuvers are more disruptive; (ii) higher bottleneck discharge rates are attained with higher diverging flow and activation of HOV lane.

This research also explored the relationship between lane flow distribution and bottleneck discharge rate at weaving bottleneck occurred due to a lane drop and a busy off-ramp. There has not been work done in the past on studying the mechanism of a weave bottleneck that occurred due to lane drop and a busy off-ramp and the results showed that the traffic patterns observed in this type of weave bottleneck are different from those mentioned in the previous studies. Data from 18 study days showed that the discharge rate diminished upon bottleneck activation and the average reduction in bottleneck discharge was found to be around 9%. It was found that the congestion occurred first in the rightmost lanes and spread progressively towards the inner lanes. LFD of the median lane is found to be positively linearly related with the pre-queue flow and LFD of the shoulder lane is negatively linearly related to the pre-queue flow. It was found that an increase in lane changing towards the median lane resulted in higher median lane utilization and higher discharge rate. The lane changes towards the off-ramp from the median lane would be disruptive and would result in lower discharge rate.

Practical implications: The regional analysis methodology employed in this research would help in identifying and prioritizing the bottlenecks by ranking them based on the capacity drop. This would aid the local governing body to focus on the bottlenecks that require immediate attention. Also the identified bottlenecks were attributed to a variety of factors, such as merging at busy on-ramps or freeway-to-freeway connectors, weaving due to busy merges followed by busy diverges (especially near major freeway-to-freeway interchanges), and curves. Since the cause of the bottlenecks was identified it would enable the local governing body to act accordingly to improve the freeway efficiency.

This research conducted detailed analysis of bottleneck features on two different types of weaving bottlenecks where there is a limited understanding of their features. The results showed

that HOV lane on a weaving bottleneck could be beneficial to the system performance. It was found that the discharge rate improved upon the activation of HOV lane and HOV lane utilization has a significant effect on discharge rate. The current highway capacity manual does not specifically address the effect of HOV lane on weaving bottleneck capacity calculations and volume adjustments were made considering the peak hour factor, heavy vehicle presence and driver population only. The findings from this research suggest that HOV lane specific adjustments on volume such as HOV lane utilization or factor representing the percent increase in total volume upon HOV activation (in this study, the average increase in bottleneck discharge rate was found to be 4%) could be included. However more weaving bottleneck sites should be analyzed to have consensus on these factors. Also it was found that the ramp to freeway maneuvers were disruptive in nature. Ramp metering (Cassidy and Rudjanakanoknad, 2005) could limit these disruptive lane changes by restricting the surge in flows from the ramp to the freeway.

Further, the effect of lane flow distribution on the bottleneck discharge rate was studied on a weaving bottleneck that occurred due to a busy off-ramp and a lane drop. This study is an important contribution given the fact that the previous studies analyzed weaving bottlenecks that occurred only due to busy on-ramp and busy off-ramps and it was found that the effect of lane changing patterns on discharge rate in this case are quite opposite to those mentioned in the previous studies. This could be due to the fact that the length of the weaving segment is different and relatively shorter than the weaving sections formed by an on-ramp and an off-ramp.

Future work: From the analysis of the weaving bottleneck with HOV lane it was found that there exist oscillations where the total flow increases and decreases alternatively with an average cycle length of oscillation is 32 minutes. It would be interesting to study the relationship

between the oscillations with discharge rate as part of the future research. Due to data limitations, detailed lane changing analysis and the effect of lane changing on the bottleneck discharge rate could not be studied in this research. However it would be interesting to investigate the lane changing patterns and their effects on the bottleneck discharge rate at these weaving bottleneck locations. As seen in the literature, the bottleneck characteristics could be site-specific and hence it is important to see if these results are reproducible at other weaving bottleneck locations. Also it would be interesting to determine the optimal level of HOV LFD that maximizes the bottleneck discharge rate.

REFERENCES

Ahn, S. (2005). *Formation and spatial evolution of traffic oscillations*. Doctoral Dissertation, Department of Civil and Environment Engineering, University of California, Berkeley.

Ahn, S. and Cassidy, M.J. (2007). Freeway traffic oscillations and vehicle lane-change maneuvers. *Proceedings of the 17th International Symposium on Transportation and Traffic Theory*, Amsterdam, Elsevier, pp. 691-710.

Amin, M.R. and Banks, J.H. (2005). Variation in freeway lane use patterns with volume, time of day, and location. *Transportation Research Record,* vol. 1934, pp. 132-139.

Banks, J. (1991). Two-capacity phenomenon at freeway bottlenecks: a basis for ramp metering? Transportation Research Record, vol. 1320, pp.83–90.

Bertini, R. L. and Leal, M. T. (2005). Empirical study of traffic features at a freeway lane drop. Journal of Transportation Engineering, vol. 131, pp. 397.

Brilon, W., Geistefeldt,J. and Regler, M. (2005). Reliability of freeway traffic flow: a stochastic concept of capacity. *Proceedings of the 16th International Symposium on Transportation and Traffic Theory*, Maryland, pp. 125-144.

Carter, M., Rakha, H. and Van Aerde, M. (1998). Variability of traffic-flow measures across freeway lanes. *Canadian Journal of Civil Engineering.*

Cassidy, M. J. and Bertini,R.L. (1999). Some traffic features at freeway bottlenecks. *Transportation Research Part B: Methodological*, no. 33 (February): 25-42. doi:10.1016/S0191-2615(98)00023-X.

Cassidy, M. J. and Bertini,R.L. (1999). Observations at a freeway bottleneck. *Transportation and Traffic Theory*, Elsevier, Amsterdam, pp. 107-124.

Cassidy, M. J. and Rudjanakanoknad, J. (2005). Increasing the capacity of an isolated merge by metering its on-ramp. *Transportation Research Part B,* Vol.39 (10), pp.896–913.

Cassidy, M.J., Jang, K. and Daganzo, C. F. (2010). The smoothing effect of carpool lanes on freeway bottlenecks. *Transportation Research Part A,* Vol. 44, pp. 65-75.

Chen, C., Varaiya, P. and Kwon, J. (2005). An empirical assessment of traffic operations. *International Symposium on Transportion and Traffic Theory.*

Chung, K., Cassidy, M. (2004). Test of theory of driver behavior on homogeneous freeways. Transportation Research Record. Vol.1883, pp.14–20.

Chung, K., Rudjanakanoknad, J., Cassidy, M. (2007). Relation between traffic density and capacity drop at three freeway bottlenecks.

Daganzo, C. F. and Cassidy, M.J.(2008). Effects of high occupancy vehicle lanes on freeway congestion. *Transportation Research Part B*, Vol 42, pp. 861-872.

Daganzo, C. F. and Cassidy, M.J. (2008). Effects of high occupancy vehicle lanes on freeway congestion. *Transportation Research Part B*, Vol 42, pp. 861-872.

Duret, A., Ahn, S., Buisson, C. (2012). Lane flow distribution on a three-lane freeway: general features and the effects of traffic controls. *Transportation Research Part-C*, Vol. 24, pp. 157-167.

Edie, L., Foote, R. (1958). Traffic flow in tunnels. *Proceedings of the Highway Research Board*, Vol. 37, pp.334–344.

Elefteriadou, L., Roess, R.P. and McShane, W.R. (1995). Probabilistic nature of breakdown at freeway merge junctions. *Transportation Research Record: Journal of Transportation Research Board*, No. 1484, pp. 91-98.

Evans, J., Elefteriadou, L., Natarajan, G. (2001). Determination of the probability of breakdown on a freeway based on zonal merging probabilities. *Transportation Research B*, Vol. 35(3), pp. 237–254.

Hall, F. L. and Agyemang-Duah, K. (1991). Freeway capacity drop and the definition of capacity. *Transportation Research Record: Journal of the Transportation Research Board,* vol. 1320, pp. 91-98.

Hall, F.L., Hall, L.M. (1990). Capacity and speed-flow analysis at the queen Elisabeth way in Ontario, *Transportation Research Record – Journal of the Transportation Research Board*, Vol. 1287, pp. 108-118.

Hong, S. and Oguchi, T. (2008). Lane use and speed-flow relationship on basic segments of multilane motorways in Japan. *Transportation Research Board.*

Kerner, B.S. (2002). Empirical macroscopic features of spatial-temporal traffic patterns at highway bottlenecks. *Physical Review E - Statistical, Nonlinear, and Soft Matter Physics*, Vol. 65(4), pp. 1-30.

Knoop, V.L., Duret, A. and Buisson, C. (2010). Lane distribution of traffic near merging zones influence of variable speed limits. *Annual Conference on Intelligent Transportation Systems,* pp. 19-22.

Koshi, M., Iwasaki, M., Okhura, I. (1983). Some findings and an overview on vehicular flow characteristics, In: Hurdle, V.F., Hauer, E., Steuart, G.F. (Eds.). *Proceedings of the 8th International Symposium on Transportation and Traffic Theory*, Toronto: University of Toronto Press, pp. 403-426.

Kwon, J. and Varaiya, P. (2008). Effectiveness of high occupancy vehicle (HOV) lanes in the San Fransisco bay area.

Laval, J.A., Cassidy, M.J., Daganzo, C.F. (2005). Impacts of lane changes at on-ramp bottlenecks: a theory and strategies to maximize capacity. In: Kühne, R., Poeschl, T., Schadschneider, A., Schreckenberg, M., Wolf, D. (Eds.), *Traffic and Granular Flow '05'*, Berlin: Springer, pp. 577-586.

Laval, J.A., Daganzo C.F. (2006). Lane-changing in traffic streams. *Transportation Research B*, Vol. 40(3), pp. 251-264.

Leclercqa, L., Laval, J.A., Chiabauta, N. (2011). Capacity drops at merges: an endogenous model. *19th international symposium on transportation and traffic theory*.

Lee, J. and Park, B. (2010). Lane flow distributions on basic segments of freeways under different traffic conditions. *Transportation Research Board.*

Lee, J.H. and Cassidy, M.J. (2009). An empirical and theoretical study of freeway weave bottlenecks. *California PATH Research Report*, USB-ITS-PRR-2009-13.

Lomax, T. (1997). *NCHRP Report 398: Quantifying congestion: volume 1 - final report*. Washington, D.C.: Transportation Research Board/National Academy of Sciences. http://onlinepubs.trb.org/onlinepubs/nchrp/nchrp_rpt_398.pdf.

Lighthill, M.J and Whitham, J.B. (1955). On kinematic waves II: a theory of traffic flow in long crowded roads. *Proceedings of the Royal Society*, A229, 317-345.

Mauch, M., & Cassidy, M.J. (2002). Freeway traffic oscillations: Observations and predictions. *Proceedings of the 15th International Symposium on Transportation and Traffic Theory*, Pergamon-Elsevier, Oxford, UK, pp.653–674.

Misiti, M., Misiti, Y., Oppenheim, G., Poggi J.M. (2010). *Matlab user guide*.

Menendez, M. and Daganzo, C.F. (2007). Effects of HOV lanes on freeway bottlenecks. *Transportation Research Part B*, vol. 41, pp. 809-822.

Muñoz, J. C. and Daganzo, C. F. (2002). Fingerprinting traffic from static freeway sensors. *Cooperative Transportation Dynamics*, vol. 1, pp. 1.1–1.11.

Newell, G. F. (1993). A simplified theory of kinematic waves in highway traffic, Part I: General theory. *Transportation Research Part B*, vol. 27, pp. 281-281.

Newell, G. F. (1993). A simplified theory of kinematic waves in highway traffic, Part II: Queueing at freeway bottlenecks. *Transportation Research Part B*, vol. 27, pp. 289-289.

Newell, G. F. (1993). A simplified theory of kinematic waves in highway traffic, Part III: Multi-destination flows. *Transportation Research Part B*, vol. 27, pp. 305-305.

Nagel K., Nelson, P. (2005). A critical comparison of the kinematic-wave model with observational data. *16th International Symposium on Transportation and Traffic Theory* (Mahmassani Ed.), pp. 145-163.

Patire, A.D., Cassidy, M.J. (2011). Lane changing patterns of bane and benefit: observations of an uphill expressway. *Transportation Research Part-B*.

Persaud, B., Yagar, S., Brownlee, R. (1998). Exploration of the breakdown phenomenon in freeway traffic. *Transportation Research Record - Journal of the Transportation Research Board*, Vol. 1634, pp. 64-69.

Polikar, R. (2001). *The wavelet tutorial*, second edition.

Polus, A. and Pollatschek, M.A. (2002). Stochastic nature of freeway capacity and its estimation. *Canadian Journal*, Vol.29, pp. 842-852.

Richards, P.I. (1956). Shockwaves on the highway. *Operations Research*, pp. 42-51.

Rudjanakanoknad, J.and Akaravorakulchai, C. (2011). Mechanism of a freeway weaving section as typical traffic bottleneck. *Transportation Research Board*, Paper#11-0747.

Sarvi, M., Kuwahara, M., Ceder, A. (2007). Observing freeway ramp merging phenomena in congested traffic. *Journal of Advanced Transportation*,vol.41(2), pp. 145-170.

Schrank, D and Lomax, T. (2012). *The 2012 urban mobility report*. Texas Transportation Institute.

Smilowitz, K. and Daganzo C. (2000). Experimental verification of time-dependent accumulation predictions in congested traffic. Transportation Research Records, Journal of the Transportation Research Board, Vol. 1710, pp. 85-95.

Yeon, J, Henrandez, S. and Elefteriadou, L. (2007). Differences in freeway capacity by day of week, time of day and segment type. *Transportation Research Board*, Report: 07-2287, pp. 27.

Zheng Z, Ahn, S., Chen, D., Laval, J. (2011). Freeway traffic oscillations: microscopic analysis of formations and propagations using wavelet transform. *Transportation Research Part B: Methodological*.